Angiogenic outgrowth from a perfused vascular explant: Design and implementation of a perfused vascular explant bioreactor

By

Michael Warren Irvin

Thesis

Submitted to the Faculty of the

Graduate School of Vanderbilt University

in partial fulfillment of the requirements

for the degree of

Master of Science

In

Biomedical Engineering

May, 2012

Nashville, Tennessee

Approved by:

Professor John Wikswo

Professor Ambra Pozzi

Professor Andries Zijlstra

ACKNOWLEDGEMENTS

I would like to first thank Dr. Wikswo for supporting and mentoring me throughout this project. He has provided great advice and education regarding the details and general concepts of this project and has provided resources and space for me to learn independently. I appreciate the great insight he brought to this project. Dr. Wikswo is someone who cares deeply for colleagues and mentees. He has patiently listened and offered honest and encouraging words to me about science, careers and life in general. I cannot fully express how grateful I am for this. I am very thankful for the chance to have worked with him. Working in his lab has been a great experience, and has shaped me into a better scientist and person.

I would also like to thank Dr. Andreas Zijlstra and Dr. Ambra Pozzi who also mentored me in this project. Dr. Andreas Zijlstra provided education and insights that motivated me to keep "the big picture" in mind as I work through the details of the project. He also dedicated a lot of time to preparing me for my professional career. I am also thankful for the equipment and space he allowed me to use to complete the project. Dr. Ambra Pozzi was awesome! Several of the experiments were conducted in her lab and therefore she would often be the first to see the data from these experiments. I am thankful for her mentoring in helping me make sense of the research. She shared in my excitement about the project and encouraged me in the more frustrating parts of the research experience. I am thankful for her generously providing me the space and equipment necessary to complete the project.

I would also like to thank Drs. Lisa McCawley, Jin Chin, and Dmitry Markov who, with Phil Sampson and Ron Reiserer helped me design and implement the device. Phil Sampson was often the first person I would consult whenever questions about the device arose. I greatly appreciate the work he put into helping develop and implement the device. I would like to also thank Dr. Masakazu Shiota who taught me how to explant the aorta and helped me develop a technique for catheterizing and loading the aorta

into the device. I would also like to thank Allison Price for editing the thesis and other writing related to this study.

I am thankful to my friends and family for their love and understanding. They listened to me and encouraged me throughout the research experience. I am thankful for their prayers and godly advice, and for being available and willing to play capoeira with me.

This work was supported in part by the Department of Defense CDMRP Breast Cancer Research Program award no. W81XWH-07-1-0507.

ABSTRACT

The importance of studying angiogenesis is underscored by its involvement in diseases such as cancer, heart disease, arthritis and diabetes. Researchers have developed disease treatments that target the molecules that drive angiogenesis in therapeutic ways. The mechanisms of angiogenesis, however, are under-characterized, and the gaps in our understanding of angiogenesis invariably limit the development of new and the efficacy of existing disease treatments. Consequently, a better understanding of angiogenesis will require new angiogenesis assays. Current angiogenesis assays strip away important components of the angiogenic process and/or limit control of the variables that direct angiogenesis. This problem is more pronounced in studies of the interaction between mechanical signals engendered in blood flow and angiogenesis. To address some of the limitations of the current armamentarium of angiogenesis assays, vascular explant assays (e.g. the aortic ring assay) were developed. Considered the best *in vitro* mimic of *in vivo* angiogenesis, the "*ex vivo*" vascular explant assay synergistically combines qualities of *in vitro* and *in vitro* angiogenesis assays to provide precise control over a biological system that recapitulates almost all of the mechanism and steps of physiological angiogenesis. However, the vascular explant assay lacks mechanical stimuli engendered in blood flow. The goal of this research was to develop a more physiologically realistic platform for studying angiogenesis by incorporating intraluminal fluid flow within the vascular explant assay. A perfused vascular explant bioreactor was developed and implemented to facilitate long-term culture and angiogenic outgrowth from a perfused mouse thoracic aorta *in vitro*. The aorta was subjected to a flow rate that would generate shear stress comparable to that experienced in post capillary venules. Finite element analysis of the reactor predicted perfusion of the aorta lumen would also cause perfusion of the abluminal space, provided the aorta contained holes through with fluid could exit. The vascular explant bioreactor developed in this study supported long-term culture of a perfused and/or perfusible thoracic aorta *in vitro*, and also demonstrated angiogenic outgrowth from the explant. When the aorta lumen was loaded with fluorescent microspheres, regions

of the angiogenic outgrowth fluoresced, suggesting that some of the nascent vasculature was patent to the aorta. However, in response to intraluminal perfusion and culturing in our bioreactor, we observed an as-yet unexplained increase in the hydraulic impedance of the aorta. The device designed in this study may allow researchers to investigate the interaction between hemodynamic stimuli and angiogenesis in an *in vitro* model that recapitulates nearly all of the mechanisms and steps of angiogenesis. Application of this technology may produce insights necessary for developing new drugs that treat diseases by targeting angiogenesis.

TABLE OF CONTENTS

Page

LIST OF FIGURES

LIST OF TABLES

CHAPTER I

INTRODUCTION

Heart disease, cancer, and stroke lead in causing death in the U.S., accounting for over half of the deaths in America in 2009[1]. Together they account for $700 billion in yearly health care and lost productivity costs in America[2, 3]. Further, for the patients battling these diseases, current treatments only marginally and temporarily improve the quality of life. Heart disease, cancer, and stroke vary widely in their mechanisms of action but share one commonality: Angiogenesis, the sprouting and subsequent stabilization of blood vessels from pre-existing blood vessels, plays a pivotal role in their pathogenesis. Angiogenesis is a hallmark of several diseases, including cancer, ischemia, hypertension, and inflammatory disorders[4]. For this reason, understanding angiogenesis is crucial to understanding, preventing, and treating many diseases. Years of study have vastly expanded the knowledge of angiogenesis but gaps remain. These gaps redound to limitations in the efficacy of available treatments for several diseases. The study of angiogenesis draws upon an armamentarium of *in vitro* and *in vivo* assays, but there is no "gold standard" angiogenesis assay. *In vitro* assays provide a platform for detailed study of biological systems that poorly mimic or recapitulate angiogenesis in humans, while *in vivo* assays provide a more relevant model at the cost of access to and control of variables that affect angiogenesis. This is especially evident in studies of the interaction between mechanical stimuli and angiogenesis.

Some diseases (e.g., tumor malignancy and hypertension) have an impact on both the mechanical forces experienced by blood vessels and angiogenesis; however, little is understood about the interaction between mechanical forces and angiogenesis or how this interaction drives the pathology of these diseases. *In vitro* mechanotransduction assays (which study the cellular response to mechanical perturbations) typically limit investigations to individual cells or two-dimensional cell monolayers in conditions that deviate greatly from their physiological context. *In vivo* angiogenesis assays offer minimal control over mechanical stimuli, and *in vivo* control of a mechanical stimulus in isolation is difficult. Blood vessels interpret the mechanical forces and biochemical cues communicated via their constant contact with flowing blood. However, blood flow and consequences of blood flow are not well mimicked *in vitro*, nor are they precisely controlled *in vivo*. Recently, improvements have allowed the introduction of blood flow mimicking mechanical stimuli to three-dimensional angiogenesis assays, but even these assays do not represent or recapitulate human angiogenesis to the full capabilities afforded by current *in vitro* angiogenesis assays.

The best *in vitro* mimic of angiogenesis *in vivo* occurs in the vascular explant angiogenesis assay, for example the aortic ring assay, in which new vessels sprout from segments of explanted vessels and to some extent stabilize. This assay presents multiple cell types with a spatial organization that is most similar to that in *in vivo* angiogenesis. In the vascular explant angiogenesis assay, the vascular explant retains more of its endogenous character than do cells used in other *in vitro* angiogenesis assays. For ex-

ample, angiogenesis only occurs when solicited, and the cells that carryout angiogenesis (endothelial cells) are typically quiescent. Isolation of endothelial cells relinquishes cell quiescence, whereas explanting vasculature does not. This assay recapitulates nearly all of the steps of *in vivo* angiogenesis while retaining much of the precision and control offered by *in vitro* angiogenesis assays. For this reason, the vascular explant angiogenesis assay overcomes several of the limitations typical of *in vitro* and *in vivo* angiogenesis assays. Unfortunately, the vascular explant angiogenesis assay does NOT accommodate simulation of blood flow or associated mechanical stimuli. In consideration of this drawback, I propose a perfused vascular explant bioreactor (PVEB) which facilitates angiogenic outgrowth from a perfused vascular explant in long-term *in vitro* culture.

The proposed PVEB would allow perfusion access to the lumen of a vessel in long-term culture and whose endothelial cells are undergoing angiogenesis. This advantage would potentially permit investigation of the influence of stimuli engendered in blood flow within the vascular explant angiogenesis assay by providing a means of monitoring and controlling intraluminal fluid composition and flow. Valuable features of the vascular explant assay (i.e. the physiological relevance of its angiogenic environment and the nearly complete angiogenic process it recapitulates) would be maintained in the PVEB. Since *in vivo* angiogenesis occurs from patent microvasculature, the addition of perfusion to the vascular explant potentially makes the PVEB angiogenic culture a better *in vitro* mimic of the *in vivo* angiogenic environment than conventional vascular explant assays. The PVEB will allow potentially more detailed and physiologically relevant study of the interactions between mechanical forces and biochemical phenomena engendered in blood flow and angiogenesis. I hypothesize that the PVEB will facilitate angiogenic outgrowth from a vascular explant whose lumen is accessible to perfusion, and that this enhancement will allow measurement and actuation of mechanical and chemical stimuli (those accompanying blood flow) in a vascular explant angiogenic culture. Insights gained by using the PVEB to study angiogenesis may prove necessary to the development of drugs and therapies that effectively target angiogenesis in the treatment of a host of diseases. The following briefly summarizes angiogenesis and reviews the assays that researchers utilize to investigate angiogenesis. Based upon this, we propose that the perfused vascular explant bioreactor as a valuable addition to the armamentarium of angiogenesis assays.

CHAPTER II

BACKGROUND

B.1. Angiogenesis

In a biological system, vital nutrients typically passively diffuse only a few hundred microns from their source. This implies that large organisms, some spanning several meters, must have an extensive network of nutrient-carrying conduits (e.g., blood vessels) in order to exist. The human circulatory system, for example, consists of miles of blood vessels assembled into a network that efficiently meets the immensely diverse needs of the body's tissues – all while maintaining fairly constant and moderate pressures and flow rates throughout. A properly functioning circulatory system is absolutely essential to human development and health. The circulatory system starts functioning before any other system in the vertebrate[5]. This incredibly adaptive and complex system assembles, maintains, and remodels itself in part via sprouting angiogenesis, commonly referred to simply as angiogenesis, which is the process of growth and subsequent stabilization of new blood vessels that bud from pre-existing ones[6-8].

Angiogenesis first occurs in early embryogenesis and continues until adulthood. During adulthood, most blood vessels remain quiescent (i.e., they do not participate in angiogenesis) until solicited to initiate angiogenesis by local ischemia, wounding, endometrial repair, or malignant tissues. Other processes (e.g., vasculogenesis and arteriogenesis) participate in vessel formation and remodeling, but angiogenesis plays the most active role in establishing and maintaining a mature circulatory system – particularly in the microcirculation domains. While the "steps" of angiogenesis are not concretely defined, one might consider angiogenic sprouting, vessel formation, adaptation to tissue needs, and stabilization as four roughly sequential events in angiogenesis. Orchestrating these steps requires the cooperation of cell types, matrix molecules, growth factors, and cytokines, each responding to certain genetic, metabolic, mechanical, and chemical cues in processes not fully understood. Researchers expect that creative innovations in assays and techniques will prove necessary for expanding the knowledge of angiogenesis. Keeping the technologies commonly utilized to study angiogenesis in mind, the following briefly overviews the current description of angiogenesis in health and disease.

B.1.1. Vascular Development and Quiescence

The first vasoformative events occur in the mesoderm of an embryo right after gastrulation[9, 10]. Here, vasculogenesis (discussed below) gives rise to a series of interconnected capillary-like tubes called the primordial blood vessel network or vascular plexus. The vascular plexus develops onward into adulthood, expanding and organizing – via angiogenesis and other vasoformative processes – into a mature, immensely complex and multifunctional vasculature. The adult vascular network is largely quiescent and arranged into blood vessels that accommodate high volume. These vessels connect to the heart and ar-

borize into smaller arteries, veins, and capillaries that populate all tissues. Anatomical and physiological features vary throughout the vascular tree and take on functional specializations to suit the needs of nearby tissues and organs. Therefore, the microenvironments that facilitate angiogenesis carry distinct cell and matrix compositions, and the cell types that most actively participate in angiogenesis vary in origin, morphology, gene expression, and responsiveness to angiogenic factors. Spatial-temporal variations of the vasculature in its quiescent state affect the likelihood and nature of angiogenesis. There exist, however, several properties that are consistent throughout the vasculature, and the quiescent vascular system, though constantly engaged in a diversity of vital tasks, stands poised to rapidly initiate angiogenesis in response to stimuli. The following describes the vascular system in its quiescent state: how the vascular system arises, what qualities define the quiescent state, and what processes maintain a quiescent vasculature until angiogenesis is induced.

Vascular system development

Vascular development begins in the embryo with vasculogenesis. In this process, endothelial cell precursors differentiate into endothelial cells – which line the entire internal surface of the vessel network – and amalgamate to form a network of primitive capillary-like tubes called the vascular plexus[9, 10]. Embryonic vasculogenesis is triggered in the mesoderm by the accumulation of fibroblast growth factors (FGFs). Cells in the mesoderm differentiate into angioblasts (embryonic precursors of endothelial cell precursors) and assemble into cell clusters called blood islands. The blood islands coalesce during vasculogenesis to form a vascular plexus. Embryonic vasculogenesis is required for organogenesis, as organs begin growing around the nascent vessels of the vascular plexus[9].

Initially thought to occur only in embryos, vasculogenesis has been observed in postnatal juveniles and adults[9]. In adult vasculogenesis, endothelial progenitor cells, mesoangioblasts, multipotent adult progenitor cells, and/or side population cells in the bone marrow assume the role that angioblasts take in embryonic vasculogenesis[9]. This has sparked interest in developing cell therapies that stimulate vasculogenesis in treating ischemia and other diseases. Embryonic and adult vasculogenesis occurs alongside angiogenesis and initiates in response to proangiogenic factors such as FGFs and vascular endothelial growth factor (VEGF)[9, 10]. In fact, embryonic models of angiogenesis can also be used to study vasculogenesis (e.g., avian embryo chorioallantoic membrane, or CAM, assays)[9]. Vasculogenesis-capable cells promote angiogenesis by secreting proangiogenic paracrine signals and by transdifferentiating into endothelial cells and vascular supporting mural cells[9, 11].

Angiogenesis begins to remodel and expand the nascent vascular plexus shortly after it arises in the embryo. Angiogenic remodeling of the vascular plexus utilizes several processes common in angiogenesis in adults (section B.1.2.) although some distinctions exist. A notable difference between embryonic and adult angiogenesis, for instance, is that embryonic angiogenesis occurs (prior to organogenesis) in anticipation of local oxygen and nutrient demands and adult angiogenesis occurs in response to it. G. Breier reviews the distinct mechanisms of embryonic angiogenesis[10]. Neuropilin and Notch signaling pathways direct embryonic angiogenesis. Angiogenic sprouting and migration (particularly in arterial fated endothelial cells) occur in response to VEGF-A signaling from the notochord and nascent neurons[10]. VEGF-A,

expressed primarily in embryos, binds to vascular endothelial growth factor receptor 2 (VEGFR2) in endothelial cells and induces expression of Notch proteins and Notch protein ligands[10]. It is suspected that VEGF-A signaling to the Notch pathway explains why arteries and neurons run alongside each other[4,10,11]. The dependence of endothelial cells on VEGF-A for angiogenesis wanes after birth[10].

Notch signaling also specifies the arterial and venous phenotype in embryonic endothelial cells. Arterial specification equips arteries, arterioles, and arterial capillaries to carry pressurized, oxygenated (except in pulmonary or umbilical arteries) blood at higher flow rates. Arterial specification coats the vessels with elastic matrix materials, pericytes, fibroblasts and smooth muscle cells which strengthen the vessels. Veins do not accommodate higher pressure flow and as a result lack some of the arterial features. Arterial/venous specification is an important step in the maturation of the vascular system and has consequences on angiogenesis. For example, arteries do not as readily respond to pro-angiogenic molecules as do veins, and it was hypothesized that tumors tend to attract angiogenic sprouting on the venous side of capillaries because of the differences that arise in arterial/venous specification. VEGF-A, secreted from notochord and neurons, suppresses venous specification and promotes stabilization of nascent arteries. Notch proteins specify the arterial phenotype, prior to blood flow[10, 11]. Notch signaling induces expression of Ephrin B2 and EphB4 (a receptor for Ephrin B2) in arterial and venous endothelial cells, respectively. EphrinB2-EphB4 signaling is critical for arterial and venous anastomoses, which demark the boundary between the arterial and venous sides of the vascular system. Researchers once suspected that Notch signaling in arterial-venous specification is nonfunctional in adults. However, endothelial cells can take on an arterial or venous phenotype in neonatal retina and even in the adult heart[11,12]. Nicosia et al. have observed arterial-venous anastomoses *in vitro*[13] . Directing the arterial/venous fate of endothelial cells might benefit angiogenic therapies in tissue regeneration and engineering.

Intussusceptive angiogenesis is a vascular remodeling process that causes transluminal endothelial pillars to form within the small vessels and capillaries and subsequently fuse, thereby delineating two new vessels[14]. Sprouting and intussusceptive angiogenesis expands the vascular plexus, but subsequent growth and remodeling occur via intussusceptive angiogenesis[14]. In adults, intussusceptive angiogenesis remodels the nascent vasculature arising from sprouting angiogenesis[14].

Once anastomotic connections between the arterial and venous trees of the vascular system form, blood flow begins[6] and arteriogenesis starts modifying the vascular system. Arteriogenesis (also termed collateral growth) is the proliferative dilation and muscularization of arterial vessels[15-17]. This process begins with activation of the endothelial cells that line arterial vessels[17]. Prolonged increases in shear stress and transmural pressure difference in the vasculature stimulate arteriogenesis. Increases in shear stress and transmural pressure that accompany arterial occlusive diseases and vascular development induce arteriogenesis, but are difficult to imitate *in vitro*. As a result, fewer of the biomolecular mechanisms of arteriogenesis have been uncovered. *Ex vivo* organ cultures have been developed and are beginning to be utilized to investigate the effects of fluid flow on endothelial and smooth muscle cell proliferation (i.e. markers of arteriogenesis)[18, 19]. Arteriogenesis also occurs by chemical induction. For example, basophilic fibroblast growth factor (bFGF) causes endothelial cells to proliferate and express cell adhesion molecules important for recruiting pro-arteriogenic monocytes from circulation[16,17]. Arteriogenesis occurs almost always in the presence of ischemia but it is not caused by ischemia[17]. Angiogene-

sis alone is only modestly effective at treating large regions of ischemia. Angiogenesis increases the vascular content in a tissue, while arteriogenesis increases the volumetric flow rate into the tissue. Treatment of coronary ischemia and blood perfusion demands in tissue regeneration applications have sparked interest in therapies that induce both angiogenesis and arteriogenesis.

Vasoformative processes that participate in the pathological vascularization of malignant tissues include vessel co-option, vessel mimicry, and tumor endothelial cell differentiation[6]. Lymphogenesis and the formation of the heart are major occurrences in the development of a functioning vascular system[20].

Vascular System Function

The mature vascular system features two closed-loop conduits: the systemic and pulmonary circulation loops. The systemic circulation loop extends from the heart via the aorta. The aorta branches into other major arteries (e.g., carotid, subclavian, femoral arteries, etc.). These arteries arborize further into arterioles, metarterioles (in some cases), and capillaries. Capillaries consist of arterial and venous sides that form anastomotic connections. Capillaries connect to venules which debouch into larger veins, and ultimately the superior vena cava (which connects to the right atrium of the heart). The pulmonary arteries carry deoxygenated blood from the right ventricle into the lungs and branch ultimately into alveolar capillaries. Oxygenated blood returns to the heart via the pulmonary veins. Anatomical and physiological features of the vascular system vary with position along the vascular tree[21]. The anatomy and physiology of the vascular system is reviewed in medical and human physiology text books (e.g., *The Review of Medical Physiology* edited by W.F. Ganong provides detailed chapters). This has important functional consequences in angiogenesis. The walls of large arteries contain three layers: the tunica adventitia, rich in elastic connective tissue; the tunica media, populated by smooth muscle cells; and the intima, comprising a single layer of endothelial cells and underlying basement membrane[21]. The elastic walls of large arteries passively distend in response to hydraulic pressure of inflowing blood[21]. The cyclic distention of arteries dampens pressure variations in downstream smaller arteries and arterioles[21]. Arterioles contain more smooth muscle cells than arteries, which allows them to actively constrict to resist blood flow[12,21]. The majority of the vasculature's hydraulic resistance arises in the arterioles[12,21]. This function of arterioles protects downstream capillaries from mechanical damage. The vascular tone of arterioles responds to noradrenergic and cholinergic nerve fibers which regulate the distribution of blood flow to different organs. Arteries and arterioles are sensitive to nitric oxide (NO) and other vasodilators[12,21, 66].

Pre-capillary sphincters regulate flow into capillaries by contricting and dilating in response to mechanical stresses (e.g. hydrostatic pressure) and metabolic demands of the surrounding tissue[21, 139]. The transition from arterioles and metarterioles to capillaries features a two- to tenfold reduction in luminal diameter (from 10-50 μm to 5 μm)[21]. But blood moves slowly through the capillaries at 0.07 m/s, with erythrocytes flowing "single file" down the capillary and having a residence time in the capillaries of 1-2 seconds[21]. This results from the tenfold increase in total cross-sectional area between arterioles and capillaries[21]. As a result, capillaries will often lack flow and exist in a collapsed state (e.g., in instances where the luminal pressure is less than the interstitial pressure, luminal diameter is less than the erythrocyte diameter, or elongation of surrounding tissue such as the alveoli or bladder applies tension on

the capillary)[21]. The capillaries in vascularized tumors contain several structural irregularities and as a result, blood flow is irregular and at times oscillatory[71].

The primary goal of the circulatory system, to affect adequate mass transfer between the blood and tissues, is met within the capillaries. Several thousand square meters of vascular endothelium lining capillaries function as a semipermeable barrier between the blood and tissue. The microvascular walls consist of a single cell layer of endothelial cells underlined with supporting pericytes and ensheathed by basement membrane. Vascular permeability mediates mass transport across the endothelium that lines capillaries and varies to suit the local demands and functions of the surrounding organ/tissue. Many vascular beds contain a continuous endothelium with 10 nm spaces between the endothelial cell junctions. Small molecules diffuse into the surrounding interstitial space through these junctions. The blood brain barrier achieves greater selectivity via its tighter junctions. The endothelial cells in some organs – particularly those that produce or remove large macromolecules (e.g., intestinal villi, kidneys, endocrine glands, etc.) – have attenuated cytoplasm, creating transendothelial pores, or fenestrae, that range from 20-100 nm. Liver sinusoidal capillaries are highly fenestrated, containing 600-3000 nm pores[21]. The existence of fenestrae is also a feature of malformed vessels grown in pathological angiogenesis (e.g., tumor vasculature). Vasicular transport and diapedesis mediate transendothelial transport of biomacromolecules and cells, respectively. Researchers assess the functional qualities of vessels grown *in vivo* angiogenesis assays by injecting fluorescent dyes and nanoparticles into the vasculature (a technique not generally amenable to use *in vitro*).

Post-capillary venules feature thin pliable walls that contain few smooth muscle cells. Veins and venules can distend greatly without pressurizing their lumens. This property protects capillaries from back pressure or fluid accumulation upstream of the venules. Low venous intraluminal pressures create a challenge to venous blood flow. Overcoming this involves skeletal muscle contractions which propel fluid in the veins and venous valves that prevent retrograde flow. Fluid entering the interstitial space from the capillaries drains into the lymphatic system and reenters the circulation at the subclavian veins. Blood flow is propelled through the circulatory system mainly by the heart, although diastolic recoil, compression of veins by skeletal muscles, and negative pressure in the lungs during inspiration also propel blood.

Blood consists of cells (erythrocytes, granulocytes, leukocytes, and platelets) suspended in plasma. Erythrocytes carry oxygen through the vasculature on hemoglobin. In the immune response to infection, granulocytes utilize the vasculature to reach a site of inflammation. Neutrophils influence vascular biology by insinuating themselves through the endothelium, degrading surrounding matrix materials, and releasing reactive oxygen species. Monocytes participate in angiogenesis by releasing proangiogenic factors and differentiating into vasosupportive cells. Leukocytes secrete immune active interleukins which activate immune cells as well as endothelial cells. Platelets facilitate clotting of the blood and influence inflammation, wound healing, and vasoformative processes (e.g., angiogenesis). Plasma contains protein biomacromolecules (e.g., antibodies, growth factors, and clotting factors), small molecules (e.g., amino acids, fatty acids, hormones, glucose, oxygen, etc.), ions, metals, and water. The vasculature responds to blood composition. Ionizable amine and carboxyl groups on proteins and cells in the blood give rise to oncotic pressure differences across the endothelium, and the resulting force influences endothelial cell

function. Clotting factors initiate thrombosis upon binding the vascular endothelium. Local oxygen concentrations regulate the initiation of angiogenesis.

The behavior of the vascular endothelium is tailored to its position along the vascular tree. This has therapeutic, tissue engineering, and disease consequences. Drug delivery is organ-specific and dependent on local vasculature properties. Fenestrated blood vessels of the liver cause the bulk of orally/intravenously administered drugs to accumulate in the liver. Vascular fenestrae also prove useful in targeting vascularized tumors. When vascularizing a tissue-mimicking biomaterial, researchers and engineers note the influence that mechanical forces have on the phenotype of the endothelium *in vivo*. This has proved critical in regenerating lung tissue, for example. Susceptibility of the endothelium to disease (e.g., arteriosclerosis and diabetic retinopathy) is a result of the spatial-temporal properties of the vascular endothelium. For these reasons it is important to study the distinct biology of individual regions of the vasculature as well as the general properties of the entire vasculature. During the quiescent state, the vascular endothelium is largely engaged in managing the mechanical forces of blood flow and carrying out transendothelial mass transport. But other processes frequently occur in the vasculature (e.g., vasodilation and constriction, hemostasis, immune response, and inflammation (reviewed elsewhere) and permeability).

B.1.2. Physiological Angiogenesis

An angiogenic stimulus will cause regions of the vasculature endothelium to undergo the drastic remodeling "steps" of vascular sprouting, vessel formation and stabilization or regression to generate new capillaries. These roughly sequential steps elicit the involvement of diverse cell types, extracellular matrix materials (ECM), growth factors and cytokines. The involvement of these angiogenic factors is reviewed in detail elsewhere[6, 22-26]. The signals that drive angiogenesis vary temporally. In fact, several inhibitors of the early steps of vessel sprouting promote later steps of vessel maturation. This poses interesting challenges and opportunities to researchers who investigate ways to interrupt disease processes by targeting angiogenesis.

Sprouting

Angiogenesis in adults begins with endothelial cell proliferation. In the absence of pro-angiogenic stimuli, endothelial cells will exist for years in a quiescent (i.e., non-proliferating) state. Endothelial cell quiescence in microvasculature is maintained by the autocrine action of endothelium derived VEGF, angiopoietin-1 (Ang-1), and fibroblasts growth factors (FGFs). Angiogenesis initiates when endothelial cells receive pro-angiogenic paracrine signals from an ischemic or growing tissue, or from injured vasculature. Potent initiators of angiogenesis, expressed by tissues demanding increased blood flow, include VEGF, FGFs and Ang-2.

Cells can sense ischemia via hypoxia inducible factors (HIFs)[27]. HIFs are a heterodimeric transcription factor composed of alpha and beta subunits. In normoxic conditions, proline residues on the alpha sub-

unit (e.g., HIF-1α) become hydroxylated by HIF prolyl hydroxylases which use oxygen as a substrate. Hydroxylation targets HIF-1α for ubiquitination and degradation. Hypoxia depletes the oxygen substrate required for HIF-1α hydroxylation. Other, metabolic consequences of hypoxia also inhibit HIF-1α hydroxylation. As a result, HIF-1α accumulates and dimerizes with HIF-1β. The HIF-1 dimer is a transcription factor that directs the expression of VEGF, Ang-2 and several other pro-angiogenic molecules. Tumor xenographs in *in vivo* angiogenesis assays contain hypoxic cells, and use the HIF pathway, in part, to generate pro-angiogenic signals. Cancer treatments that target angiogenesis by inhibition of the HIF-1 pathway have been developed[28].

In several *in vitro* and *in vivo* angiogenesis assays (vascular explant assay, *in vivo* Matrigel invasion assay, and the cornea angiogenesis assay) angiogenesis can occur in response to wounding. The wound healing response begins with vascular or tissue injury. Expression of a Glucose Analog of Blood Group H Antigen, (H-2g also called 2-fucosyl lactose) increases in endothelial cells exposed to damaged tissue. H-2g induces endothelial cell release of bFGF and VEGF[29]. The resulting, short-term surge in bFGF and VEGF initiates angiogenesis. H-2g also induces endothelial cell expression of intercellular adhesion molecule 1 (ICAM-1) which attracts leukocytes and other immunologically active cell types[30, 31]. Several pro-angiogenic factors are synthesized by immunologically active cells, including tumor necrosis factors (TNFs), interleukins, bFGF and VEGF[32]. In the vascular explant assay, resident adventitial macrophages secrete these growth factors as part of the wound healing response, and ablation of macrophages from the aortic ring assay, for example, abrogates the angiogenic potential of the explant[33]. Platelet activation during wound healing causes expression and activation of plasminogen activator (PA), a fibrin degrading protease. NO also has a pro-angiogenic effect as it elicits VEGF expression[34].

Upon angiogenic activation of a vessel, pericytes (in response to Ang-2) detach, proliferate and migrate into the interstitium. Pericytes burrow through the basement membrane by expressing matrix metalloproteases (MMPs) which degrade the ECM. Fibroblasts also migrate outward, laying a provisional extracellular matrix (composed of collagen, fibronectin, and heparan sulfate proteoglycans) for the growing angiogenic sprout. In addition, fibroblasts secrete pro-angiogenic signaling molecules (e.g., VEGF, tumor growth factor (TGF-β), and platelet derived growth factor (PDGF)). Various *in vitro* co-culturing and vascular explant assays have provided insights about involvement of pericytes and fibroblasts in angiogenic sprouting.

Endothelial proliferation and migration occur in the presence of pro-angiogenic cues (e.g., VEGF, Ang-2 and bFGF). So that endothelial cells do not migrate *en masse* toward the angiogenic stimuli, delta-like 4 (Dll4) -Notch1 signaling pathways select a tip cell to lead the angiogenic sprout[35]. The Notch signaling pathway is active in differential cell fate decisions such as the selection of a tip cell phenotype. Tip cells express increased levels of VEGFR2, platelet-derived growth factor B (PDGFB), and the Notch ligand DLL4 over those of adjacent endothelial cells[36]. The increased VEGFR2 in tip cells makes them more responsive to the chemotaxis stimulus, VEGF[36]. DLL4 secreted by the tip cell has an inhibitory effect on adjacent stalk cells. Tip cells chemotax toward VEGF, while adjacent stalk cells proliferate and migrate behind the tip cell to form the growing sprout.

Several of the existing angiogenesis assays incorporate a means for investigating the mechanisms of endothelial cell proliferation and migration. When studying endothelial cell proliferation, researchers note that the *in vitro* angiogenesis assays (discussed in section A.2.) utilize endothelial cells that upon isolation have lost their quiescence and with culturing have been selected for their proliferative ability.

Vessel Formation

Endothelial cells acquire a lumen once they have migrated outward from their parent vessel. In this process, endothelial cells and stalk cells form vacuoles via pinocytosis. These vacuoles coalesce into larger contiguous lumens which eventually span the multiple endothelial cells.

Fibroblasts induce tube formation in the angiogenic sprout. Fibroblasts deposit extracellular matrix molecules which signal to stalk cells. Interstitial collagen-I and fibrin/fibronectin signal to endothelial cells through integrin pathways[37]. Vascular endothelial cadherin which establishes intercellular junctions between endothelial cells also mediates tube formation[38]. Fibroblasts secrete tubulogenesis-stimulating molecules when co-cultured with endothelial cells (without direct contact between them)[37]. Fibroblasts secrete VEGF, TNF and PDGF, but these alone did not induce tube formation in collagen *in vitro.* In co-culture with endothelial cells, fibroblasts produced several diffusible extracellular matrix precursors and it is suspected that these matrix precursors were required for tube formation[37, 39]. Tube formation occurs in the absence of fibroblasts when human umbilical vascular endothelial cells (HUVECs) are plated on Matrigel (a gelled murine tumor basement membrane extract)[40].

Branching in angiogenesis is thought to have mechanistic similarities to tip cell activation and migration. Endothelial cells in the stalk of an angiogenic sprout may assume a tip cell phenotype. Geudens and Gerhardt describe competition between endothelial cells in an angiogenic sprout for the role of tip cell[36]. It is suspected that branching utilizes this mechanism. Notch signaling suppresses tip cell migration, which in turn limits branching[41, 42]. Inhibition of Notch signaling induces hyperbranching[41]. Much of the work elucidating the mechanisms of vessel lumen and branch formation was carried out in *in vitro* tube formation assays and in zebrafish embryos.

Adaption to Tissue Needs and Stabilization

Once angiogenesis has produced a network of endothelial tubes, the angiogenic outgrowth undertakes key steps of vascular regression (which prunes parts of the angiogenic outgrowth) and vessel stabilization/maturation (which equips the nascent vessels to function long-term). Nascent angiogenic sprouts must decide whether to regress or stabilize. An abrupt loss of pro-angiogenic factors coupled with a lack of blood flow prompt endothelial tubes to regress and undergo apoptosis[43]. Signals that prompt vessel stabilization include angiogenic signaling molecules, PDGF and Ang-1, and blood flow.

Angiopoietin-2, which enhances vessel formation, also actively promotes vessel regression. Effects of Ang-2 signaling include detachment of pericytes (which promote vessel stability) and generation of MMPs (which inhibit endothelial cell viability by proteolytically degrading extracellular matrix proteins

that support endothelial cell adhesion). The effect of Ang-2 on vessel stability depends on the overall composition of growth factors. Together, VEGF and Ang-2 promote vessel formation but, in the absence of VEGF, Ang-2 causes vessel regression[44]. Prolonged exposure to other pro-angiogenic growth factors (e.g., VEGF and bFGF) inhibits stabilization of endothelial tubes can causes persistent formation of malformed vasculature[45, 46]. A cleavage fragment of collagen XVIII, endostatin, causes vessel regression by disrupting endothelial cell bFGF and VEGF signaling[47]. Vessel regression is observed *in vivo* and in angiogenesis assays that generate endothelial tubes/vascular sprouts *in vitro*.

Stabilization/maturation of nascent vessels involves processes that are the opposite of those that carry out the early steps of angiogenesis. During vessel stabilization, the endothelium abandons its proliferative and invasive phenotype in order to recover a non-proliferative state, with tight adhesion between cells and to the extracellular matrix, characteristic of quiescent vasculature. Pericytes and other mural cells get recruited to the vessel, matrix degradation is inhibited and new matrix materials are deposited to generate a basement membrane for the vessel. Attached pericytes and extracellular matrix proteins inhibit further migration and proliferation of and provide pro-survival signals to the endothelial cells. Eventually, anastomoses between the vascular sprouts allow blood flow in the capillaries. Hemodynamic forces engendered in blood flow are suspected to also stabilize the capillaries.

Four signaling molecules have been identified as playing a significant role in vessel stability[48]. PDGF secreted by endothelial cells causes recruitment and proliferation of pericytes, smooth muscle cells, fibroblasts and other mural cells. Sphingosine-1-phosphate-1 is released from endothelial and mural cells and also causes mural cell recruitment[48, 49]. Ang-1, expressed by pericytes and other mural cells, stabilizes nascent vessels by promoting the interaction between endothelial cells and pericytes, and stimulating monocyte recruitment[6, 48]. Pericytes recruited to the nascent vessels supply the endothelium with pro-survival and proliferation inhibiting signals. Pericytes also inhibit leakage of the endothelium. Monocytes are recruited to and immobilize where the ends of two vascular sprouts come in contact and promote anastomosis[50]. TGF-β inhibits extracellular matrix degradation and stimulates production of the extracellular matrix molecules that compose the basement membrane (e.g., collagen IV and laminin)[48]. The extracellular matrix plays a dynamic role in stabilizing a vascular sprout. The extracellular matrix harbors angiogenic signaling molecules that become liberated as regions of the extracellular matrix get degraded by MMPs. As a result, the composition of the available angiogenic signals varies spatially and temporally about the growing vascular sprout. Tissue inhibitors of metalloproteases become active and slow extracellular matrix degradation by inhibiting MMPs[51]. This helps stabilize the nascent vessels. As vessels mature, they become invested in a layer of laminin and collagen IV (i.e. the basement membrane)[48]. Collagen-endothelial cell binding promotes endothelial cell survival[26].

Blood flow aids vessel stabilization by generating potent pro-survival signals. Shear stress is mechanically transduced into the PI3K/Akt pathway in ways that mimic signaling by VEGF and Ang-1. Nitric oxide, produced by endothelial cells subjected to shear stress, inhibits endothelial cell apoptosis[43].

Angiogenesis gives rise to vessels that meet the organ-specific needs of their surroundings. The mechanisms involved in tailoring the nascent vasculature to suit its tissue needs are largely uncharacterized, though it appears to result from the concerted actions of VEGF and distinct signals from the host[52].

Hemodynamic force in angiogenesis

Hemodynamic forces engendered in blood flow (shear stress, pressurization and vessel wall tension) have an impact on angiogenesis *in vitro* and *in vivo*; for instance, administration of an adrenoreceptor agonist, prazosin, causes increased capillary shear stress. Increased shear stress induced by prazosin results in high capillary content and increased VEGF[53, 54]. High and low shear stress conditions also generated capillaries with differing morphologies in skeletal muscle[55]. Hemodynamic signals in angiogenesis have attracted research interests. It is suspected that mechanotransduction of blood flow-generated forces plays a more prominent role in physiological angiogenesis than in pathological angiogenesis, whereas chemotransduction directs more of the pathological angiogenic processes than the physiological angiogenic processes[56]. Studying hemodynamic effects on angiogenesis may allow researchers to piece together the molecular mechanisms that form the basis for adequate feedback control of capillary expansion and rarefaction to suit local tissue needs[56]. The impact of hemodynamic properties on angiogenesis is poorly understood in part because of the limitations of current *in vitro* and *in vivo* angiogenesis assays. Still, some mechanisms have been elucidated. Endothelial cells detect hemodynamic forces and in response cause increased expression of pro-angiogenic cytokines.

Endothelial cells detect shear stress via mechanosensory molecules in the extracellular matrix and in cell-extracellular and cell-cell adhesion complexes[57]. For example, in response to shear stress, platelet endothelial cell adhesion molecule (PECAM or CD31), VE cadherin and VEGFR2, assemble into a mechano-sensory complex and activates, via Ras and Src signaling cascades, pro-angiogenic genes[56]. PECAM is thought to serve as the primary shear stress transducer. VE cadherin functions here as an adapter that brings VEGF receptor 2 into the complex[56]. Glycocalyx, a dynamic polymeric coating on the luminal side of the endothelium, plays a role in regulating vessel permeability, leukocyte extravasation and mechanic transduction. Glycocalyx was shown necessary for flow-induced nitric oxide production[56]. Caveolae, invaginations in the cell membrane of cells, may contain mechanosensory molecules. Caveolin-1, a transmembrane protein that causes formation of caveolae, mediates blood flow-dependent vascular remodeling and vasodilation[57]. Flow-induced release of endothelial nitric oxide synthase (eNOS), which catalyzes the production of nitric oxide, was observed to initiate with local Ca^{+2} increases in the vicinity of the caveolea[58].

Shear stress promotes expression of potent pro-angiogenic molecules: PDGF, bFGF and TGF-β[59-62]. Nitric oxide is considered a principal mediator of flow-induced changes in the endothelium that give rise to angiogenesis. Nitric oxide is produced by three isoforms, in mammals, of the nitric oxide synthase protein family: eNOS, iNOS and nNOS. The current understanding of how nitric oxide promotes angiogenesis is incomplete. Nictric oxide has been linked to increased VEGF and bFGF expression[63, 64]. Shear-stress-induced nitric oxide increases the permeability of the endothelium. This causes blood-borne proteins to flow into the interstitium, where they would provide a scaffold for migrating endothelial cells. Nitric oxide also suppresses expression of the angiogenic inhibitor, angiostatin[65]. Nitric oxide may transmit flow-induced vasostimulatory signals in resistance arteries to downstream vessels. Nitric oxide can bind hemoglobin in red blood cells and therefor travel to downstream sites of slowed blood flow and/or low oxygen tension, where it is released[66]. The physiological consequence of this phenomenon is controversial[67, 68].

B.1.3. Angiogenesis in Disease

The vascular network exists predominantly in a quiescent state. Therein, endothelial cells retain the capacity to create new vasculature in response to a physiological stimulus: endometrial repair during ovulation, vascularization of the placenta during pregnancy and vascularization of the skeletal muscle after exercise. Angiogenesis is controlled by a balance of endogenous pro- and anti-angiogenic signaling molecules (i.e. an angiogenic switch)[69]. In disease, the angiogenic switch is frequently disregulated or subverted by the pathology. Cases where the angiogenic switch is "on" include cancer, retinopathies, and inflammatory disorders[69]. These diseases generate powerful inducers of angiogenesis, some of which are distinct to the diseases (e.g. HIV-1 Tat protein activates endothelial cells)[70]. Ischemia elicits an angiogenic response to several diseases. Tumors expand until they have regions that can no longer access adequate nutrient and oxygen exchange. Retinal diseases damage fragile retinal vessels and, as a result, they poorly perfuse regions of the retinal tissue. Vasculature produced as a result of pathological angiogenesis lacks morphological and functional features of healthy vasculature. Tumor vasculature, for instance, is characterized by leaky, disorganized vessels (many tumor angiogenic sprouts terminate and are non perfusable)[71]. Tumor cells may also line the walls of tumor vessels and differentiate into endothelial-like cells in a process called vascular mimicry[70, 71]. Flow in tumors is irregular and at times even oscillatory[71]. The high morbidity of diseases that induce angiogenesis has prompted more attention from researchers than have diseases that suppress angiogenesis. Research efforts have been successful generating anti-angiogenic compounds that disrupt these diseases and have been applied in clinic. Cases where the angiogenic switch is "off" or insufficient to support local demands for oxygen and nutrients include cardiac ischemia, neurodegenerative disorders, and hypertension[70].

B.2. Angiogenesis Assays

Recognizing its involvement in several pathologies, researchers have begun investigating angiogenesis to identify potential targets in the treatment of disease. Great strides have been made in elucidating the complex mechanisms of angiogenesis, but large gaps in the current knowledge base still exist. Diseases employ or disrupt the angiogenic process in ways not yet fully defined. The development of therapies that intercept disease actions on angiogenesis requires a more thorough understanding of the angiogenic process. Researchers use an array of *in vitro* and *in vivo* assays in their study of angiogenesis[72-74]. There is no "gold standard" angiogenesis assay. Therefore, angiogenesis studies rely heavily on the appropriate selection of multiple assays. In determining how well suited the assay is for a particular study, researchers consider the nature of the study and what is being investigated. Investigations of the molecular mechanisms of angiogenesis require assays that resolve individual components of the angiogenic process with high precision and recapitulate the particular mechanism being investigated. *In vitro* angiogenesis assays only recapitulate a few steps of the angiogenic process. In contrast, *in vivo* models facilitate the whole angiogenic process but key aspects cannot be controlled or studied. Investigating the action of a particular pro- or anti-angiogenic substance requires an assay whose overall angiogenic behavior best mimics angiogenesis in humans. In general, *in vitro* angiogenesis assays offer high precision and control of components of the angiogenic process isolated from confounding variables resident in

the whole organism. In contrast, *in vivo* assays trade precision for increased predictability/translatability and relevance to angiogenesis in humans. Results of angiogenic studies may vary depending on the assays utilized (e.g., observations *in vitro* that do not occur *in vivo*, and vice versa). Therefore, researchers carefully consider the relevance of the model organism, tissue type, test site, matrix material, and cell type to human angiogenesis in the physiological or pathological context being investigated. Typically an angiogenesis study pairs *in vitro* and *in vivo* angiogenesis assays to harness the power and overcome the limitations of both. Still, the current armamentarium of angiogenesis assays presents a gap between the capabilities of the assays and the requirements of some angiogenesis investigations. This gap makes it difficult to reach conclusions about key aspects of angiogenesis or design therapies that take these aspects into account (e.g., mechanotransduction effects on the long-term development of nascent angiogenic sprouts cannot be fully investigated in either *in vitro* or *in vivo* models). The following describes and compares common angiogenesis assays.

B.2.1. Types and Applications of Angiogenesis Assays

In vitro assays, experimentation on cells and tissues isolated from an organism, permit reduction of complex biological processes into units that can be tractably studied in detail. They are usually required to resolve the individual functional components of the angiogenic process. Data from *in vitro* assays inform the design of *in vivo* assays that ultimately translate to innovations in the clinic. However, *in vitro* assays create a synthetic environment that bears little similarity to the physiological environment being investigated. Angiogenesis *in vitro* does not always represent *in vivo* angiogenesis well (e.g., in several *in vitro* angiogenesis assays vascular maturation steps do not occur). Results of *in vitro* studies frequently do not translate and should be interpreted carefully and confirmed *in vivo*. In an effort to get more translatable results, researchers try to controllably reconstruct the complex mesh of features that exist physiologically. Still, no *in vitro* assay incorporates mural cells, extracellular matrix, flow (shear stress, pressure, and tension), and humoral interactions. The following describes common *in vitro* and *in vivo* angiogenesis assays.

In vitro angiogenesis assays

In vitro assays of angiogenesis typically study the behavior of endothelial cells within a tightly controlled environment, in isolation from other cells or in co-culture with another cell type. This allows researchers to study particular mechanisms or drug actions in angiogenesis while controlling nearly all other influencing variables. Such studies identify target molecules and pathways. Several angiogenic signals (cell types, matrix materials, mechanical cues, structural organization, etc.) are stripped away in *in vitro* studies. Therefore, endothelial behavior in these experiments differs considerably from that *in vivo*. *In vitro* studies of angiogenesis are highly dependent on the endothelial cell source[72-74]. As described above (Section B.1.1.), endothelial cells vary greatly with respect to position along the vascular tree, organ, and age of the donor. Functional heterogeneity of the endothelium brings about diverse findings *in vitro*[75]. Angiogenesis models should utilize endothelial cells that best resemble the context being studied. How-

ever, the technical difficulty of isolating endothelial cells from some tissues limits the selection of available endothelial cells for *in vitro* study[74]. Isolation disrupts the quiescent state of endothelial cells and induces proliferation[72-74]. Quiescence can be recovered via serum starvation[74]. The proliferative state of endothelial cells *in vitro* is short-lived in culture and endothelial cells become senescent after multiple passages[74]. Prolonged culturing of endothelial cells selects for more proliferative subpopulations[74, 75]. Isolation and culturing of endothelial cells also compromise the organotypic phenotype of endothelial cells[74]. These problems have an impact on the characterization of pro- and anti-angiogenic compounds and pathways[72,73]. Still, *in vitro* assays of endothelial cell behavior contribute greatly in advancing the current understanding of angiogenesis. *In vitro* endothelial cell assays typically assess proliferation, migration and tube formation as measures of angiogenesis[72-74].

Angiogenic sprouting involves endothelial cell proliferation and outward migration toward an external angiogenic activator. Assays that monitor proliferation of endothelial cells (ECs) in culture have the benefit of being rapid, reproducible, precise, and quantifiable. Measures of endothelial cell proliferation include increases in the endothelial cell number and progression of an endothelial cell population through a single cell cycle. Experimental designs should also account for observed decreases in cell number due to apoptosis in order to avoid mistaking the cytotoxic effect of a test substance for inhibition of proliferation. Cell number can be measured by various automated cell counters, some of which distinguish between live and dead cells. MTT assays measure metabolic reduction of MTT [3-(4,5-Dimethylthiazol-2-yl)-2,5-Diphenyltetrazolium Bromide, a yellow tetrazole, to purple formazan in cells as a measure of cell number. However, this assumes that cell metabolism primarily depends on and is roughly proportional to cell number. Changes in DNA content also provide measures of cell number. Thymidine [H^3], BrdU (Bromodeoxyuridine) and various dyes incorporate into or stain DNA, making it detectable. However, these molecules become incorporated as a result of DNA repair as well[15]. Cell cycle progression is measured by allowing incorporation of BrdU and staining with propidium iodide. Endothelial cells in G_1 stain with only propidium iodide while cells that have progressed through the S phase of the cell will stain with both propidium iodide and BrdU. However, DNA repair can inflate this readout as well. Proliferation assays typically lack a three-dimensional manifold, non-endothelial cell populations, an extracellular matrix, and blood flow (mechanical and humoral stimuli). Researchers also note the impact endothelial cell isolation and culturing has on proliferative behavior when conducting these studies. These deviations from the *in vivo* context prevent results of proliferation assays from translating to *in vivo* studies. Mechanical stimulation has been achieved by culturing cells on distendable diaphragms and in flow cells[77].

Proliferating endothelial cells in an angiogenic sprout migrate or chemotax in response to a local gradient of angiogenic stimulus. Boyden chambers position endothelial cells on one side of a filter (that contains an extracellular matrix material) and facilitate chemotaxis toward a chemoattractant on the other side of the filter. Boyden chambers and variations thereof provide fast, quantitative, three-dimensional assays of endothelial cell chemotactic migration in an extracellular matrix. Quantitation of endothelial cell migration is accomplished by measuring the number of cells that completely traverse the filter in a finite time. A concentration gradient exists in the filter. Automated counters lose accuracy by mistaking pores for cells. Recent advancements allay this error by imaging fluorescently labeled cells against an

opaque (black) filter. The high sensitivity of endothelial cell chemotaxis to the magnitude of the gradient provides the advantage of allowing detailed mechanistic analyses of angiogenesis migration. Drawbacks of the Boyden chamber migration assays include the difficult and time-consuming nature of quantitation and loss of the gradient over time. The Boyden chamber does not readily incorporate mechanical stimuli, but endothelial cell migration from a perfused and/or pressure-controlled channel into a three-dimensional collagen layer was accomplished using a microfluidic culturing platform. A two-dimensional model of endothelial cell migration in wound healing angiogenesis makes use of the scratch assay and variations thereof. In a scratch assay experimenters monitor closure of a denuded area – made in a confluent layer of endothelial cells via scratching or other means – as endothelial cells migrate into the denudation. Scratch assays are fast and allow continuous monitoring of angiogenesis. However, the extent of confluence and scratch size vary, and quantification methods are arbitrary and prone to bias errors. Use of stencils overcomes variations in scratch size (e.g., magnetically attachable stencils or MATs create a smooth, controlled denudation area)[77]. Stencils also permit application of an underlying gradient of surface bound ligands, as could advanced protein printing techniques[153].

Endothelial differentiation in angiogenesis is modeled by tube formation. Tube formation assays are conducted by placing a layer of endothelial cells on or inside an extracellular matrix (fibrin, collagen, or Matrigel) and monitoring tube formation over time. Quantitation is accomplished by counting the lengths and number of the formed tubes and the number of branch points. Tube formation assays can be two-dimensional (plating on top of a thin layer of extracellular matrix) or three-dimensional (placing cells within extracellular matrix). These assays are rapid, reliable, and sensitive to composition and mechanical properties of the extracellular matrix[74.78]. However, the tubes that form are homogeneous in length (i.e., not representative of *in vivo* angiogenesis). Quantitation of tube formation assays requires technical skill, and three-dimensional assays have the additional technical challenges of processing confocal images. Variations in seeded cell distribution and matrix composition cause variability in the results[74]. Biochemical gradients and mechanical stimuli have been incorporated into a tube forming assay using a microfluidic culturing platform[79].

A major disadvantage of *in vitro* endothelial cell assays is the exclusion of non-endothelial cell types. As described above, non-endothelial cell types play an indispensable role in angiogenesis. Therefore, results of angiogenesis studies that lack non-endothelial cell types are less likely to translate to *in vivo* studies. Non-endothelial cell types find utilization in *in vitro* angiogenesis assays in co-culture setups that allow direct contact between the different cell types (for juxtacrine signaling) or separation between the cell types (for paracrine signaling). Simply mixing or layering different cell types accomplishes direct contact between cell types. Permeable membranes (e.g., filters and hollow fibers) and layers of extracellular matrix provide a physical barrier for separating cell types. In proliferation and two-dimensional tube formation assays, non-endothelial cell types can be mixed with or layered on endothelial cells. The addition of fibroblasts, for example, promotes tube formations that contain lumen and better resemble *in vivo* angiogenesis[80]. Three-dimensional Boyden chamber migration assays incorporate non-endothelial cell types on the opposite side of the filter. Co-culturing organ specific non-endothelial cell types with endothelial cells in *in vitro* angiogenesis assays allows researchers to probe mechanism of angiogenesis that are distinct to a particular organ. Martin-Green et al. co-cultured, within the three-dimensional

tube formation assay, several cell types present in skin[149]. By doing so, they were able to recapitulate characteristics of skin tissue (e.g., production ECM and cytokines unique to skin tissue)[149]. The tubes formed in this assay better resembled microvasculature in the skin; they organized into tubes with supporting mural cells with karatinocytes and skin specific ECM surrounding[149]. Fluorescent labels are essential for distinguishing between the different cell types in cell co-culture assays. Some problems with co-culturing angiogenesis studies arise from the fact that the secretome of non-endothelial cell types is not well characterized. Biochemical gradients and mechanical stimuli have been incorporated into the aforementioned *in vitro* assays wherein multiple cell types were cultured. When suspended in collagen gels containing channels to permit perfusion, disintegrated microvascular fragments self-assembled into a network of interconnected patent vessel tubes[81]. Using microfabricated scaffolds, Liu et al were able to encourage tube formation in the direction of the structural support provided by the scaffolds[150].

Organ explant cultures provide the best *in vitro* mimic of *in vivo* angiogenesis[73, 74]. Described in detail in the following section B.2.2., organ explant cultures facilitate spontaneous angiogenic sprouting, vessel formation, and to some extent adaptation to local needs from a slice or piece of vasculature or bone cultured in an extracellular matrix material. Organ explant cultures feature near-physiological spatial arrangements of multiple cell types and extracellular materials, and isolation of the tissues does not alter the proliferative state (e.g., quiescence) of the endothelial cells. Such assays typically lack the gradient of angiogenic stimuli and the mechanical/humoral influence of local blood flow that occur *in vivo*. Some limitations include the assays' requirement for growth serum, variability between animals, and difficulty of quantification. The sensitivity and applicability of organ explant assays have not been proven[74].

In vivo angiogenesis assays

In vivo angiogenesis assays, i.e., experiments utilizing an entire organism to model angiogenic behavior, present a fully intact and functional angiogenic process that acts alongside a complete set of processes maintaining the state of the organism. *In vivo* models of angiogenesis carry out all the steps of angiogenesis and vessel maturation to produce fully functional vascular networks or vessels characteristic of certain disease states. In contrast, *in vitro* angiogenesis assays do not produce vascular sprouts capable of accommodating blood flow or carrying out other functions of the microvasculature. The completeness of the angiogenic process in *in vivo* angiogenesis assays makes its response to an experimental condition strongly predictive of angiogenic behavior in humans. *In vivo* angiogenesis assays typically investigate drug effects on angiogenesis and validate observation about the molecular mechanisms of angiogenesis from *in vitro* studies. The reliability or translatability of *in vivo* angiogenesis assays comes at the expense of precision and access to individual functional components of the angiogenic process. Precise measurement and control of experimental conditions in and around a test site within the model organism are often not possible. *In vivo* angiogenesis assays typically restrict experimentation to sites within a few hundred microns of the surface of the organism. More internal sites of angiogenesis lie outside the range of commonly utilized imaging technologies, and access therefore requires less precise, indirect measures of angiogenesis. Measurement of internal angiogenesis often requires *post hoc* explanting, sectioning, and staining of the test site (making repeated/time-course imaging impossible). The

angiogenic response of an *in vivo* angiogenesis assay to an experimental condition or test substance is subject to influences (noise) from other processes also functioning to maintain the state of the organism. A common example involves disturbances due to irritation or inflammation caused by the route of administration of the test substance. Metabolic depletion, diffusion, and drainage from the test site and dilution in the peripheral blood of a test substance make its concentration and spatial distribution difficult to control and maintain. Genetic engineering of cells and organisms provides a powerful means of elucidating the mechanisms of angiogenesis. However, genetic engineering *in vivo* presents a limitation in that it compromises the viability of the organism. Mechanical stimuli (e.g., tensional forces, pressure, and shear stress) are difficult to control in isolation from other variables affecting angiogenesis. Problems with precision and control in *in vivo* angiogenesis assays make several mechanisms of angiogenesis difficult or impossible to investigate *in vivo*. Researchers have designed assays that harness the strengths of *in vivo* angiogenesis models while overcoming one or more of the aforementioned limitations. As a result, *in vivo* angiogenesis assays have proven indispensable to furthering the current understanding of angiogenesis and the development of angiogenic therapies.

Because of their simplicity of use and lack of immune response to exogenous cells and tissues, the chick chorioallantoic membrane (CAM) assay has become the most utilized *in vivo* angiogenesis assay[74, 82]. In the chick embryo, a change in vascular density in and around a test site on the CAM results from the topical or intravenous addition of test substances to the CAM. This change in vascularization implies an effect on the angiogenesis. Test substances include soluble angiogenic growth factors, angiogenic inhibitors, tumor cells, and tissues. Encapsulation or immobilization of the test substance in polymer pellets, gelatin sponges, and air-dried filters accomplishes slowed or controlled release of the test substance. The chick CAM assay can be conducted *in ovo* with the test substance added to the CAM through a small hole cut into the shell of the chick's egg, or *ex ovo,* where the entire embryo and CAM are cultured outside of the shell[72,74,15,151,152]. *In ovo* experiments require less maintenance, and angiogenesis can be tracked through the later stages of embryo development. *Ex ovo* models permit repeated administration of the test substances, repeated time-course imaging, and multiple test sites per embryo. Angiogenesis is measured visually by counting vessels or semi-quantitatively by scoring vascular density. Dyes and fluorescent micro- and nanoparticles injected into the vasculature better resolve the sprouts and identify patent vessels. Biomolecular analysis of angiogenesis or cell-vasculature interaction can be accomplished via RNA and protein extraction. The chick CAM is simple, scalable, and allows repeated/time-course imaging. Pre-existing vasculature on the CAM makes quantitation of angiogenesis difficult. For example, small vessels initially overlooked may widen and become visible during the course of the experiment and could be mistaken for neovascularization. The chick embryo lacks an immune system until day 7-8 in culture, which allows administration of exogenous cells and tissues[73]. However, it should be considered when interpreting data that developmental angiogenesis occurs until day 11 in culture[74]. Chemical and physical irritation of the CAM elicits an inflammatory response which gives rise to angiogenic cytokines.

The zebrafish model of angiogenesis provides a powerful and inexpensive *in vivo* screening of angiogenesis stimulators and inhibitors. One mating can produce over 200 embryos. Zebrafish angiogenesis assays are conducted by injecting a biomolecular test substance into the yolk sac of a zebrafish embryo.

Conveniently, lipophilic test substances added to the water can freely diffuse into the embryos. Utilization of mutagens and antisense morpholinos facilitates genetic engineering of the zebrafish model for investigating the molecular mechanism of angiogenesis. The fact that zebrafish embryos develop outside the mother and are transparent allows researchers to measure angiogenesis via visual inspection. Patent vasculature is visualized via injection of fluorescent dye, quantum dots, or microspheres, followed by confocal microscopy and image reconstruction[83]. Transgenic zebrafish with GFP-labeled endothelial markers (Fli-GFP, mTie2-GFP, and Flk-GFP) grow fluorescent vasculature which eases visualization. When using fluorescently labeled zebrafish, however, researchers consider that the GFP-labeled markers may confer fluorescence to non-endothelial cell types (e.g., Fli-GFP is also expressed in the neural crest)[74]. A Fli-GFP::GATA-dsRED zebrafish exists with green-labeled endothelium and red-labeled erythrocytes, which allows differentiation between nonfunctional and patent vessel formation[74]. The zebrafish angiogenesis assay is inexpensive, scalable, rapid, and quantifiable via imaging, but there are some drawbacks. The relevance of angiogenesis in the zebrafish embryo as a model of angiogenesis in human adults has been questioned. In the zebrafish assay, neovascularization results from vasculogenesis and angiogenesis. Distinguishing between the two is difficult. Regions that participate only in angiogenesis are debated, but angiogenesis is accepted to occur in the subintestinal vein.

Once considered the “gold standard” assay of angiogenesis, the cornea angiogenesis assay features angiogenesis from mammalian vasculature, which better represents angiogenesis in humans[72,74]. Cornea angiogenesis assays are conducted by cutting a pocket into the corneal stroma of a mouse, rat, rabbit, etc., and implanting into it a test substance (e.g., tumor (or other) tissue or cells, conditioned media, growth factors, etc.). To overcome the difficulty of controllably delivering the test substance to the corneal pocket, various slow-release polymer pellets have been employed[72,74]. Angiogenesis can also occur in response to injury to the cornea, delivered via chemical cauterization or mechanical scraping. Quantification or analysis of the angiogenic response is accomplished visually, by explanting the cornea and counting the number of vessels and measuring the length, caliber, or density of the new vessels. The corneal angiogenesis assay is reliable and quantifiable. Genetic engineering in mice allows investigation of the molecular mechanisms of angiogenesis using the cornea angiogenesis assay. The initially avascular cornea permits a low background measurement of angiogenesis. However, researchers question the relevance of ectopic angiogenesis into the normally avascular cornea[74]. The cornea is a two-dimensional environment for angiogenesis, while human angiogenesis typically occurs in three dimensions. Other limitations of the assay include that it is time-consuming, expensive, and technically demanding to run (more so in smaller mammals). Angiogenesis in this assay is not amenable to repeated or time-course imaging. There also exist ethical qualms regarding the invasive use of a major sensory organ.

In vivo matrix invasion assays facilitate mammalian angiogenesis in a natural extracellular matrix biomaterial (e.g., Matrigel)[84]. Such assays are performed by injecting Matrigel (which gels into a plug upon injection) or implanting a polymer scaffold subcutaneously in the mouse, rat, or rabbit, then monitoring for angiogenic ingrowth. Synthetic sponge matrices, composed of polyvinyl acid, polyethylene, or polyurethane, have been utilized in the matrix invasion assays as a scaffold. The Matrigel plug or scaffold material typically contains a test substance (e.g., growth factor, cells, tumor, and tissue explant). Measurements of angiogenesis occur at the end of the assay, when the matrix material plug or scaffold material

is explanted, sectioned, and stained for endothelial markers. The hemoglobin content in the matrix material or scaffold provides an indirect measure of angiogenesis, but may become inflated by deposition of hemoglobin due to hemorrhaging. Starting with a defined matrix material background allows researchers to investigate *in vivo* the interaction between the extracellular matrix and angiogenesis. Measurements of matrix metabolism and deposition are possible in this assay. The amount of fibrovascular tissue in the matrix plug indicates neovascularization via wound healing. Cell proliferation and macrophage innervation can also be monitored. Quantitation of neovascularization is helped by the fact that the Matrigel and scaffold implants are initially avascular. Initial concentrations of a test substance in the Matrigel plug or scaffold implant can be precisely controlled. The mammalian microenvironment in which the assay takes place makes it relevant to angiogenesis in humans. However, the injection of Matrigel creates an undefined geometry that contributes to variability in the results of the assay[74]. To overcome this limitation, polymer scaffolds and sponges with defined geometries are implanted. This approach utilizes unnatural polymers, and the rigid shape of the implant elicits an inflammatory response which produces angiogenic cytokines. An alternate approach utilizes Matrigel injected into a polymer container (with defined shape) then implanted, providing a natural matrix material, although one still subject to inflammation[85]. Other limitations of the assay include the difficult and time-consuming nature of quantitation. The measurement of angiogenesis in this assay is destructive and repeated/time-course measurements are not possible. The assay is also expensive, and angiogenesis that occurs in the assay is strongly sensitive to the shape, material, rigidity, porosity, etc. of the Matrigel plug or scaffold material implant.

The dorsal air sac model of angiogenesis is constructed by lifting the dorsal skin on a mouse, injecting air, and implanting a chamber through a transverse section cut on the back[86]. The chamber is loaded with a test substance such as tumor tissue or cells or angiogenic cytokines. The angiogenesis response is assessed upon explantation of the chamber by counting the newly formed vessels. In this approach, it is difficult to distinguish neovascularization from the pre-existing vasculature. Indirect measures of angiogenesis are accomplished by injecting dye or ^{51}Cr erythrocytes into the mouse and measuring the volume of dye or ^{51}Cr that accumulates in the chamber. This assay is simple, amenable to genetic engineering, and permits facile administration of the test substance. However, the dorsal air sac assay is difficult to quantitate and does not permit repeated or time-course measurement of angiogenesis.

Efforts to overcome these limitations resulted in the use of chamber assays. Chamber assays are prepared by assembling a chamber around a region of thin tissue (e.g., rabbit or mouse ear, and dorsal skinfold). The chamber is typically loaded with a test substance (e.g., tumor (or other) tissue or cells, growth factors, cytokines, and angiogenic inhibitors). The thinness of the tissue inside the chamber allows repeated/time-course measurements of angiogenesis to be performed visually via translumination. Vessel density and diameter are measures of angiogenesis utilized in the chamber assay. Injection of fluorescent dyes allows nonfunctional and patent vasculature to be distinguished and can be used to measure vascular permeability. Transgenic mice expressing GFP-labeled proteins are employed to analyze gene expression during the angiogenic process. A significant advantage of the chamber assay is that it allows repeated measurements on a mammalian model of angiogenesis. Windows implanted into the cranial bone or across the mouse femur window allow visualization of angiogenesis in organotypic sites (the

brain and femur). The chamber assay and dorsal air sac assays are reliable and amenable to genetic engineering; however, they are prone to irritation from the surgery and implant. As a result angiogenesis is subject to influences (noise) from cytokines released by inflammatory and wound healing responses to the surgery. The assay is also expensive, difficult, and invasive.

In vivo models of pathological angiogenesis include tumor mouse models and premature and diabetic retinopathy models, and rheumatoid arthritis mouse models[74, 87-89]. These models incorporate test substances or conditions that establish, within the model, aspects and symptoms of the disease being investigated. For instance, tumors form via excessive cell proliferation that occurs as a result of mutations that relinquish proliferative control of the cell. Avascular tumors grow until they encounter a size limitation where oxygen, metabolites, and wastes no longer adequately transfer to and from all the regions of the tumor. Some tumor types form avascular dormant lesions where cell proliferation rates match cell apoptosis rates[90]. Tumor growth and progression beyond this size limitation and into subsequent pathological stages rely heavily on angiogenic neovascularization of the tumor. Vascularization permits further growth of the tumor and provides the route by which tumor cells metastasize into the rest of the body. The dependence of tumors on vascularization and angiogenesis, combined with the fact that an epigenetically homogeneous vascular endothelium (relative to tumors) is more amenable to growth inhibition than are tumor cells, attracts research interests in therapies that target angiogenesis in the treatment of cancer (e.g., Bevacizumab). Investigation of tumor angiogenesis generally involves direct/indirect incorporation of tumor cells, tumor tissue, or conditioned media to the *in vitro* and *in vivo* assays described in this section. Mouse tumor angiogenesis assays are conducted by subcutaneously implanting a tumor, injecting tumor cells orthotopically, or utilizing transgenic mice that overexpress a particular oncogene. Quantitation of angiogenesis occurs after explanting the tumor. The tumor is sectioned and stained for endothelial markers, then scored for extents of angiogenesis, tumor size, etc. Subcutaneous implantation, though easy, does not create the tumor microenvironment representative of tumorigenesis in humans. Orthotopic injection of tumor cells overcomes this limitation but is harder to perform. Transgenic oncogene overexpressing mice typically form and vascularize tumors at about the same age. This allows analysis of the angiogenic response to test substances. Quantitation of this assay is time-consuming and difficult, and hence prohibitive for repeated measurements. The use of fluorescently labeled tumor cells in the nude mouse (i.e., AngioMouse®) allows repeated non-invasive measurements of tumor size and observation of metastases[96]. Quantitation of angiogenesis is accomplished by imaging. Under stereo microscopy, non-fluorescent vessels appear as dark networks against a green background[73]. Use of GFP fluorescently labeled mice (e.g., Flk-eGFP) with RFP-labeled tumors allows further analysis of tumor-host interactions. Monitoring tumor angiogenesis via fluorescence suffers the limitation that light absorption and scattering by the tissue and skin reduce the image resolution. Tumor cell expression of GFP decreases in hypoxia, thereby influencing quantitation[74].

Table B.1. Angiogenesis Assays			
Assay	**Description**	**Uses**	**References**
In Vitro Cell Proliferation Assay	Measure EC proliferation at baseline or in the presence of angiogenic factors.	Investigate effect of test substance on angiogenic initiation (specifically EC proliferation). Investigate the molecular mechanisms of EC proliferation.	74,
In Vitro Migration Assay	Scratch assay; ECs migrate across a 2D denuded area. Boyden chamber assay with ECs migrating across a filter/matrix within a gradient of angiogenic factor.	Investigate molecular mechanisms of EC chemotaxis, wound healing.	74, 92,
In Vitro Tube Formation Assay	ECs plated on 2D or in 3D matrices and quantification of a representative measure of tubule formation.	Investigate effect of test substance on EC differentiation as marked by tube formation. Investigate *in vitro* angiogenic potential.	40,
Organ Explant Assays	Segments of vessels cultured in 3D matrices are monitored for angiogenic outgrowth.	Investigate effect of test substance on angiogenesis. Investigate the molecular mechanisms of angiogenic sprouting, vessel formation, and regression.	73-74, 93, 94
Chorioallantoic Membrane Assay (CAM)	Test substances (e.g., xenograft material, cell, or tissue) are applied on or within the CAM, in order to continuously monitor local angiogenesis.	Investigate the effect of test substances on angiogenesis. Investigate the interaction between CAM vasculature and the test substance.	72-74, 82
In vivo Matrix Invasion Assay	Test substances (e.g., xenograft material, tissue, cell, cytokine, or small molecule) are loaded into Matrigel or matrix containing polymer scaffold. The Matrigel or polymer scaffold is loaded subcutaneously. Explanted Matrigel plugs or polymer scaffolds are evaluated for invasion of angiogenic sprouts post-hoc.	Investigate the effect of test substances on angiogenesis. Investigate the molecular mechanisms of angiogenic sprouting, vessel formation, regression, and stabilization.	72-74, 84

Table B.1. Angiogenesis Assays (Continued)			
Assay	**Description**	**Uses**	**Cited**
Retinopathy of Prematurity Model	Retinopathy is induced in neonatal mammals by exposure to hyperoxia followed by normoxia. Explanted retina are evaluated for angiogenesis *post hoc*.	Investigate the effect of test substances on angiogenesis in retinopathy. Investigate the molecular mechanisms of angiogenic sprouting, vessel formation, regression, and stabilization in retinopathy.	87
Fluorescent Zebrafish Assay	Live transgenic fluorescent embryo is exposed to small molecule angiogenic inhibitors and extent of angiogenesis is measured via fluorescence confocal imaging.	Investigate the effect of test substances on angiogenesis. Investigate the molecular mechanisms of angiogenic sprouting, vessel formation, regression, and stabilization.	83, 95,
Dorsal Air Sac Model and Chamber Assay	A chamber is implanted across dorsal skin of the mouse, or (in some chamber assays) across thin layers of tissue (e.g., the ear or mouse femur). Test substances are introduced in the chamber. Local angiogenesis is measured *post hoc* (dorsal air sac model) and throughout the experiment (chamber assay).	Investigate the effect of test substances on angiogenesis. Investigate the molecular mechanisms of angiogenic sprouting, vessel formation, regression, and stabilization.	74, 86
Tumor Mouse Model	Fluorescent tumor cells are implanted subcutaneously in nude mice. Other test substances are administered as well. Vascularization and growth of the tumor is monitored throughout the experiment, as well as occurrence of metastases.	Investigate the molecular mechanisms of tumor angiogenic sprouting, vessel formation, regression, and stabilization. Investigate tumor-host interaction.	74, 91, 96

B.2.2. Aortic Ring Assay and Other Organ Explant Angiogenesis Assays

In 1982, Roberto Nicosia's lab published its first observation of spontaneous angiogenic outgrowth from a rat aorta *in vitro*[97]. From this observation, the aortic ring assay and other organ explant assays arose and have since developed into the most complete *in vitro* mimic of *in vivo* angiogenesis[72-74]. Table B.2. lists organ explants that are utilized as a platform for studying angiogenesis. In a vascular explant assay, the explanted vessel is carefully cleaned of surrounding fibroadipose tissue, cut into 1 mm slices, and imbedded in collagen, fibrin, or Matrigel[93, 94,] . With culturing in media (some vascular explants do not require media with serum) vascular outgrowths spontaneously occur from the vascular explant[93]. Other

organ explant cultures are performed similarly. Organ explant assays provide a convenient, cost-effective, reliable way to investigate the mechanisms of angiogenesis and the effects of test substances (e.g., potential therapeutic agents) on angiogenesis[72-74]. Qualities that define these assays as *in vitro* mimics of *in vivo* angiogenesis include the near-physiological spatial organization of endothelial and non-endothelial cell types, paracrine and juxtacrine signals, and endogenous matrix materials[72-74, 93]. Organ explant assays permit the study of more of the "steps" of angiogenesis than any other *in vitro* assay[73, 93]. Endothelial cells in vascular explants retain their endogenous quiescent phenotype after explanting, a feature that allows investigation of aniogenesis initiation[72-74,]. Vascular sprouts originating from an organ explant contain lumen, supporting pericytes, and basement membrane. Considered essentially the same as capillary sprouts arising from angiogenesis *in vivo*, these vessels feature nearly all the functional similarities to those *in vivo* except vascular maturation brought on by blood flow[93].

Angiogenic outgrowth from a vascular explant is typically analyzed via visual inspection[93]. The number of sprouts resulting from a vascular explant provides a measure of the extent of angiogenesis[93]. Vascular sprouts can be counted manually or using image processing software. The count includes vessels appearing at different depths in the sample via focusing[93]. The number of branch points in the outgrowth also provides a useful measure of the extent of angiogenesis[74]. A more rapid quantitation of the extent of angiogenesis comes from measuring, via image processing software, the area covered by the angiogenic outgrowth[74]. Quantitation of the organ explant assay is non-standard, difficult, and subject to bias, and is a limitation of the assay. Vessel maturity is assessed by the number of pericytes lining the vessel and by the vessel caliber[74, 93]. Whole mount immunostaining of the angiogenic sprouts is possible in vascular explants cultured in a 0.5 mm layer of collagen[98]. RNA and protein isolation from angiogenic sprouts allows biomolecular analysis of nascent sprouts, but multiple samples are often required to yield an analyzable amount of RNA or protein.

Table B.2. Organs used in the vascular explant assay

Vessel Type[28]	Species
Aorta	Rat, Mouse, Chick, Rabbit, Cow, Dog, Human
Carotid Artery	Rat, Pig, Cow
Saphenous Vein	Human
Vena cava	Rat
Thoracic Duct	Rat, Mouse
Fetal Metatarsals	Mouse
Placental Vein	Rat, Mouse

Organ explant assays offer several advantages in angiogenesis research because they readily combine the capabilities of common *in vitro* and *in vivo* angiogenesis assays[93]. The native endothelial phenotype retained in organ explant assays allows researchers to study *in vitro* the early steps of angiogenesis initiation[72-74, 93]. The presence of non-endothelial cell types supplies the complex signaling events necessary to carry out the steps of angiogenesis[72-74, 93]. The near-physiological spatial organization of endothelial and subjacent non-endothelial cell types and extracellular matrices provides a strong representation of *in vivo* angiogenesis[72-74, 93]. Organ explant assays lack confounding variables that influence *in vivo* studies, such as inflammation, hemostasis, and uncontrolled blood flow[93].

Limitations of organ explant assays in angiogenesis research include the use of vascular explants that poorly represent the microvasculature (where angiogenesis occurs), the difficulty of quantitation, and variability in the results. Described in section A.1.1., notable differences in the morphology and function of endothelial cells exist between the microvasculature, which participates in angiogenesis *in vivo*, and

larger arteries, which do not. In consideration of this, researchers have cultured the mouse and rat vena cava, placental vein, chick embryonic aortic arch, and mouse embryonic metatarsals[73]. Veins bear more similarities to the microvasculature than do arteries. Embryonic vessels are more similar to the microvasculature than veins in postnates. However, these tissues are harder to isolate, and differences between them and the microvasculature still exist. Mouse embryonic metatarsals contain plugs of highly vascularized marrow tissue. Angiogenic outgrowths from the fetal metatarsals sprout from the microvasculature. However, embryonic endothelial cells are actively proliferating while adult microvascular endothelial cells are not. Human vessels are difficult to acquire. As a result, organ explant assays cannot fully represent angiogenesis *in vivo* in humans. As discussed above, quantitation of angiogenesis in the organ explant assays is difficult and prone to error. Variability in angiogenesis in the organ explant cultures arises from variability in the matrix and serum utilized in the assay and the difference between animals utilized in the study. While the rat aortic ring will spontaneously produce angiogenic sprouts, the mouse aortic ring and several other vascular explants require serum, whose protein content is not completely defined[74, 93]. Exposure of the organ explant to subphysiological temperature and alkalinity arising from low carbon dioxide pressures during preparation of the organ explant assay impedes angiogenesis and may give rise to variations in the results of the assay[94]. Variations between organ explants from the same animal are small compared to variations between animals. In mice, for example, age and genetic background strongly influence the results of the organ explant assay[99]. Provided the variations in endothelial phenotype along the vascular tree, discrepancies in the results between studies may arise from differences in the vessel type utilized[100].

While other animals are utilized, the mouse model provides advantages which have popularized its use in organ explant assays. The mouse genome has been sequenced, and its human homologues have been identified[99]. A repository of transgenic and knockout mice is readily available. Genetic background influences the amount of angiogenic outgrowth in the assay, with C57 mouse aortic rings producing more angiogenic sprouts in culture than aortas from other mouse strains[99]. The smaller size of aortic rings retrieved from mice necessitates the use of serum in aortic ring assays[101].

Organ explant cultures are tenable to adjustments that permit detailed investigation of the mechanisms of angiogenesis and overcome some limitations of common organ assays. Organ explants produce angiogenic sprouts in response, in part, to wound healing mechanisms induced during explanting. When investigating some mechanisms of ischemia-induced angiogenesis in the organ explant assay, researchers may halt the wound healing response by inducing an “angiogenically quiescent state” wherein the aorta no longer spontaneously produces angiogenic sprouts. Suspending the rat aorta in media without serum for 14 days induces an angiogenically quiescent state capable of identifying initiators and enhancers of angiogenesis from the set of ischemia- (or other process)-induced angiogenic cytokines[33]. Angiogenic initiators (e.g., VEGF) induce angiogenesis in angiogenically quiescent aortic rings, but angiogenic enhancers (e.g., Ang-2) alone do not induce sprouting in this model. Genetic manipulation of vascular explants can be accomplished via gene transduction via virus prior to embedding in matrix[104]. Electroporation of DNA plasmids through the matrix containing the vascular explant accomplishes genetic manipulation of vascular explants in culture[102]. The cellular composition of vascular explants can be tractably controlled. For example, the use of liposomal clondronate, which is selectively cytotoxic to mi-

crophages, ablates them from vascular explants assays[101]. The vascular explant assay has also accommodated direct and indirect addition of organ-specific non-endothelial cell types (e.g., microglial) using techniques employed in *in vitro* co-culture assays[103]. Co-culturing the rat aortic and vena cava rings produced more mature vascular sprouts than either of the vascular explants alone and with arterial/venous anastomoses[100]. Significant limitations of conventional vascular explant assay are the lack of a maintained external gradient and the lack of mechanical stimuli (e.g., intraluminal blood flow). Occurring *in vivo*, these phenomena have an impact on angiogenesis, and researchers recognize the importance of studying their effect on angiogenesis *in vitro*. Researchers have used microfluidic devices to enhance the vascular explant assay by imposing a defined exogenous concentration gradient around the vascular explant[105]. Perfusion of vascular explants has been accomplished in the short term as a way to analyze the extent of functional angiogenesis *in vivo* and to investigate vascular tone of resistance arteries. Short-term perfusion of an intact mouse resistance artery was accomplished by fixing the artery within a microfluidic device and perfusing the lumen and abluminal space with media[106]. Long-term culture of perfused rabbit and porcine thoracic aorta was carried out in efforts to study arteriogenesis[18, 19]. These techniques, however, maintain the artery in a fluidic bath (in the abluminal space) that does not permit angiogenesis. The perfused organ cultures utilized in arteriogenesis studies are carried out in reactors that position the aorta beyond the working distance of optical microscopes. These reactors rely on vessels dissected from larger animals that are not amenable to genetic manipulation. To my knowledge, long-term perfusion of a vascular explant (i.e., allowing angiogenic outgrowth) has not been accomplished.

B.2.3. Mechanical Stimulation in Angiogenesis Assays

Angiogenesis is a mechanical process. As cells carry out the steps of angiogenesis (proliferation, migration, etc.), they interact mechanically with their surroundings. The growing cells exert forces on the ECM, which presents opposing forces that resist the generated forces of and provide traction to motile cells. Adjacent and nearby cells answer these mechanical perturbations by generating their own forces. Meanwhile, the chemical processes that drive much of angiogenesis act and cooperate with the mechanical processes. Information conveyed via mechanical force gets transduced and relayed throughout the tissue via mechanochemical signaling pathways. This information ultimately directs angiogenic behavior. Angiogenesis responds to mechanical cues, thus aberrant mechanical stimulation of endothelial cells is a hallmark of many diseases, including those that influence angiogenesis (e.g., hypertension). Unfortunately, there exists a dearth of information about the influence of mechanical forces and signals on angiogenesis. Few *in vitro* assays currently permit detailed study of the effect of mechanical stimulation on the later steps of angiogenesis. *In vivo* angiogenesis assays offer only limited control over the mechanical forces acting on the endothelium. Researchers are working to expand the selection of assays that allow investigation of mechanical signaling in angiogenesis. The following describes ways in which researchers have incorporated controlled mechanical stimulation in angiogenesis assays.

The cells and supporting extracellular matrix materials that compose a tissue exhibit a range of mechanical properties. Tissues passively (i.e., without expending metabolic energy) respond to an applied force

or physical deformation according to their viscoelastic properties. Viscoelasticity is the property of tissues that causes them to initially deform or strain under an applied force and then gradually strain or creep further as long as the force is applied. The deformed tissue also relaxes so that the amount of force needed to maintain the deformed state gradually diminishes. The Maxwell, Kelvin-Voigt, and standard linear models of viscoelastic deformation approximate the passive mechanical behavior of biological materials[107]. Extracellular materials can only produce a passive response to mechanical forces, but cells can respond passively or actively (i.e., utilizing metabolic energy in their response). Cells involved in angiogenesis sense local deformations and stresses in their surroundings. In response, they may apply tension and compression on subjacent cells, the entire vessel and/or their surroundings. Such actions are responsible for vasoconstriction and dilation of arterial vessels and endothelial, mural, and smooth muscle cell migration in angiogenesis. The mechanical forces that act in angiogenesis include compression and tension, shearing and bending of pliable tissues, and flow-induced hydrostatic pressure and shear stress[108, 109].

The introduction of a mechanical stimulus or the measurement of mechanical changes in an angiogenesis assay entails three heavily interdependent actions: the application of exogenous force or deformation, the passive response of pliable extracellular matrix materials, and the cell-mediated endogenous force generation in reaction to the study conditions. Studies of mechanotransduction in angiogenesis seek to isolate and precisely control and/or measure one of these three actions. As with conventional angiogenesis assays, assays that incorporate mechanical stimulation trade precision and control for maintenance of a relevant biological context. The long-established and highly quantitative laws of continuum mechanics make mechanical process more amenable to precise measurement and control than many biomolecular processes. For example, devices exist that measure the forces acting on and generated by biological materials with pico-Newton sensitivity[110]. Attaining such high precision and sensitivity requires *in vitro* assays that remove several features of the cells' endogenous environment, and they are therefore poorly representative of *in vivo* biology. In contrast, *in vivo* assays are more relevant to biological processes in humans, but *in vivo* mechanical stimulation and measurement methods are rare and seldom quantitative.

In vitro mechanotransduction assays apply a mechanical stimulus to or measure mechanical properties of a single cell or a two-dimensional cell monolayer. Micro- and nano-scale BioMEMS (biological microelectrical/mechanical system) devices make possible the isolation and study of the mechanics of single cells with pico-Newton precision. Addae-Mensah and Wikswo review measurement techniques using BioMEMS, while Desmaele and coworkers review actuation techniques using BioMEMS[110, 111]. The small volumes utilized by BioMEMS devices allay solute dilution, thereby allowing detection of rare mechanochemical conversion. One drawback of BioMEMS is that it can be time-consuming to load BioMEMS devices. Mechanical stimuli delivered to two-dimensional cell cultures include compression or hydrostatic loading, distension, and fluid shear stress[76]. Hydrostatic loading of cells in two-dimensional culture is accomplished by culturing the cells under a controlled pressure. A two-dimensional cell monolayer with overlying cell culture media can be incubated in a container pressurized with air and 5% CO_2. This simple procedure provides quantitative homogeneous, temporally controlled application of pressure to the cells. However pressurization of the incubator air increases the partial pressures of oxygen and carbon

dioxide beyond their physiological concentrations. Also, purely hydrostatic loading (i.e., in the absence of shear or tensional stresses) does not well represent the physiology being modeled. Culturing cells on a flexible polymer substrate or diaphragm and applying tension to the substrate or diaphragm accomplish controlled distension of a cell monolayer. Pressure differences across the diaphragm or platen abutments are commonly utilized means of distending the cell monolayer. Platen abutment techniques have been miniaturized for use in BioMEMs[110]. Various directionalities of distension are accessible; these include in-plane longitudinal, biaxial, radial tension and out-of-plane longitudinal bending, and radial curvilinear and irregular shaped distension[76]. This simple and controllable procedure provides a quantitative mechanical stimulus that is relevant to physiological situations. The technology suffers limitations, however, of anisotropy and spatial heterogeneity of distension. This is more so along the edge of the culture, where the flexible polymer connects to rigid walls of the culturing dish. Movement of the diaphragm also causes movement of the overlying cell culture media, thereby introducing uncontrolled shear and normal stresses to the assay[112]. Application of a fluid shear stress to cells in a monolayer commonly utilizes one of two techniques. A cell monolayer is positioned beneath a cone whose central axis is perpendicular to the plane of the cell culture. The cone rotates around its central axis, providing roughly spatially uniform (because of its conical shape) shear stress to the underlying cell culture. This technique, though simple and spatially homogeneous, is cumbersome when imaging the cells. Alternatively, laminar flow is maintained in a parallel plate flow chamber. Pumps or gravity drive fluid flow. Cells cultured on the floor of the chamber experience controlled shear stress. Flow chambers have been miniaturized for use in BioMEMS[110, 111]. Cell monolayers established on the inside walls of cylindrical tubes (e.g., glass capillary tubes) have provided a more physiological geometry for studying fluid shear stress[113]. Flow chambers offer simple, quantitative delivery of controlled shear stress. Transient shear stresses and media sampling and exchange are also possible in flow chambers. Parallel plate flow chambers are also easy to image. However, the edges of the parallel plate flow chamber make shear stress spatially nonuniform. Considering that mechanical stimuli rarely act in isolation, researchers have designed ways to controllably deliver, simultaneously, multiple mechanical stimuli[76]. For example, laminar flow over cells cultured in a flexible cylindrical tube provides controlled application of distension and shear stress. A pressure gradient down the axis of the cylindrical flow chamber drives flow, while a pressure difference across the flexible wall of the flow chamber actuates distention. Both mechanical stimuli can be controlled separately from each other.

Two-dimensional biological assays lack several aspects of the environments they model. Concomitantly, two-dimensional angiogenesis assays do not recapitulate many steps of the angiogenic process. Three-dimensional angiogenic cell and tissue cultures better represent angiogenesis in humans and model more of the angiogenic process. Researchers and engineers have designed strategies for incorporating mechanical stimuli into three-dimensional cell cultures. Cells in a three-dimensional matrix material generate forces that mechanically deform their surroundings[117]. Deformations, measured by clamping a matrix between a fixed boundary and a force gauge, provide a semi-quantitative assessment of force generation by a collection of cells[114, 115]. More precise measurement of forces generated by cells in a matrix material requires detailed imaging of matrix strain along three axes and computational modeling local force generation using the finite element method[116]. Measurements of cell mechanics in three-dimensional culture are semi-quantitative or they are time-consuming and complicated. Variability re-

sulting from non-uniform cell seeding and heterogeneous matrix properties also affects the quality of the measurement[117]. Current techniques do not permit measurement of force generation by individual cells in three-dimensional culture.

Static and dynamic compression of tissues, cells, and extracellular matrix material is accomplished via platen abutment [76]. Such compression can be unconfined (i.e., space is provided for the material to spread out under the platen) or confined (i.e., walls prevent spreading and the deformation decreases the specimen's volume). Compression of three-dimensional cultures better mimics instances of compression *in vivo*. However, anisotropy and heterogeneity of the surrounding matrix make the delivery of compressive stress to cells less precise and controllable. Commercially available devices (e.g., the Flexcell®Tissue train® culture system) apply tension or distension to three-dimensional cultures by placing them inside a flexible mold or on a flexible diaphragm. The mold or diaphragm is equipped with mesh-like anchors along the periphery which maintain attachment to the tissue. Bioreactors have been engineered to apply tension or distension to tissues and extracellular matrices while permitting imaging. These bioreactors apply tension or strain by clamping thin sheet-like constructs or fibers of extracellular matrix material (e.g., collagen) between two moveable connectors[118]. Attachment or clamping of the matrix is non-uniform and subject to variability, and the strength of the attachment can decrease with time.

The interstitial matrix materials surrounding microvasculature accommodate Darcy's Law flow. *In vitro* perfusion of the matrix materials mimics Darcy's Law or Starling flow in the interstitium. Controlled perfusion of matrix materials is accomplished by placing the matrix against a supporting micropore filter and maintaining a pressure difference across the filter[119]. The filter permits flow of cell culture media through the matrix while resisting deformation and displacement of the matrix. Tein and colleagues applied fluid shear stress to endothelial cells in collagen. A perfusable tube was cast into collagen and seeded along its walls with endothelial cells. This setup mimics the microvascular geometry while providing a biologically relevant extracellular substrate. However, fluid shear stress is difficult to isolate from other mechanical stimuli. The soft material substratum can deform under the pressure driving perfusion, which causes distension of the cell layer and introduces spatial heterogeneities of flow. Darcy's Law flow of perfusate through underlying collagen substratum accompanies perfusion of a tube cast into extracellular matrix material[120]. This extraluminal flow mimics a property of interstitial tissue surrounding the microvasculature but also introduces variability. Spatial-temporal control of the mechanical stimuli is complicated by changes undergone by the matrix as a result of angiogenesis.

Angiogenesis studies often consider the interaction of multiple cell types. Fluid shear stress can be added to a study of the interaction between multiple cell and extracellular matrix types. For example, Hoying and colleagues cast hollow tubes into collagen doped with disintegrated microvasculature[81]. Upon culturing and perfusion of the collagen tube, a network of patent vascular tube was assembled. This setup allows the most biologically relevant application of fluid shear stress *in vitro* currently available. Endothelial cells are immediately juxtaposed to physiologically relevant cell and matrix materials. However, the device does not accommodate imaging, and the initiation of angiogenesis in the device occurs in separation from flow. Three-dimensional mechanotransduction-angiogenesis assays recapitulate more

steps of angiogenesis under more biologically representative applied mechanical stimuli, but at the cost of precise control of the mechanical stimuli. Three-dimensional assays contain a deformable, perfusable, anisotropic and heterogeneous extracellular matrix material which introduces several sources of variability. Deformation of the extracellular matrix shields the cells from the applied mechanical stimuli. Pressure differences that drive perfusion also deform the matrix material, and matrix deformation has an impact on matrix perfusion. Perfusion and deformation, whether intended or not, vary with the anisotropic and heterogeneous nature of the matrix. As a result, some three-dimensional mechanotransduction assays yield only semi-quantitative information. Despite these limitations, three-dimensional assays have a place in biological research because two-dimensional assays cannot mimic the biology well enough to provide relevant information about some processes, and *in vivo* assays do not sufficiently permit precise control of the stimuli to investigate the details of some processes. For this reason three-dimensional mechanotranduction assays are necessary for elucidating the interaction between mechanical stimulation and angiogenesis.

B.3. Summary and Aims

Angiogenesis is a complex process that is essential to both health and disease. Through angiogenesis, blood vessels sprout from preexisting ones and subsequently stabilize to supply local oxygen and nutrient demands. Angiogenesis initiates in response to biochemical/mechanical stimuli that signal the presence of ischemia, development, wound healing, endometrial repair, and disease. The environments that host angiogenesis vary throughout the body and life of the organism. As a result (in part), angiogenic mechanisms and features vary spatially and temporally, displaying distinct characteristics at different sites along the vascular tree and within different organs, at different ages, and in different physiological/pathological states. Endothelial cells conduct angiogenesis with the aid of supporting cells (e.g., fibroblasts, pericytes, monocytes, and smooth muscle cells), extracellular matrices, and angiogenic signaling molecules (VEGF, Ang-1 and -2, FGFs, etc.). These factors participate in a complex network of interactions to drive angiogenesis. However, aberrant functions of just a few of these components can derail the entire process, giving rise to any of several diseases. The involvement of angiogenesis in diseases such as cancer, ischemia, hypertension, and inflammatory disorders demonstrates the value of understanding angiogenesis. Great strides have been made in elucidating the details of angiogenesis, but unfortunately the process remains under-defined, and the full potential of therapies that intelligently target angiogenesis has yet to be harnessed. The complexity of angiogenesis is a primary reason for our current limited knowledge. Further, several parts of this process cannot be directly accessed (i.e., measured, quantitated, or actuated). Human tissues are inaccessible in most studies for obvious ethical reasons, so human angiogenesis is modeled in animals or by cell and tissue explants. Test sites within animals have limited relevance to the angiogenic context they model. Cell and tissue isolates can come from a wider range of sites, but the endogenous phenotype of cells distorts upon isolation and distorts further with continued culturing. Current technologies permit measurement and actuation of angiogenic factors with finite precision and control, and typically precision and control in angiogenesis assays come at the expense of relevance to the biological context being studied. *In vitro* angiogenesis assays offer

detailed study of angiogenic cells and tissue components, albeit in synthetic environments that lack several of the features experienced *in vivo*. In contrast, *in vivo* angiogenesis models present a complete angiogenic process capable of producing functional vasculature but suffer from limitations of imaging and difficulty measuring angiogenic factors. *In vivo* assays also pose a challenge to controlling factors that drive angiogenesis (e.g., maintenance of gradients of growth factors). The limitations of *in vitro* and *in vivo* angiogenesis assays are exacerbated in assays that seek to control or study mechanical forces in angiogenesis. Measurement and actuation of mechanical influences on angiogenesis are generally restricted to single cells and two-dimensional cell monolayers, which lack several pertinent features of *in vivo* angiogenesis. Mechanotransduction, though most easily investigated in two-dimensional cell monolayers, can also be studied in detail in three-dimensional angiogenesis. These assays, however, often prohibit certain modes of mechanical actuation and still lack the physiological relevance of *in vivo* angiogenesis assays. *In vivo* angiogenesis assays provide little to no control over the mechanical stimuli that affect angiogenesis. Studies of mechanical force in angiogenesis provide a notable example of the general limitations of *in vitro* and *in vivo* angiogenesis assays.

As an intermediate method between more physiologically relevant *in vivo* angiogenesis assays and more precise *in vitro* angiogenesis assays, the organ explant angiogenesis assay has gained wide use. Organ explant assays initiate angiogenic sprouting, outward growth and (to an extent) stabilization of new blood vessels from explanted segments of vasculature, bone, or embryonic tissue. Often termed an "*ex vivo*" model, organ explant assays are considered the most complete *in vitro* model of *in vivo* angiogenesis. These assays undergo nearly all the steps of angiogenesis. The *in vitro* setup has the advantage of facilitating repeated imaging and quantitation of angiogenesis, precise measurement of angiogenic factors, and control of angiogenic stimulators. The *ex vivo* character of the organ explant assay recapitulates the spatial organization of heterogeneous cell types and extracellular matrices, the multitude of paracrine and juxtacrine signaling events, and the endogenously generated spatial-temporal gradients of angiogenically active biomolecules of *in vivo* angiogenesis. Therefore, researchers utilize the organ explant assays to reliably investigate angiogenic mechanisms (including vessel stabilization and regression steps not accessed in the other angiogenesis assay) and the test substances that influence angiogenesis. Insights gained from the study of angiogenesis using organ explant assays have informed the development of therapies that impact angiogenesis. Still, the organ explant assay suffers limitations common to *in vitro* angiogenesis models (e.g., absent endocrine signals, mechanical stimuli, and local blood flow). Mechanical stimuli have been incorporated into various angiogenesis assays but are largely absent from the organ explant assay. Local blood flow and mechanical properties of the surrounding tissue signal to the angiogenic process. Diseases which pathologically influence angiogenesis also create mechanical perturbations. However, the interaction between mechanical stimulation and angiogenesis remains under-characterized. If the organ explant assay with its advantageous *in vitro* and *in vivo* characteristics were adapted to accommodate some mimic of local blood flow, it would yield new information about the interaction between mechanical stimuli and angiogenesis necessary to the treatment of disease. For this reason, we have designed and implemented a bioreactor that facilitates angiogenic sprouting and outgrowth from a perfused vascular explant.

The Perfused Vascular Explant Bioreactor

The perfused vascular explant bioreactor, shown in Fig B.1 was conceived to address limitations of *in vitro* and *in vivo* angiogenesis assays, particularly those relating to studies involving hemodynamic stimuli. The primary design target of the proposed work was to culture (over the long term) and encourage angiogenic sprouting of a vascular explant while maintaining a perfusion access to the lumen of the vascular explant. The successful design also sought to implement this without sacrificing advantageous features of the conventional vascular explant angiogenesis assay (e.g., amenability to repeated non-invasive imaging of angiogenesis). These design targets were put forth with the expectation that a perfusable connection to the lumen of a vascular explant would enable researchers to mimic aspects of physiological and/or pathological blood flow in the vascular explant angiogenesis assay. Researchers recognize the importance of blood flow and the mechanical and chemical signals it generates, and they have incorporated stimuli engendered in blood flow into *in vitro* angiogenesis assays; however, the vascular explant angiogenesis assay has yet to see such enhancement. Our work explores the potential of the PVEB to incorporate measurement and/or actuation of mechanical and chemical stimuli (engendered in blood flow) into the vascular explant angiogenesis assay.

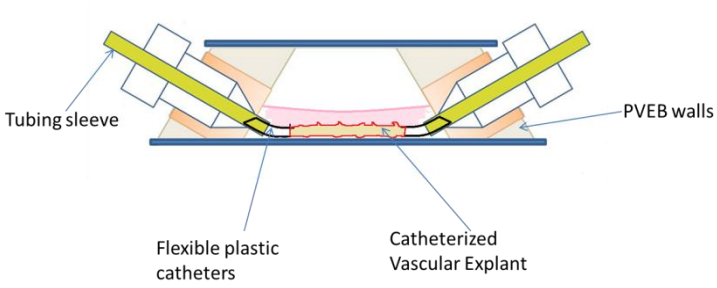

Figure B.1. Schematic of the perfused vascular explant bioreactor (PVEB). A mouse thoracic aorta is embedded in Matrigel and housed inside the PVEB. Flexible plastic catheter inserts connect the aorta to tubing sleeves. The tubing sleeves are fixed in the walls of the PVEB via commercially available ferrule fittings and nuts. The ends of the tubing sleeves that are outside of the PVEB are connected to tygon tubing. This assembly allows media to be pumped through the lumen of an aorta that is undergoing angiogenesis.

The PVEB would allow researchers to study the interaction between signals produced by flowing blood and angiogenesis, in a platform that presents potentially the most complete *in vitro* model of *in vivo* angiogenesis. The PVEB was conceived with the goal of eventually controllably delivering mechanical signals (e.g., shear stress) to vascular explants undergoing angiogenesis, and measuring changes in mechanical properties of blood vessels (e.g., impedance to fluid flow) which accompany long-term culture and angiogenesis. An *in vitro* experimental model such as the PVEB would also allow researchers to further probe chemical consequences of blood flow and their impact on angiogenesis. For example, mass transport of small molecules, radially diffusing from patent blood vessels, could be better mimicked in the PVEB. Similarly, the PVEB would allow the biomolecular properties of the luminal and abluminal spaces to be controlled independently of each other. These features may enhance the ability of the vascular explant assay to mimic physiological or pathological features of angiogenesis.

Constraints considered in the design and fabrication of the PVEB were that it maintain a clean (i.e., free of contamination) environment with physiological temperature, pH, pO_2, and pCO_2. The design should provide liquid-tight volume that opens only to the perfusion connection. The liquid-tight seal should withstand internal pressures at least as great as physiological pressures. Leaks arising from failure of the leak-tight seal introduce uncertain and uncontrolled influence on the angiogenesis and provide route for contamination and loss of perfusate. Components of the PVEB should also be inert and withstand sterili-

zation, thereby permitting repeated usage of the device. Quick assembly and facile implementation of the PVEB were important design constraints. The explanting and loading of the vascular explant into the PVEB should require little or no more time and expertise than the conventional vascular explant assay, since prolonged exposure to non-physiological temperature, pH, pO_2, and pCO_2 threatens the viability and angiogenic phenotype of the explant. Finally, the vascular explant should sparingly use matrix materials and culturing media to minimize the cost of the assay and the dilution of paracrine and autocrine signals secreted by the explant.

We achieved a perfusible connection to the lumen of the aorta by catheterizing the aorta. Commercial ferule fittings and nuts were incorporated into the custom-machined polycarbonate walls of the PVEB to accommodate perfusion of the catheterized aorta while also maintaining a liquid-tight reactor. The PVEB end walls were slanted inward in order to position the aorta near the floor of the bioreactor and within the working distance of common microscope objectives. The PDMS gasket placed between the polycarbonate walls and the floor of the reactor had an approximately 0.6 x 1.2 cm rectangular cutout that provided clearance for the aorta to rest against the floor of the reactor and allowed the aorta to be completely submerged in a small volume of matrix material. Because of their common use in the aortic ring assay, endothelial growth media-2 (EGM-2) and growth factor reduced Matrigel were utilized in the PVEB culture. The goal of this study was to accomplish as a “proof of principle” angiogenic outgrowth from a perfused vascular explant without necessarily investigating specific mechanisms of the angiogenic outgrowth. Considering this, Matrigel was selected over collagen and fibrin because of its ease of use and its greater capacity to induce angiogenesis.

The aorta was perfused at flow rates between 50 and 100 μL/min. This would generate (considering that the mouse thoracic aorta is roughly 0.5 mm in diameter) shear stresses along the wall of the aorta that were comparable to that in the post capillary venule where angiogenesis typically occurs (~1 dyne/cm^2). In this way, the perfusate flow rate was relevant to physiological angiogenesis. EGM-2, commonly used to investigate effect of shear-stress on endothelial cells *in vitro*, was utilized as the perfusate in the PVEB. The following details the design and implementation of the PVEB.

CHAPTER III

METHODS

We now describe the three experimental assays that were utilized: the classic mouse aortic ring assay, a whole-aorta angiogenesis assay in a cell culture dish, and the perfused vascular explant bioreactor (PVEB) assay. We follow this with the methods for small molecule perfusion experiments, and conclude this section by describing a COMSOL model of small molecule diffusion and convection in the PVEB and the equipment used in the experiments.

All experiments conformed to the *Guide for the Care and Use of Laboratory Animals* published by the U.S. National Institutes of Health and were approved in advance by the Vanderbilt Institutional Animal Care and Use Committee.

C.1. Mouse Aortic Ring Assay

A 30-50 µL thick layer of Matrigel was pipetted into each well of a 96-well plate and allowed to cure. Thoracic aortas from four-to-ten-week-old wild-type or Tie-2::GFP mice were sectioned into six parts and centered, one per well, on top of the Matrigel layer. A second 20 µL layer of Matrigel was pipetted into the wells on top of the slices of aorta and allowed to cure. The aortas were cultured for at least six days with EGM complete media, in the dark at 37°C with humid 5% CO_2, 95% air. The extent of angiogenic sprouting was inspected visually under a microscope at 4x to 20x magnification.

C.1.1. Equipment List

1. Corning sterile 100 mm x 20 mm cell culture dishes.
2. Microtest^{TM} sterile 96-well flat bottom tissue culture plate.
3. Syringe needles (24G) were used repeatedly to pin down the euthanized mouse and were therefore not sterile.
4. A 1L Nalgene jar served as a chamber for euthanizing the mouse. Paper towels were placed at the bottom of the jar, and a plastic grate was situated approximately 1 cm above them. This assembly was stored in a chemical fume hood when not in use.
5. A Styrofoam box lid, covered by a sheet of cloth, served as a dissecting tray.
6. Dissecting tools: Roboz 24 mm carbide blade micro-dissecting scissors, Roboz Bonn 15 mm curved sharp tip micro-dissecting scissors, Roboz serrated straight fine tip (0.5 mm) micro-dissecting forceps and Roboz McCullough cross serrated straight blunt tip (1.5 mm) micro-dissecting forceps were washed with Roboz surgical instrument cleaner and warm water and

then stored in 70% v/v ethanol or under UV radiation for at least 30 minutes prior to use. Feather® sterile stainless steel disposable scalpels were also used. In repeated uses, the scalpels were stored in 70% v/v ethanol for at least 30 minutes prior to use. The dissection equipment was sterilized via autoclaving whenever yeast contamination was a concern.

7. P100 and P1000 pipettes.
8. AmScope 4X magnification desktop dissecting scope.
9. AmScope 4-40X magnification microscope.
10. Nikon Ti Eclipse microscope with attached photometric Coolsnap HQ^2 digital camera and NIS-Elements AR software.
11. Tissue culture incubator.

C.1.2. Materials

1. BD Biosciences Growth Factor Reduced Matrigel™ Matrix was stored in 800 µL aliquots at -20°C until use, which was within 6 months of purchase. The Matrigel was thawed and stored on ice no earlier than 8 hours prior to use.
2. Complete Clonetics® Endothelial Cell Growth Media (EGM-2) was stored in 40 mL aliquots at -20°C until thawed for use within 6 months. Upon thawing, the EBM-2 aliquot was stored in darkness at 4°C until use.
3. Phosphate buffer solution (1x PBS) was prepared using a standard recipe starting with dry FisherReagent® laboratory grade chemicals and DI water. The solution was mixed and sterilized via autoclaving weeks or months prior to use.
4. IsoThesia™ Isoflurane, USP was stored in bulk at room temperature in the absence of light.
5. Four-to-ten-week-old C57, BALB-C or SV-129 wild–type or hemizygous Tie2::GFP (Jackson Laboratories STOCK Tg(TIE2GFP)287Sato/J mice) were kept until use in standard mouse facilities.

C.1.3. Euthanasia

Mice were euthanized immediately prior to use via barbiturate overdose followed by cervical dislocation (as a precautionary measure). To accomplish this, approximately 0.5 mL of IsoThesiaTM Isoflurane, USP was added to a 1L Nalgene jar containing several paper towels; a plastic grate situated above the paper towels prevented the mouse from directly contacting the liquid isoflurane. Immediately afterwards, the mouse was placed inside the jar and the lid was screwed shut. The mouse was exposed to isoflurane gas for 2 to 10 minutes. Immediately after, cervical dislocation was performed manually.

C.1.4. Explanting the Aorta

The dissection procedures were developed under the guidance of Dr. Masakazu Shiota in arranged individual training sessions at Vanderbilt University, and by Dr. Robert Nicosia as part of the National Institutes of Health and the Foundation for the Advanced Education in the Sciences (NIH/FAES) Analytical

Techniques for the Quantitation of Angiogenesis and Lymphoangiogenesis Course, TRAC28, developed by Mark Nardone[93, 121]. During the dissection, when not being used all dissection tools were stored in 70% v/v ethanol. Immediately following euthanasia, the mouse was pinned to the dissecting tray by inserting 25G syringe needles through the fore- and hind-paws with palmar and dorsal surfaces facing up, respectively. The ventral side of the mouse was facing up. To reduce the risk of contamination, the mouse was sprayed thoroughly with 70% v/v ethanol.

Carbide blade micro-dissecting scissors were utilized to make an incision into the skin along the sagittal axis from the base of the abdomen to the middle of the sternum. Horizontal incisions were made into the skin across the base of the abdomen and across the chest. The skin and fur were peeled away from the underlying abdominal and thoracic muscle using the micro-dissecting forceps. The skin was pinned down using 25G syringe needles. Vertical incisions were made into the abdominal muscle using either of the two micro-dissecting scissors. This opened the peritoneal cavity and exposed intestine. The intestine, stomach, liver and kidneys were gently pushed to the dextral side of the peritoneal cavity using the blunt tip micro-dissecting forceps.

In subsequent steps, all dissection tools were rinsed in an approximately 5 mL reservoir of sterile 1x PBS (in a 100 mm x 20 mm cell culture dish) before contact with the mouse. This was to prevent ethanol poisoning of the vascular explant. The diaphragm was punctured, and the sinistral side of the rib cage was cut open using the carbide blade micro-dissecting scissors, to expose the lungs and heart in the thoracic cavity. The rib cage was partially cut away. The lungs were gently pulled toward the dextral side of the thoracic cavity using blunt tip micro-dissection forceps, thereby exposing the aorta. While grasping the posterior end of the thoracic aorta with the fine tip micro-dissecting forceps, the thoracic aorta was cut away (using curved tip microdissecting scissors) from the underlying rib cage from the posterior end toward the anterior end. The explanted aorta was stored in 1x PBS until further use.

Under the 4X magnifying dissecting scope the aorta was cleaned of fibro-adipose tissue. A ~2 mL droplet of 1x PBS was placed in the center of the lid of a 100 mm x 20 mm cell culture dish. This dish was placed under the objective of the dissecting scope and the aorta was placed inside the 1x PBS droplet. Pieces of fibro-adipose tissue were grasped and pulled apart using the micro-dissecting forceps. In an effort to maintain the endogenous angiogenic potential of the aorta, this was done with minimal manipulation of the underlying aorta. Once there was a break in the fibro-adipose tissue, large segments of it could be gently pulled off of the aorta (ideally). On occasion, additional manipulation was required. Care was taken not to disturb the endothelial cell layer in the intima of the aorta.

C.1.5. Culturing the Aortic Ring Assay

Prior to performing the dissection, a 30-50 µL aliquot of Matrigel was pipetted into each of six wells in a 96-well plate for each aorta. This layer of matrix was allowed to cure inside the tissue-culturing incubator for the duration of the dissection. After explanting the aorta, five cuts were made (with the scalpel) in planes perpendicular to the axis of the aorta, resulting in six segments of roughly equal size. An aorta segment was removed from the 1x PBS using the fine tip micro-dissecting forceps. A small droplet of 1x

PBS can be held between the tips of the forceps by surface tension. With the aorta segment enclosed inside this droplet it is possible to transfer the aorta from 1x PBS to a well in the 96-well plate without the forceps contacting the aorta. One aorta segment was placed on top of the Matrigel and centered inside a well on the 96-well plate, and 20 µL of Matrigel was pipetted into the wells on top of the aorta slices. The additional Matrigel was allowed to cure inside the tissue-culturing incubator for at least 20 minutes. Afterward, 150 µL of media was added to the well, and replenished every four to six days in culture. Aorta slices were cultured at least six days in the dark at 37°C with humid 5% CO_2, 95% air.

C.1.6. Data Acquisition

The aortic ring assay was used to investigate angiogenesis. Angiogenic sprouting was inspected visually, using a 4-40X magnification Amscope microscope and a Amscope camera or a Nikon Eclipse Ti equipped with a photometric Coolsnap HQ^2 digital camera and NIS-Elements AR software. Fluorescent images of the Tie-2 mouse aortas were acquired at the FTIC emission wavelength (515-555 nm), 700 ms exposure and 4x gain (10X objective). Excitation of fluorescent materials was accomplished using a Nikon arc lamp on its minimum output setting (delivering an excitation wavelength of 475 to 490 nm).

C.2. Whole Aorta Angiogenesis Assays in Cell Culture Dish

Whole thoracic mouse aortas were placed in a 35 mm x 10 mm cell culture dish and overlaid with a 150 µL bubble of Matrigel. The aortas were cultured for at least six days with EBM-2 complete media, in the dark at 37°C with humid 5% CO_2, 95% air. Angiogenic sprouting was inspected visually under a microscope.

C.2.1. Equipment

The same equipment was used in the Whole Aorta Angiogenesis Assay in Cell Culture Dish as in the Mouse Aortic Ring Assay (Section C.1.1). Cell culture (35 mm X 10 mm) dishes were used to culture the whole aorta instead of the 96-well plates. In some experiments Exel Safelet shielded 24G catheters and Myco silk suture thread were also used.

C.2.2. Materials

The same materials were used in the Whole Aorta Angiogenesis Assay in Cell Culture Dish as in the Mouse Aortic Ring Assay (Section C.1.2).

C.2.3. Explanting the Aorta

The mouse euthanasia and the aorta explantation in the Whole Aorta Angiogenesis Assay were conducted as in the Mouse Aortic Ring Assay (Sections C.1.3 and C.1.4). After explanting, the aorta was occasionally catheterized as described in PVEB Mouse Aorta Assay (Section C.3.5).

C.2.4. Culturing the Whole Aorta Angiogenesis Assays in Cell Culture Dish

After explanting and cleaning the aorta, it was transferred to the center of a 35 mm X 10 mm cell culture dish using the fine tip micro-dissecting forceps. A 150 µL bubble of Matrigel was overlaid on the aorta using a P1000 pipette. The Matrigel was allowed to cure inside the tissue-culturing incubator for at least 20 minutes. Afterward, 2000 µL of media was added to the well using a micropipetter, and replenished every six to eight days in culture. Two thousand microliters of media sufficiently submersed the bubble of Matrigel. Whole aortas were cultured at least six days in darkness at 37°C with humid 5% CO_2, 95% air.

C.2.5. Data Acquisition

The Whole Aorta Angiogenesis Assay in Cell Culture Dish was used to investigate angiogenesis. Angiogenic sprouting was inspected visually, using a 4-40X magnification Amscope microscope and a Amscope camera or a Nikon Eclipse Ti equipped with a photometric Coolsnap HQ^2 digital camera and NIS-Elements AR software.

C.3. Perfused Vascular Explant Bioreactor (PVEB) Assay

C.3.1. Equipment

Dissection Equipment

The same equipment was used in the PVEB Mouse Aorta Assay as in the Mouse Aortic Ring Assay (Section C.1.1). The PVEB, peristaltic pump, and perfusion tubing were used to culture the whole aorta instead of the 96-well plates. In addition, Exel Safelet shielded 24G catheters were used. Occasionally, Myco or Ethicon silk suture thread was utilized to secure the aorta on the catheter.

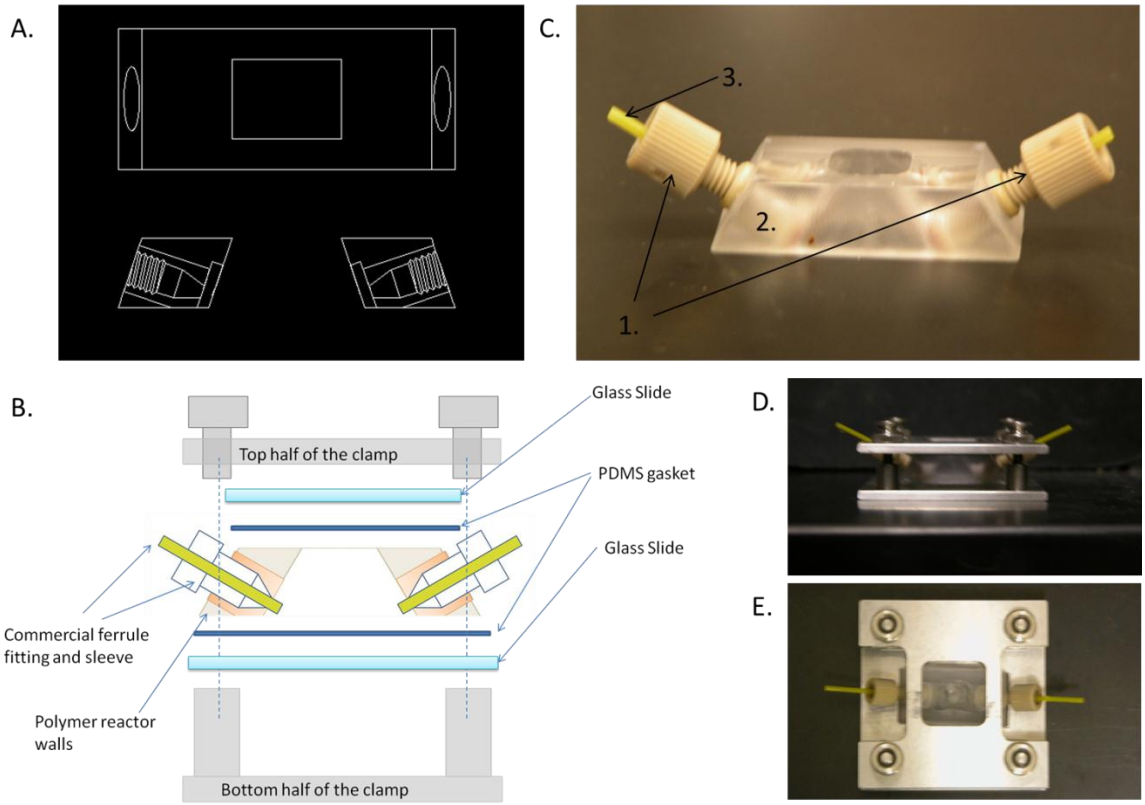

Figure C.1. Schematics (A and B) and photographs (C, D and E) of the Perfused Vascular Endothelial Bioreactor (PVEB). Commercial ferrule fittings (1) were fixed, using epoxy, into the polycarbonate walls (2) of the bioreactor. Commercial tubing sleeves (3) served as an adaptor between the ferrule fitting and the smaller diameter catheter tubes. A coverglass (0.5 mm thick), the bottom PDMS gasket, PVEB, top PDMS gasket and glass slide were stacked and clamped to create a liquid tight environment for the aorta. Parts are numbered in Table C.1.

The PVEB

The walls of the bioreactor, ferrule fittings and nuts, and tubing sleeves in the bioreactor were assembled as in Fig. C.1. prior to use. A polycarbonate reactor (2) shell was manufactured by the Vanderbilt Physics Department machine shop. The bioreactor featured two sloped walls with circular openings and two solid, vertical walls. The walls with openings were tilted inward at 60° relative to the floor of the reactor. UpChurch ferrule N-333 fittings (1) were held in each opening by Epoxy. The ends of these ferrule fittings were filed at a 120° angle so that they lay flush with the floor of the reactor and the hole of the ferrule was 2mm above the floor. This assembly is referred to in this section as the PVEB. PDMS gaskets (4 and 5) were made by pouring a ~2 mm thick layer of PDMS elastomer and curing agent mixture into a plastic dish. This was cured at 60°C overnight in the absence of light, then cut, using a Feather® sterile stainless steel disposable scalpel, into rectangles that matched the dimensions of the top and bottom of the PVEB. The bottom gasket had an approximately 5 mm X 1.2 cm rectangle cut out of the center. This allowed clearance for the aorta to be positioned against the floor of the reactor. The PDMS mixture was prepared by mixing 10:1 Sylgard PDMS elastomer with Sylgard curing agent using a minute-mixer. Using a stainless steel or brass/plexiglass compression clamp, a liquid-tight seal was created in

the PVEB. The PVEB, bottom (4) and top (5) PDMS gaskets, coverglasses, and clamps were immersed in 70% v/v ethanol for at least 30 minutes prior to use.

Table C.1. Parts List for the Perfused Vascular Endothelial Bioreactor (PVEB)			
Part No.	**Equipment**	**Manufacturer/Other**	**Material**
1	Ferrule fittings and nuts	IDEX Health&Science N333	PEEK
2	PVEB polymer walls	VIIBRE	Polycarbonate
3	Tubing sleeves	IDEX Health&Science F247X	FEP and Teflon
4	Top PDMS gasket	VIIBRE	PDMS
5	Bottom PDMS gasket	VIIBRE	PDMS
6	Studs	VIIBRE	Stainless steel
7	Compression clamp base	VIIBRE	Stainless steel
8	Compression clamp lid	VIIBRE	Stainless steel
9	Compression clamp base (alternate)	VIIBRE	Brass
10	Compression clamp lid (alternate)	VIIBRE	Plexiglas
11	Miniature incubator	Bioscience tools	NA
12	Temperature controller	Bioscience tools	
13	Persitaltic pump	Ismatic	NA
14	Liquid-gas separator	VIIBRE	Polycarbonate
15	PVC Solv tubing	Cole-Parmer 95712-26	PVC Solva
16	CO_2 tank	AL Compressed Gas	
17	Sterile filter	Pall Life Sciences®	0.45µm Supor® Membrane
18	Reflux trap (flask)	Unknown	Glass
19	Humidifier flask	Unknown	Glass
20	Media/CO2 Equilibrator (flask)	Unknown	Glass
21	Peristaltic pump tubing	Cole-Parmer 95712-26	PVC Solva
22	Polyethylene tubing (CO_2 delivery)	Bioscience tools	Polyethylene
23	Polyethylene connectors	Bioscience tools	Polyethylene
24	Silicone tubing	Bioscience tools	Silicone
25	Luer adaptor	Bioscience tools	Polyethylene
26	Polyurethane tubing (bubbler)	Bioscience tools	Polyurethane
27	Luer adaptor 2	Bioscience tools	Polyethylene
29	Polyethylene flask lid		Polyethylene
30	Straight tubing connectors 1/16"ID	Cole-Parmer C0-1HDPE	Polypropylene
31	Luer adaptor 3	Unknown	Nylon
32	Silicone tubing	Bioscience tools	Silicone
33	Luer adaptor 4	Value Plastics SMTLL-J1A	Kynar PVDF
34	1/4-20 screw to Luer adaptors	Unknown	Nylon
35	O ring	Unknown	Buna-N
36	Thumb screws	Microplastics 092520050TEG	Economy Nylon
37	25G syringe needles	Becton Dickinson &Co 305122	Stainless steel & unspecified
38	PVEB2 polymer walls	VIIBRE	PDMS
39	Hollow fiber	Spectrum Technologies	Unknown
40	T-Joint Tubing Connectors 1/16" ID	Cole-Palmer 5(53-2032W)	PVC Solva

Incubation and Perfusion Equipment

Two approaches were utilized in incubation and perfusion of the mouse aorta in the PVEB. This section lists the equipment utilized in each.

1. An alternate clamp (9 and 10) was designed to accommodate use within the Bioscience Tools miniature incubator. The Bioscience Tools miniature incubator was connected to a Bioscience Tools temperature controller (12) and a cylindrical tank charged with 5% CO_2, 95% air as diagrammed in Fig. C.2. The perfusion circuit was connected to a Bioscience Tools incubator through ports described in Section C.3.1.4. Gaseous 5% CO_2, 95% air was delivered to the miniature incubator at a rate that allowed one bubble to go through the humidifier per sec. At least 4 hours before use, the perfusion circuit was disconnected from the sterile filter and sterilized with ethanol (Section C.3.1.4).
2. A tissue culture incubator was modified to accommodate a perfused connection to the PVEB it contained. Perfusion tubing, described in the next section, was wedged into the door of the incubator. Structural support was provided by plastic syringe pistons which were taped to the incubator, flanking the tubing and also wedged into the door of the incubator. This setup was assembled prior to sterilization of the perfusion tubing (Fig. C.3).

Perfusion Circuit

The perfusion circuit comprises all the equipment and tubing that carries sterilized CO_2 /air and media to the miniature incubator and PVEB. Described in Section C.3.4., a modified perfusion circuit delivered media to a PVEB that was housed within a conventional tissue culture incubator. Experiments utilized the miniature incubator and the larger conventional tissue culture incubator. When sterilizing the circuit, the PVEB is replaced by a 1/8" piece of tubing sleeve (3). This serves as a place holder and closes the loop that will carry media to and from the aorta lumen in the PVEB. The perfusion circuit was assembled as diagrammed in Fig. C.4 prior to use and sterilized by perfusing the closed loop path with 1-2 mL/min of 70% v/v ethanol for at least 30 minutes. After sterilization, the perfusion circuit was perfused at 1-2 mL/min with sterile DI H_2O for at least 30 minutes, then perfused at 1-2 mL/min with 1x PBS. The CO_2 and humid air delivery path in the perfusion circuit is not a closed loop. This path was filled with 70% v/v ethanol by injecting it (using a 10 mL syringe) directly into the silicone tubing (24), followed by DI water. All internal surfaces of the perfusion loop were exposed to 70% v/v ethanol for at least 30 minutes, followed by DI water for at least 30 minutes.

C.3.2. Materials

The same culture materials were used in the PVEB Mouse Aorta Assay as in the Mouse Aortic Ring Assay (Section C.1.2). The EGM-2 was separated into two allotments, one (10 mL) for perfusing the lumen of the aorta and another (2 mL) for culturing in the abluminal space of the PVEB. The latter was stored inside the tissue culture incubator for at least 30 minutes to equilibrate it to 5% CO_2.

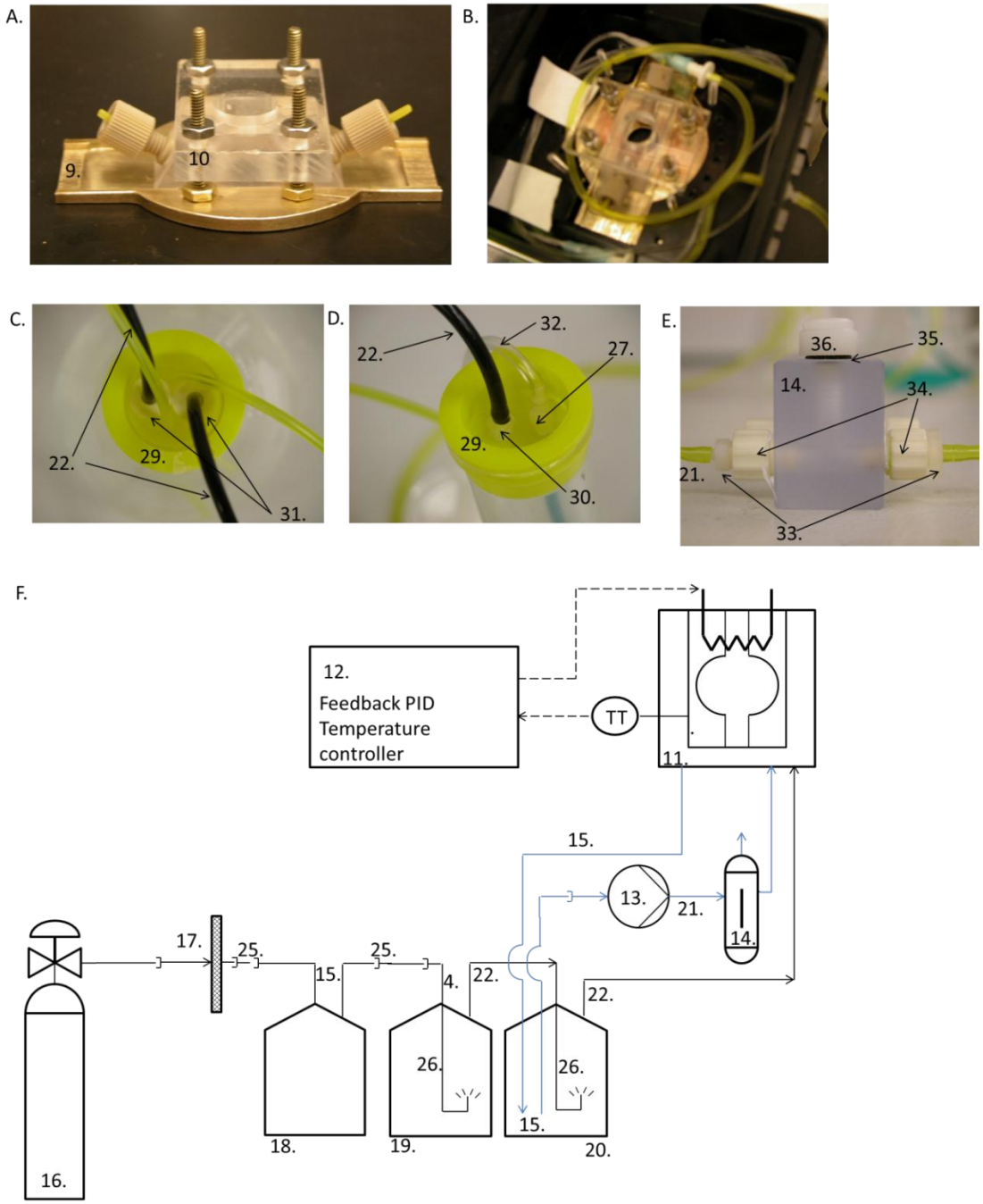

Figure C.2. An alternate compression clamp was designed (A and B) that allowed the PVEB to fit inside a Bioscience Tools miniature incubator (11). A 2 mm thick brass compression clamp base (9), in the shape of the incubator stage inset, was made at the Vanderbilt Institute for Integrative Biosystems Research and Education (VIIBRE), as were an accompanying plexiglass compression clamp lid (10) and nuts. As shown in a schematic F) of the Bioscience Tools miniature (11) incubator and supporting temperature controller (12), the miniature incubator was connected to a perfusion circuit which consisted of a peristaltic pump (13), liquid-gas separator (14) E) and (depicted in blue) Tygon tubing (15). Gaseous 5% CO_2, 95% air was delivered from the pressurized cylinder(16) through a 0.02 µm pore-sized sterile filter(17) and reflux trap (18), bubbled through a humidifier (19) and media reservoir (20) (C and D) and finally flowed into the miniature incubator. Bubbling 5% CO_2, 95% air through the media reservoir (20) equilibrated the media to 5% CO_2. The resulting color change was noted as an indicator of 5% CO_2 equilibration of the media. A 15 mL conical tube was placed inside the media reservoir flask. A detailed parts list (Table C.1.) provides the names and suppliers of the numbered components in this figure.

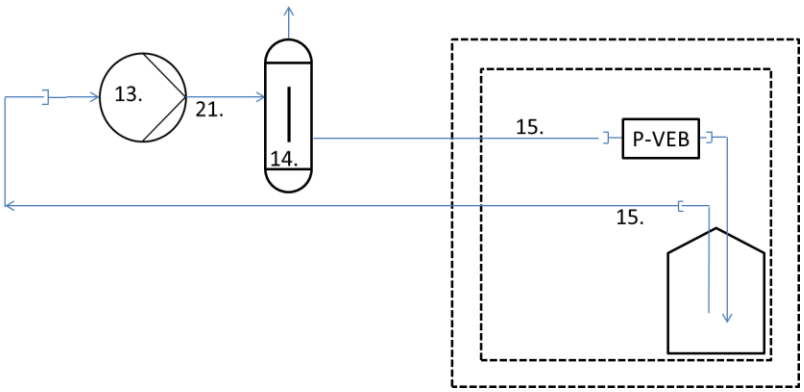

Figure C.3. Schematic depicting the perfusion circuit and PVEB in a large incubator. A tissue culture incubator (depicted by dashed lines) was modified to accommodate a perfused connection to the media reservoir and the PVEB it contained.

C.3.3. Initiating the Temperature Controller and Perfusion Loop

After sterilizing and rinsing the perfusion circuit, 1x PBS was decanted from the media reservoir and replaced by 10 mL of complete EGM, which was pipetted into the media reservoir (which also served as a CO_2/media equilibrator (20). The perfusion circuit was reconnected to the sterile filter (17) that is connected to the CO_2 tank. The volumetric flow rate of CO_2/air into the reactor was not measured. Flow was slow enough to produce in the humidifier and media reservoir one or two bubbles per second. On occasion, to insure adequate delivery of CO_2 to the miniature incubator, a small culture dish of EBM-2 complete media was incubated inside the incubator for at least 30 minutes and inspected visually for the color change that accompanies CO_2 equilibration.

The temperature controller was turned on, and the electronic connections of the miniature incubator and lid (11) were made at least 30 minutes prior to culturing the aorta. After sterilization and rinsing, the perfusion circuit was perfused using the peristaltic pump (13) at 1-2 mL/min with complete EBM-2 for at least 30 minutes.

C.3.4. Alternate Assembly of Perfusion and Incubation Equipment

In some Perfused Vascular Explant Bioreactor (PVEB) Mouse Aorta Assays, the perfusion circuit consisted of a closed loop of Tygon tubing (15) connecting a media reservoir to the peristaltic pump (13), debubbler (14) and PVEB, and then returning to the media reservoir (Fig. C.3). When sterilizing this circuit, the PVEB is replaced by a 1/8” piece of tubing sleeve (3). This serves as a placeholder and closes the loop that will carry media to and from the aorta lumen in the PVEB. Sterilization was accomplished by perfusing the closed loop path with 1-2 mL/min of 70% v/v ethanol for at least 30 minutes. After sterilization, the perfusion circuit was perfused at 1-2 mL/min with sterile DI H_2O for at least 30 minutes, then perfused at 1-2 mL/min with 1x PBS. Adequate temperature and carbon dioxide concentration were maintained for the duration of the assay using a standard tissue culture incubator, as described below (Section C.3.7).

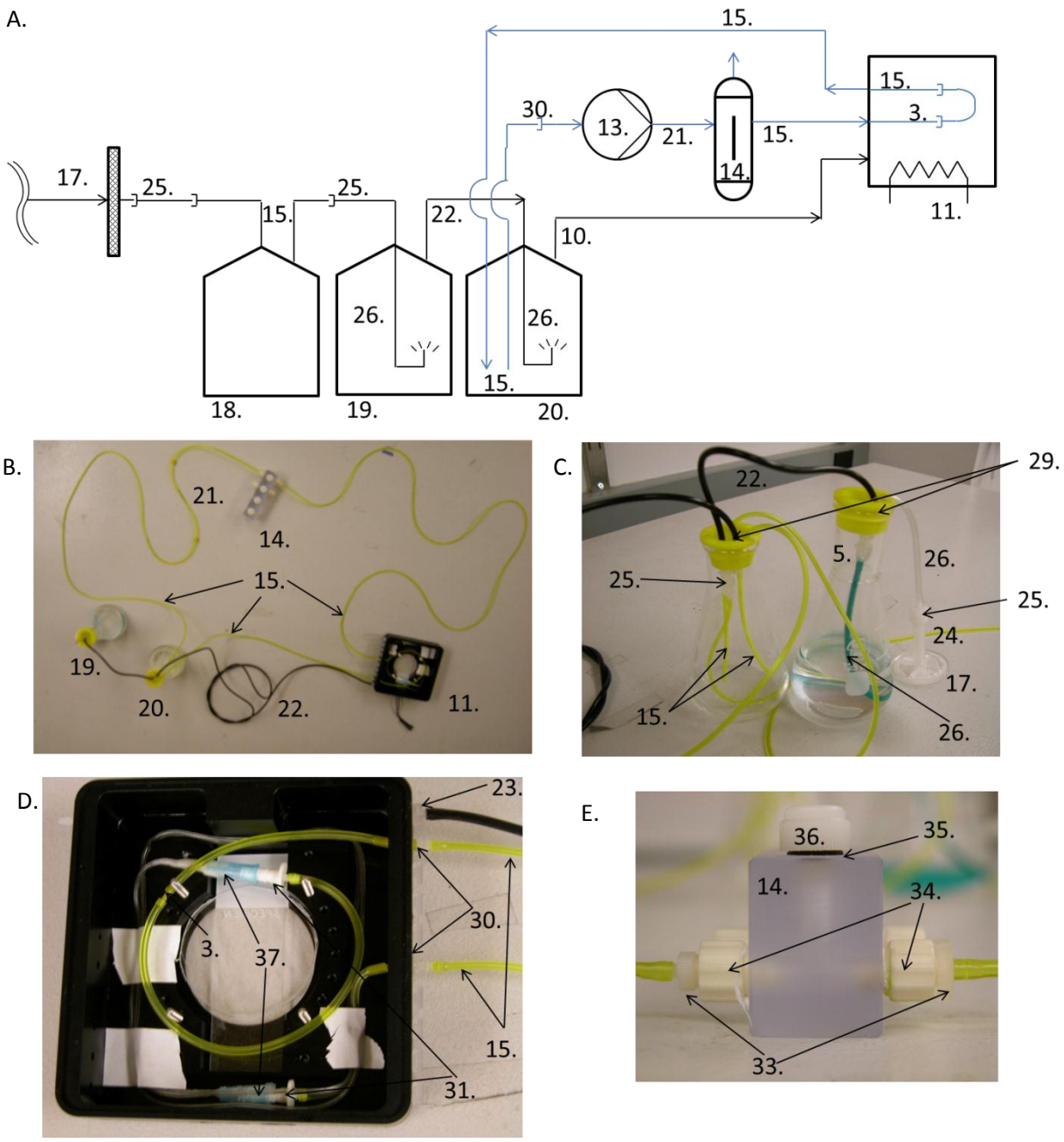

Figure C.4. The perfusion circuit was assembled as diagrammed above. The sterile filter (17) was not connected until after sterilization of the rest of the perfusion circuit. Sterilization was accomplished by using the peristaltic pump to perfuse the closed-loop circuit (depicted in blue) with 70% (v/v) ethanol in water, followed by DI water then 1x PBS. The CO_2 delivery line which connects to the sterile filter was filled with 70% (v/v) ethanol in water, followed by DI water then 1x PBS. The tubing in the CO_2 delivery line was exposed to 70% (v/v) ethanol in water, DI water and 1x PBS by injecting it into the tubing (24).

C.3.5. Explanting the Aorta

The mouse euthanasia and the aorta explantation in the PVEB Aorta Assay were conducted as in the Mouse Aortic Ring Assay (Section C.1.3 and C.1.4).

C.3.6. Catheterizing the Aorta

Exel safelet sterile shield catheters (24G X ¾") were inserted into the ends of the explanted aorta. These catheters feature a flexible ¾" plastic catheter tube that slightly tapers at its end. The plastic catheter tube is attached to a "quick connect" syringe tip which is capable of fitting on commercially available syringes. Underlying the syringe tip and catheter shield is a 24G X 2" stainless steel needle. The end of the needle is beveled (useful for carefully inserting into the aorta), and fixed at the other end to a plastic support for safe handling. The needle can be withdrawn from the syringe tip and catheter shield by applying gentle force. Under the 4X magnifying dissecting scope, the aorta, once cleaned of fibro-adipose tissue, was catheterized and loaded into the PVEB. A ~2 mL droplet of 1x PBS, placed in the center of the lid of a 100 mm x 20 mm cell culture dish, held the explanted aorta. To accomplish this catheterization, one end of the aorta was grasped using the fine tip micro-dissection forceps in the left hand. The right hand was used to insert the Exel Safelet shielded catheter into the lumen of the aorta. Using the thumb and index finger it is possible to smoothly slide the catheter back and forth along the underlying syringe needle. While holding the aorta in place using the fine-tip micro-dissection forceps, the catheter was gently slid into the lumen of the aorta. Immediately after, the catheter shield was cut away from the rest of the syringe tip using the curve tip micro-dissecting scissors, leaving a 3 to 7 cm long segment of the catheter inside one end of the aorta, with the other end of the catheter free and open. The aorta was rotated 180° so that the non-catheterized end of the aorta could be grasped using the fine tip micro-dissection forceps in the left hand, and the catheterization step was repeated for the other end of the aorta. Catheterizing the aorta occurred without removing the aorta from the ~2 mL droplet. The catheterized aorta was laid flat inside the droplet and both catheter shields were then cut in planes 45° from the axis of the catheter, such that the whole length of the aorta plus catheters was ~2.5 cm (shown in Fig. C.5.A). A ruler was placed under the culturing dish in order to accurately judge the distance between the two cuts.

Occasionally, silk thread suture knots were tied around the aorta in order to secure the aorta-catheter connection. In these cases, silk thread was tied into loose double-square knots and sterilized in ethanol for at least 30 minutes, followed by immersion in sterile DI water for at least 30 minutes. These knots were slid onto the aorta and tightened around the aorta-catheter connection using the micro-dissecting forceps.

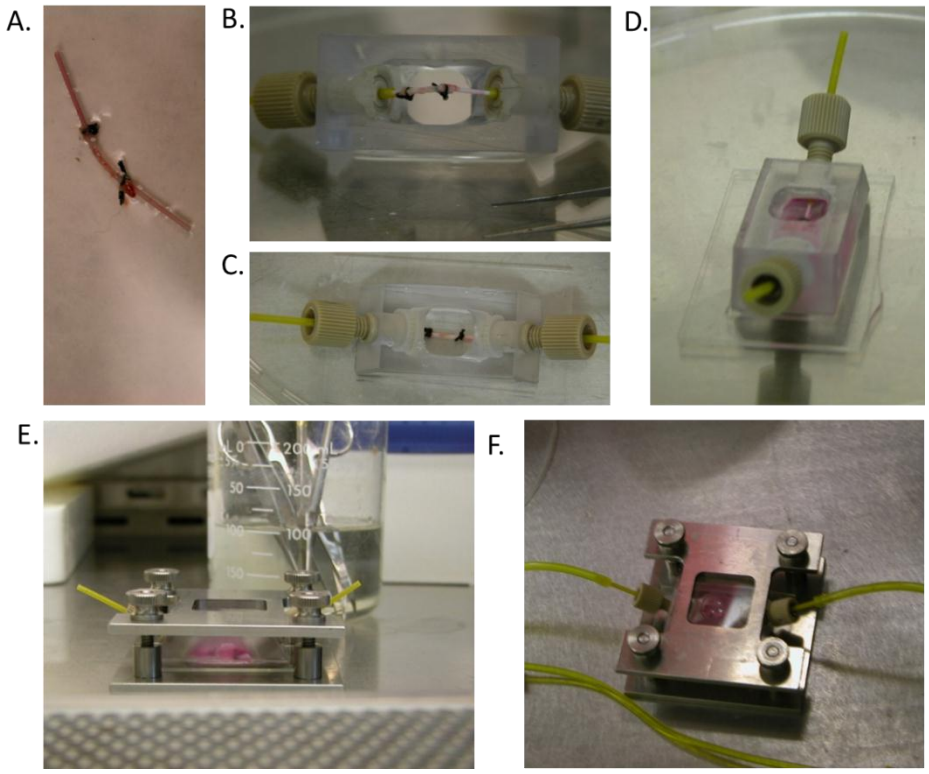

Figure C.5. Major steps of that assembly of the PVEB: A) Extract, clean, and catherize the aorta, (B and C) load the aorta into the ferrule fittings, D) cover the aorta in Matrigel, allow it to cure at 37 degrees, and fill the remaining volume with EGM-2, E) seal the reactor, F) perfuse the aorta. On average it takes 40 minutes to extract and catheterize the mouse aorta, connect to the ferrule fitting, assemble the bioreactor and supply it with Matrigel/media.

C.3.7. Loading the PVEB

Prior to loading the PVEB, the coverglass and bottom PDMS gasket were stacked on the floor of the incubator or stainless steel clamp (in that order), and the top PDMS gasket was placed against the coverglass. Using the blunt tip micro-dissecting forceps in the left hand, the PVEB was picked up by the left ferrule fitting. The left hand is rotated ~180° such that the reactor is upside-down and hovering over the thenar space of the hand with the forceps around the *now right* ferrule fitting. This positioning allows added clearance for the right hand and makes it possible to load the aorta without raising the right elbow to uncomfortable heights. The catheter was inserted 1-4 mm into the left tubing sleeve inside the PVEB using the fine tip micro-dissecting forceps. Immediately thereafter, the PVEB was placed into a 2-3 mL droplet of 1xPBS. The PVEB was rotated 180°, and the loading of the second catheter was done exactly as the first. Care was taken not to pull the aorta off of the catheters or to stretch or flex the aorta.

C.3.8. Culturing the PVEB Mouse Aorta Assay

The compression clamp lid was placed above the PVEB and tightened without the top coverglass and PDMS gasket. This provided a leak-proof seal between the walls and the floor of the PVEB. Excess liquid in the PVEB was aspirated using a P1000 micropipetter. Matrigel (300 µL) was deposited on the aorta using a P1000 pipette. The Matrigel was allowed to cure inside the tissue-culturing incubator for at least 20 minutes. Afterward, the compression clamp lid can be removed momentarily without disrupting the

seal between the walls and the floor of the PVEB. The compression clamp lid was removed and 1000 µL of CO_2 equilibrated complete media was quickly added to the PVEB using a P1000 micropipetter. Immediately afterward, the top PDMS gasket and coverglass were gently placed on top of the PVEB and the clamp was tightened down. The perfusion circuit was connected to the PVEB by using the forceps to remove the tubing sleeve (3) that served as a place holder up until now. The perfusion circuit was connected to the external ends of the tubing sleeves of the PVEB. Finally, the perfusion circuit was reconnected to the sterile filter (17) that connects to the CO_2 mixer and the peristaltic pump. The aorta lumen was perfused inside the PVEB, with media (that contained 75% of the growth factors in complete EGM-2) from the media reservoir flask or CO_2/media equilibrator (20), at 0-500 µL/min continuously for at least six days.

In an alternate approach to the assay, the PVEB, coverglass and PDMS gaskets are held between the compression clamp base and compression clamp lid, as shown in Fig. C.3. Instead of incubating the PVEB in the miniature incubator, the PVEB is stored in the tissue culture incubator. A peristaltic pump that pumps the perfusate through the aorta bioreactor was located outside the incubator. Tubing connecting the aorta bioreactor to the perfusate and pump was wedged into the door of the incubator. The incubator door closed and sealed around the tubing. Plastic syringe pistons served as structural support and were situated around the tubing to prevent the door seal from collapsing the tubing. The aorta lumen was perfused inside the PVEB, with media from the media reservoir flask or CO_2/media equilibrator (20), at 50 µL/min continuously for at least six days. The PVEB and perfusate were kept in the dark at 37°C with humid 5% CO_2, 95% air.

C.3.9. Data Acquisition

Angiogenic sprouting was inspected visually, using a 4-40X magnification Amscope microscope and a Amscope camera or a Nikon Eclipse Ti equipped with a photometric Coolsnap HQ^2 digital camera and NIS-Elements AR software. Fluorescent images of the Tie-2 mouse aortas were acquired at the FITC emission bandpass of wavelengths (500-540), 700ms exposure and 4x gain (10X objective). Excitation of fluorescent materials was accomplished using a Nikon arc lamp on its minimum output setting (delivering a passband of excitation wavelengths, 475-490nm).

After four to seven days in culture, aortas were retrieved from the PVEB. Using forceps, the aortas were manually separated from the glass floor of the PVEB, or from the cell culturing dish. Aortas were fixed in 10% formalin at room temperature for 24 hours, followed by incubation in ethanol. Fixed samples were sliced and hematoxylin and eosin stained.

C.4. Small Molecule Perfusion Experiments

C.4.1. Hollow Fiber Dye Rinse Out Experiment

C.4.1.1. Equipment List

1. Perfused vascular explant bioreactor model 2 (PVEB2).
2. Ismatec pump and perfusion circuit.
3. Microtest^{TM} sterile 96-well flat bottom tissue culture plate.
4. UV-VIS Spectrometer.
5. Rubber band.

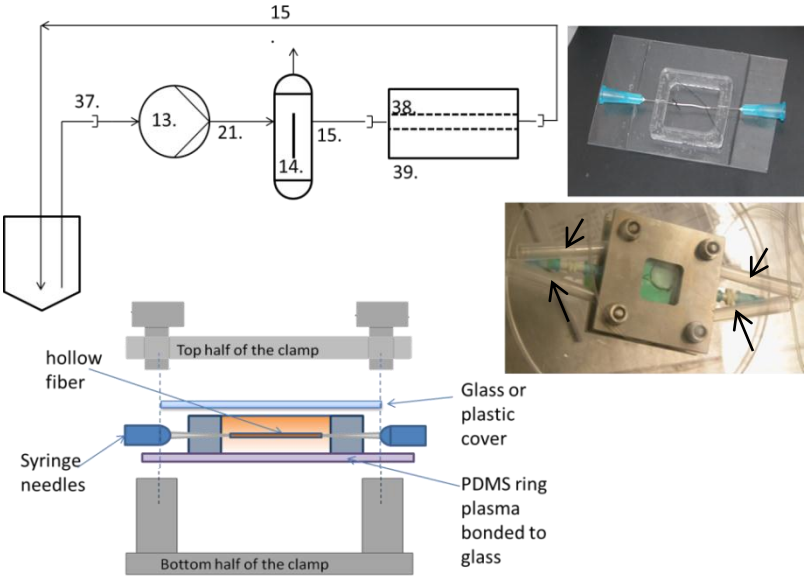

Figure C.6. An earlier version in the evolution of the PVEB, the PVEB2, was fabricated by casting a PDMS square ring (38) and plasma-bonding it to a glass slide. The PVEB2 featured a slit in the PDMS ring. Syringe needles 25G were tied, using Myco silk suture thread to 0.50 diameter hollow fiber (39). The PVEB2 was sealed using a stainless steel compression clamp. Lateral compression was occasionally applied, by wedging plastic P1000 pipette tips between the PDMS walls of the PVEB and the screws of the compression clamp, in an effort to quell leaks from where the needles passed through the slits in the PDMS. Above is the schematic of the perfusion circuit utilized in the hollow fiber bioreactor dye rinsing experiment (Section C.4.1.)

Perfusion Circuit

The perfusion setup was assembled as schematized in Fig. C.6. A 50 mL conical tube served as the reservoir for the perfusate. The perfusion circuit was sterilized by perfusing with 1-2 mL/min of 70% v/v ethanol for at least 30 minutes.

Perfused Vascular Explant Bioreactor PVEB 2

The previous section describes the procedures for the final version of the PVEB. An earlier implementation is worthy of note, as it was used for dye rinsing experiments. The second of five major iterations in the evolution of the PVEB was assembled prior to experimentation as in Fig. C.6. PDMS elastomer and curing agent were mixed in a 10:1 ratio, then poured into a 1 inch X 1 inch square, ring-shaped brass mold and cured at 60°C overnight. The resulting PDMS ring (39) was plasma-bonded to a 75 mm X 50 mm X 1 mm glass microscope slide. Afterward, a vertical slit was cut partially into opposite sides of the ring using a razor blade. Syringe needles (24G) were inserted into the ends of an approximately 1 inch segment of 0.5 mm polyacetylnitrile hollow fiber (38). The syringe needles were secured by using silk suture thread to tie a square knot around the hollow fiber with the needle underneath. The syringe needle/hollow fiber assembly was inserted into the slits of the PDMS. This assembly was sterilized prior to use via exposure to UV radiation overnight or by submersion in 70% (v/v) ethanol for at least 30 minutes, followed by submersion in DI water for at least 30 minutes.

C.4.1.2. Materials

Non-sterile 1x PBS was prepared months before use and stored at room temperature. A non-sterile 100 mM stock solution of fluorescein in DI water was prepared months before use and stored at room temperature in the absence of light.

C.4.1.3. Dye Rinsing Experiment

The P1000 pipette tips (indicated by the arrows in Fig. C.6.D) were wedged between the walls of the PVEB2 and the screws of the clamp immediately prior to experimentation (Fig. C.6.D). This was done in order to prevent leaks through the slits in the PDMS walls of the PVEB2. The PVEB2 was connected to the perfusion circuit. Non-sterile 1x PBS (4500 µL) was pipetted into a microcentrifuge tube and mixed via pipetting with 500 µL of fluorescein stock solution. Of the resulting fluorescein solution, 3 mL was pipetted into the abluminal space of the PVEB2. Immediately afterward, the glass cover of the PVEB2 was quickly placed on top of the reactor and the steel clamp was tightened around the reactor. The hollow was perfused inside the PVEB2 with 1x PBS from the reservoir at 400 µL/min continuously for at most 1 hour. Aliquots (100 µL) of the outflow from the PVEB were taken every minute by allowing it to drip into the wells of a 96-well plate. After a sample was dispensed into a well of the 96-well plate, that well would be covered with tape to reduce the evaporative loss from the sample.

C.4.1.4. Data Acquisition and Analysis

Of the samples that dripped into the wells of the 96-well plate, 50 µL of each was transferred into another well. This was done in order to keep the volume of each sample constant. Since it was observed that intense fluorescent emissions could scatter into adjacent wells, the 50 µL samples were not placed in adjacent wells. Fluorescence intensity of the 96-well plate was measured using a SPECTRAmax Plus 384 UV/Vis spectrometer. Alternatively, the 96-well was stored overnight at 4°C in the absence of light before measuring.

The fluorescence intensity of the eluent samples were plotted vs. time. The fluorescein concentration in the eluate from the reactor approaches pseudo-equilibrium. (If the volume of the abluminal space were infinite, the fluorescein would approach a true equilibrium.) The equilibrium concentration can be modeled using equations that describe membrane reactors.

$$\frac{dn_A}{dx} = r_A + R_A$$

Here, n_A is the molar flux of a reagent, A, L is unit length of the hollow fiber, r_A is reactive accumulation (zero in our case) per unit volume of the reagent and R_A is trans-membrane flux of reagent into the perfusate. This equation was simplified, by assuming that the perfusate flow rate and the reagent (fluores-

cein) concentration in the ablumenal space are constant along the length of the hollow fiber. The effect of radial variations of the perfusate velocity on trans-membrane fluorescein flux was neglected.

$$Q_V \frac{dC_A}{dx} = Ps\ (C_A - C_{ablumenal})$$

$$Q_V \ln\left(\frac{C_{A,x=L} - C_{abl}}{C_{A,x=0} - C_{abl}}\right) = P_S L$$

$$\frac{Q_V}{L} \ln\left(1 - \frac{C}{C_{abl}}\right) = P_s$$

Q_V is the volumetric flow rate of media in through the PVEB2, C_A, $C_{A,\ x\ =\ 0,}$ $C_{A,\ x\ =\ L}$ and C_{abl} are the fluorescein concentration along the length of the hollow fiber, at the entrance, at the exit and in the ablumenal space of the hollow fiber. P_S is the small molecule permeability per length of the hollow fiber. The concentration of the eluite reaches a pseudo-equilibrium. Consequently, the fluorescence intensity is roughly asymptotic. The average fluorescence intensities of the samples that appeared to be close to an asymptote were used in the following calculation in order to get a measure of small molecule permeability per length of hollow fiber, P_s,

$$P_S = \frac{Q_V}{L} \ln\left(1 - \frac{I}{I_0}\right), \quad (1)$$

where Q_V is the volumetric flow rate of media in through the PVEB2, L is the length of the hollow fiber, I is the fluorescent intensity of the eluent and I_0 is the fluorescent intensity of the solution in the abluminal space at the end of the experiment. This assumes that the fluorescent intensity was directly proportional the fluorescein concentration.

C.4.2. Mouse Aorta Fluorescent Microspheres Perfusion Experiment

At day 6 in culture and once angiogenic sprouting had occurred in the PVEB, the lumen of the aorta was exposed to a 1% w/w solution of 0.04 µm diameter fluorescent (in all channels) microspheres via injection. This procedure was adapted from Weinstein and colleagues who used fluorescent microspheres to image neovascularization in zebrafish[83]. The aorta was incubated with the fluorescent microspheres solution for 36 hours. The presence of microspheres inside angiogenic sprouts was detected using fluorescence microscopy.

C.4.2.1. Equipment

The same equipment was used in the Mouse Aorta Fluorescent Microspheres Perfusion Experiment as in the PVEB Mouse Aorta Assay (Section C. 3.1). Since this experiment was short-term, lasting only several hours, the CO_2 controller and CO_2 delivery path were not necessarily included in the perfusion circuit.

C.4.2.2. Materials

The same materials were used in the Mouse Aorta Fluorescent Microspheres Perfusion Experiment as in the Mouse Aortic Ring Assay (Section C.1.2). A sterile 5% w/w stock solution of fluorescent microspheres in DI water was purchased months before use, and stored at 4°C in the absence of light. A sterile 10% bovine serum albumen (BSA) in PBS stock solution was prepared using the standard recipe months before use, and stored at -20°C.

C.4.2.3. Culturing and Perfusing the Mouse Aorta with Microspheres

The aorta was explanted, catheterized and loaded into the PVEB as in the PVEB Mouse Aorta Assay (Sections C.1.3, C.1.4, C.3.5 and C.3.6). The aorta was cultured for six days until the appearance of angiogenic sprouts.

C.4.2.4. Loading Microspheres into the Aorta

The microsphere stock solution was sonicated using a Heat Systems Ultrasonics Model W-375 Sonicator™ (with water bath) on its highest setting, pulsed, for 2 minutes with a 25% duty cycle. A sterile solution containing 1% w/w microspheres and 2% BSA in PBS was prepared. The solution was drawn into the PVEB (into the aorta lumen). The catheter shield was placed onto a 1 mL syringe. About 150 µL of the microsphere solution was drawn into the syringe tip of the catheter shield. The syringe was connected to the upstream tubing sleeve (3) of the PVEB. The syringe was carefully disconnected from the syringe tip. Downstream, tubing was disconnected or vented, thereby creating a hydrostatic head of a few decimeters. Flow under this hydrostatic head was halted by manually reconnecting the downstream tubing once the microsphere solution had flowed down the length of the aorta. The PVEB was incubated under this no-flow configuration for 36 hours.

C.4.2.5. Data Acquisition and Analysis

Microsphere diffusion was inspected visually, using a 10-40X magnification Fluorescence Nikon Eclipse Ti equipped with a photometric Coolsnap HQ^2 digital camera and NIS-Elements AR software. Images were acquired at the TRITC emission bandpass of wavelengths (590-650), 50 ms exposure, and 1x gain (10X objective). Excitation of fluorescent materials was accomplished using a Nikon arc lamp on its minimum output setting (delivering a passband of excitation wavelengths, 475 -490 nm).

C.5. COMSOL Model of Small Molecule Diffusion and Convection in the PVEB

A mathematical model of small molecule transport via diffusion and convection in the PVEB2 was generated and solved using the finite element method. The mathematical model of bulk fluid flow utilized Navier-Stokes equations and Darcy's Law in the luminal and abluminal spaces of the PVEB, respectively. Fick's Law of diffusion and mass transport equations modeled solute mass transfer. COMSOL version 3.4 was utilized to integrate and solve the modeling equations.

C.5.1. Assumptions

This mathematical model of the bulk flow utilizes the following assumptions:

1. Perfusate is incompressible and Newtonian with spatially uniform and temporally constant viscosity.
2. End effects on axial flow in the hollow fiber or explant are neglected.
3. The velocity of perfusate leaking from the hollow fiber (i.e., filtrate) is continuous in the direction normal to the hollow fiber. A slip condition along the wall of the hollow fiber, however, is allowed.
4. The hollow fiber resistance to filtrate flow was considered small in comparison to resistance imparted by the matrix.
5. The matrix in the abluminal space was incompressible. The permeability of the matrix was isotropic, spatially uniform, and temporally constant.

Assumptions utilized in the solute transport model are as follows:

1. The small molecule solution is ideal (i.e., the enthalpy of mixing is zero and the solution density is independent of concentration).
2. Density is therefore constant and uniform.
3. Diffusivity of the solution is isotropic, spatially uniform and temporally constant.
4. The solute concentration is small enough to allow us to neglect osmotic effects.

Commonly used assumptions and approximations were also utilized in the model:

1. Constant and uniform temperature.
2. The model is at steady state.
3. Gravitational force is neglected.

C.5.2. Geometry

The PVEB geometry that was modeled was 1 cm x 1 cm x ~0.5 mm. The centerline of a 0.5 mm diameter straight hollow fiber passed through the center of the reactor parallel to the 1 x 1 cm square. The mathematical model of the PVEB was solved for a planar cross-section that was through the centerline of the

hollow fiber and parallel to the floor of the reactor. The cylindrical geometry of the hollow fiber was neglected.

C.5.3. Equations

Bulk fluid flow was modeled using the continuity (2), Navier-Stokes (3) and Darcy's Law (4) equations.

$$\nabla \cdot \boldsymbol{V} = 0 \ , \tag{2}$$

$$\frac{\partial \boldsymbol{V}}{\partial t} + \boldsymbol{V} \cdot \nabla \boldsymbol{V} = \ -\frac{1}{\rho}\nabla p + \ \vartheta \nabla^2 \boldsymbol{V} + \boldsymbol{F} \ , \tag{3}$$

$$\boldsymbol{V} = \ -\frac{K}{\mu}\nabla p \ . \tag{4}$$

In these equations, $\boldsymbol{V}$ is the velocity vector, p is pressure and $\boldsymbol{F}$ is force vector acting on the bulk of the fluid (assumed to be zero). Constants, ρ, ν, μ and K are fluid density, kinematic viscosity, dynamic viscosity and matrix permeability, respectively. Solute transport was modeled using the mass transport equation (5)

$$\frac{dC}{dt} = D\nabla^2 C - \boldsymbol{V} \cdot \nabla \mathrm{C} + \mathrm{R} \ . \tag{5}$$

C and D are concentration and diffusivity of the solute, respectively; R is a reactive consumption of the solute (e.g., metabolism). Boundary conditions were assigned as follows: The inlet was fully developed Poiseuille flow (in a cylindrical tube), as given by

$$\frac{2Q_V}{\pi R^2}\left(1 - \frac{r^2}{R^2}\right) = V_Z \ . \tag{6}$$

In this equation, Q_V is the volumetric flow rate in the tube, and V_Z is the fluid velocity in the axial direction. R and r are the tube radius and radial position of the fluid stream, respectively. The radial component of velocity at the inlet is zero. Pressure was also continuous across the hollow fiber membrane. Pressure at the outlet is zero. Velocity component normal to the hollow fiber is continuous across the hollow fiber membrane. The walls of the reactor are insolating (i.e., the velocity component normal to the walls is zero).

Material properties, density (ρ) and viscosity (μ) of water at 37°C were assigned to the solution. The matrix permeability, K, was assigned that of 1% collagen 1000 nm^2. The diffusivity of the small molecule was assigned that of sugar in water at 25°C, 0.66 $m^2/sec \times 10^9$. The volumetric flow rate Q_V and the hollow fiber radius were values used in experiments (100 μL/min and 0.25 mm, respectively). Reactive consumption, R, was selected arbitrarily such that the negative values for solute concentration did not result $1mol/sec \times 10^{-10}$.

C.5.4. Numerical Methods

COMSOL Multiphysics 3.4. was used to integrate and solve Equations 2-6 and boundary conditions. A mesh that was fine near the hollow fiber and coarse further away (Fig. D.7 (A)) was created. The mesh contained 12000 elements. The fluid flow solution for the Navier-Stokes region was computed for an impermeable tube. The pressure in this solution provided the boundary condition for the Darcy's Law region. The Navier-Stokes region was re-solved using the fluid velocity along the edge of the hollow fiber (computed via Darcy's Law). This process was iterated until the solutions for pressure converged exactly. The solution for fluid velocity was used in the convective term of the solute mass transfer equation (5).

C.6. Hydraulic Impedance Measurements of a Perfused Aorta *In Vitro*

The impedance to fluid flow, imparted by a perfused mouse aorta, was monitored over time. Manometers placed immediately upstream and downstream of the PVEB provided a measure of the pressure (head) difference across the PVEB. This pressure (head) difference was used to calculate the impedance for a particular flow rate.

C.6.1. Equipment

C.6.1.1 Dissection Equipment

The same equipment was used in Impedance Measurement Experiments as in the Mouse Aortic Ring Assay (Section C.1.1). The PVEB, peristaltic pump, and perfusion tubing were used to culture the whole aorta instead of the 96-well plates. In addition, Exel Safelet shielded 24G catheters were used. Occasionally, Myco or Ethicon silk suture thread was utilized to secure the aorta on the catheter.

C.6.1.2. Incubation and Perfusion Equipment

The same incubation and perfusion equipment was used in the Impedance Measurement Experiment as in the PVEB Mouse Aorta Assay (Section C.3.1.2). The perfusion circuit that used the Bioscience Tools miniature incubator was used in the Impedance Measurement Experiment. Polypropylene 1/16" ID barbed T-joint tubing connecters (41) were added to the perfusion circuit upstream and downstream of the PVEB and miniature incubator. A manometer (i.e., Tygon tubing (15) extending vertically for about 1.5m from the PVEB and opening to the room) was connected to the perfusion circuit at these T-joints (40). Prior to experimentation, the perfusion circuit was sterilized and rinsed as in the PVEB Mouse Aorta Assay (Section C.3.1.3). The ends of the two manometers were connected using a 1/8" piece of tubing sleeve (2) during the sterilization step. The PVEB was assembled and sterilized as in the PVEB Mouse Aorta Assay (Section C.3.1.4).

C.6.2. Culturing the Aorta and Measuring its Impedance to Fluid Flow

The mouse was euthanized and the aorta explanted in the Impedance Measurement Experiment as in the Mouse Aortic Ring Assay (Sections C.1.3 and C.1.4). The aorta was catheterized and loaded into the PVEB as in the PVEB Mouse Aorta Assay (Sections C.3.6 and C.3.7). The aorta was maintained in culture as in the PVEB Mouse Aorta Assay.

C.6.3. Data Acquisition

Columns of EBM-2 media accrued inside the manometers. The following equation relates the difference in the heights of these columns of fluid to the impedance (*Z*) imparted by the aorta underflow

$$Z = \frac{\rho g(h_0 - h)}{Q}, \tag{7}$$

where h_0 and h are the respective heights of the manometers upstream and downstream of the PVEB, Q is the volumetric flow rate of perfusate (as set by the peristaltic pump), ρ is the density of the media (approximated as that of water) and g is the acceleration of gravity (9.8 m^2/s). The pressure readings of the manometers were converted to from Pascals to mmHg by dividing by 133.33 mmHg/Pa.

CHAPTER IV

RESULTS

Current technologies facilitate the study of angiogenesis in organ explant cultures. Variations to the organ explant culture, particularly the aortic ring assay, have been implemented to improve mass transport in and investigate (in the short term) mechanical properties of the aorta. We further expand the capabilities of the organ explant cultures to:

1) accomplish long-term culture of a whole aorta,
2) facilitate angiogenic outgrowth from the whole aorta,
3) maintain a perfusable connection to the aorta lumen, and
4) facilitate angiogenic outgrowth from a perfused aorta.

We accomplished these tasks using the PVEB. We also demonstrated (in principle) the potential of the PVEB, or future improvements to the PVEB, to control mass transport and measure mechanical properties of the aorta.

D.1. Mouse Aortic Ring Assay

Our study began with the already established technique: the mouse aortic ring assay. This starting point for the development and implementation of the PVEB served as a standard with which angiogenesis in the PVEB was compared. Representative aortic ring assays are shown in Fig. D.1. While variations in the extent and rate of angiogenesis were observed, the mouse aortic ring assay has, by day 6 in culture, produced a densely vascularized, roughly continuous tubule network that extended radially from the aortic ring. The tubule network was highly branched and branch points occurred uniformly throughout the outgrowth. Angiogenesis typically favors the ends of the aortic rings or severed arborizing arterials, but angiogenic outgrowth was routinely observed along the sides of the aortic rings as well. Prolonged culturing of the aortic ring assays produced angiogenic sprouts that were highly branched and disorganized, with several discontinuities. In Fig. D.1, an example of this is labeled (C6). The morphological changes that accompany prolonged culturing typically occur by day 8 in culture. It was observed that the rate and extent of angiogenesis assay varies with mouse genetic background (BALB/C, C57, etc.), age and sex (data not shown). In an aortic ring assay which used Tie-2::GFP positive mice, fluorescent vascular sprouts extended from the aortic ring. The fluorescence intensity of the vascular sprouts was much less than that of the much larger aortic ring.

D.2. Evolution of the Perfused Vascular Explant Bioreactor

The design of the PVEB underwent several modifications. Concurrently, the vasculature (aorta) explanting and PVEB loading techniques underwent iteration. In this way, the PVEB design and vasculature handling techniques were tailored to each other. While the aorta explantation technique was being developed, a hollow fiber served as a model of the aorta in initial designs of the PVEB. Problems with initial designs included leaks and contamination, excessive use of materials (e.g., Matrigel), difficult and time-consuming loading of the aorta and poorly maintained temperature and pH. The first design of the PVEB (PVEB1) featured a one-inch square PDMS ring that was plasma-bonded to glass. Plastic gel loading tips that were pushed through the walls of the PVEB served as perfusion connectors for the aorta. A coverglass served as a lid to the PVEB1, and VELAP was utilized to seal the reactor. This design suffered all the aforementioned drawbacks. VELAP did not adequately seal the PVEB1, and the perfusion connectors were fixed to the walls of the PVEB1 (and often misaligned), making it difficult to load an aorta onto them. It was observed that small slits in the PDMS would self-seal, thereby preventing leaks. The PVEB2, shown in Fig. C.6, featured a slit in the PDMS ring, allowing catheterization of the aorta (*in situ* or *ex vivo*) prior to loading it into the reactor. The slit also accommodated easy loading of the syringe/catheter-aorta assembly. The slit reduced sample loading times to less than an hour for hollow fibers. VELAP and a compression mechanism – utilizing magnets placed on the PVEB2 lid and magnetite dopant in the PDMS ring – were explored as means of suppressing leaks through the lid of the reactor. They were unsuccessful. A steel clamp was developed to prevent leaks through the lid of the PVEB2, but this design had problems too. To prevent leaks the depth of the slit had to be small relative to the height of the ring. This situated the aorta toward the top of the reactor (away from the objective of the microscope). Simple approaches to sealing leaks through the slit in the PDMS using various lateral compression devices were ineffective. The device was leak–prone, especially when larger slits were cut into the PDMS walls. The volume of the reactor was still excessive. Nonetheless, this device was employed in experiments.

Other PVEB designs sought to accommodate aortas that had been catheterized prior to loading into the PVEB. These designs presented movable Luer connectors onto which the catheter could fit. Unfortunately, these designs also excessively used materials and situated the aorta far from the objective. The most recent PVEB designs (described in the Methods sections) were sufficient to culture an aorta and facilitate angiogenic outgrowth from an aorta that was connected to an external perfusion setup. Here, we adapted the catheterization of the aorta using shielded cannulae to fit commercial ferrule fittings. The polycarbonate walls of the reactor were sterilizable via ethanol. The angled design of the bioreactor serves two functions: 1) to provide clearance for the forceps when loading the reactor, and 2) to locate the aorta closer to the objective. This design, the PVEB5, resisted leaks and contamination and successfully maintained and grew angiogenic sprouts from an aorta that was connected to an external perfusion setup.

D.3. Whole Aorta Angiogenesis Assay

To investigate biological morphological consequences of culturing the whole mouse thoracic aortas (as opposed to sub-millimeter slices used in the aortic ring assay), whole aortas were cultured in Matrigel and angiogenic outgrowth was observed. The Whole Aorta Angiogenesis Assay also served as a platform for developing and implementing aorta explantation and catheterization strategies. Catheterized aortas embedded in Matrigel and cultured in a Petri dish with complete EBM-2 routinely produced angiogenic outgrowths from the aorta that consisted of densely vascularized, roughly continuous tubule networks similar to those observed in the mouse aortic ring assay (Fig. D.2.). The tubule network was highly branched, and branch points appeared uniform throughout the outgrowth. Angiogenesis occurred along the side and ends of the aorta and typically favored severed arborizing arterials. Myco or Ethicon suture threads were occasionally utilized to secure the aorta on the catheter. Angiogenesis did not occur near the sutures. In whole aorta assays lacking suture thread, angiogenesis occurred along the entire length of the aorta, including sections that contained the catheter. Although variations in the extent and rate of angiogenesis were observed, the whole aorta angiogenesis assay produced angiogenic outgrowth typically by day 6 in culture. Initial whole aorta angiogenesis assays took more than an hour to assemble, but with practice, the technique improved and decreased the amount of time required to 30 minutes or less. In earlier assays, angiogenesis occurred more slowly. Prolonged culturing of the whole aorta angiogenesis assay produced angiogenic outgrowth with disorganized and discontinuous structure similar to that in Fig. D.1. (labeled C6).

After seven days in culture aortas were retrieved from the cell culture dish, fixed in 10% formalin for 24 hours, sliced and hematoxylin and eosin (H&E) stained (top row of Fig. D.4). Structure features of surrounding angiogenic outgrowths were lost as the aorta was manually separated from the cell culture dish. The medial region of the aorta was stained violet and pink with dark spots scattered throughout. The medial region also contained layers of ribbon-like folds. In contrast, a dead aorta (i.e. one that suffered prolonged exposure to ambient conditions (room temperature and low CO_2 and humidity)) stained more orange and lacked the dark spots (Bottom row of Fig. D4). The media was also smooth. The top row of Fig. D.4 shows a small puncture or rupture in the medial region of the aorta. The dark dots were more frequent in this region.

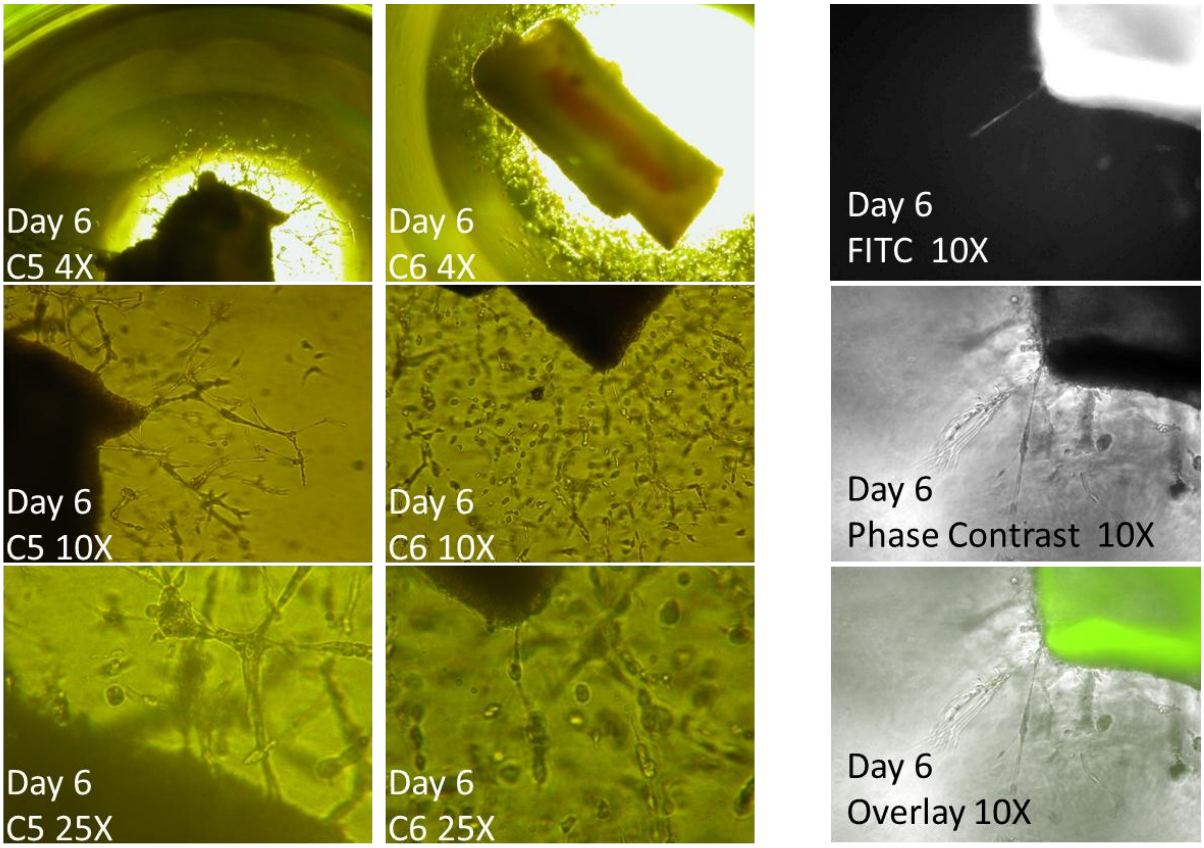

Figure D.1. Demonstrative aortic ring assay. Two slices from the same aorta, embedded in Matrigel and cultured in complete 150 µL EBM-2 for six days produced angiogenic outgrowths that extended radially from the aorta segment. The tubule network was roughly continuous and highly branched, with branch points existing uniformly throughout the outgrowth. In the aortic ring assays, angiogenic outgrowth favored the ends of the aorta slice, although angiogenesis occurred on severed arterials and along the sides of the aorta slice as well. Angiogenic sprouts tended to become disorganized after prolonged culturing. The larger aorta slice in this assay (C6) has a highly branched capillary network with several discontinuities in the tubes characteristic of angiogenic outgrowths subjected to prolonged culturing. This would begin at different points in culture typically after 8 days.

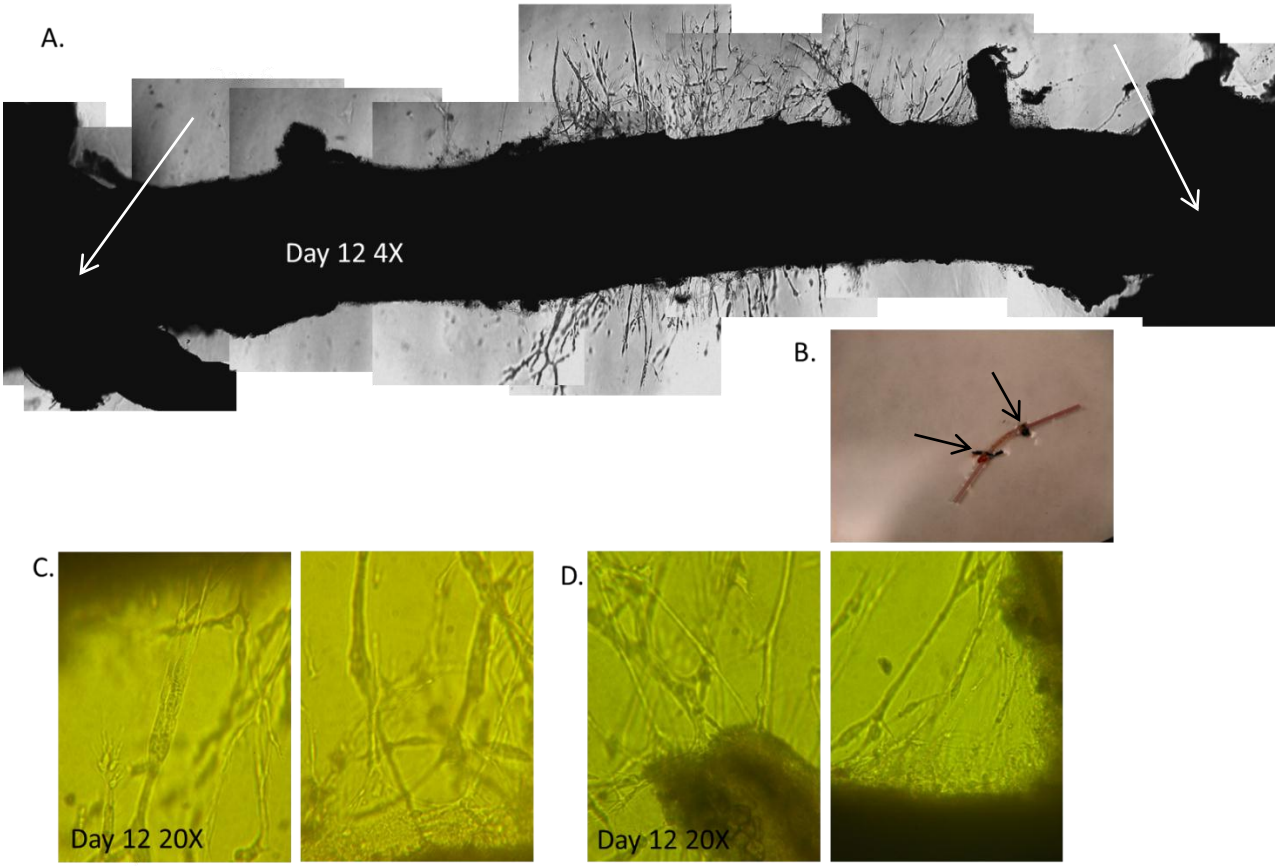

Figure D.2. Demonstrative whole aorta angiogenesis assay. This aorta was catheterized, embedded in Matrigel and cultured in a Petri dish with complete EBM-2. Angiogenic sprouting was observed by day 12 (but typically earlier) in culture. Angiogenic outgrowth extended from the aorta, except near the knots in the Ethicon suture thread,indicated by arrows in (A) and (B). The outgrowth consisted of densely vascularized, roughly continuous tubule networks similar to those observed in the mouse aortic ring assay (Fig. D.1). The tubule networks were highly branched, with bifurcating branch points appearing uniformly throughout the outgrowth. Angiogenesis occurred along the sides (C) and from severed arborizing arterials (D).

D.4. Perfused Vascular Explant Bioreactor (PVEB) Mouse Aorta Assay

The PVEB enabled long-term (up to two weeks) culture of the whole aorta while maintaining a perfusable connection to the aorta lumen. The PVEB also facilitated angiogenic outgrowth from a perfusable and a perfused aorta. Sections D.4.1 and D.7. provide details of these observations.

D.4.1. PVEB Mouse Aorta Assay without Flow

Catheterized aortas that were embedded in Matrigel and cultured with complete EBM-2 inside the PVEB routinely produced angiogenic outgrowths that resembled those grown in the whole aorta angiogenesis assay (Section D.3.) Tubular networks were largely similar to those observed in the whole aorta angiogenesis and the mouse aortic ring assays: densely vascularized and highly branched with bifurcating

branch points appearing uniformly throughout the outgrowth (Fig.D.3.). Angiogenesis occurred in vented PVEBs (i.e., having the lid and top gasket removed from the assembly) and sealed PVEBs. Evaporative loss of media from the abluminal space was noticeable in the vented PVEB. In the sealed PVEB, angiogenesis did not occur if the media added to the abluminal space had not been equilibrated to 5% CO_2 beforehand. The angiogenic outgrowth in the PVEB without flow occasionally contained regions whose morphology differed from that observed in the mouse aortic ring and whole aorta angiogenesis assays. In these regions, outgrowths extended from the aorta without traversing much into vertical axis. The tubules appeared smoother and fainter than those occurring in the aortic ring assay. They are highly branched, and branch points appeared uniformly throughout the outgrowth. These branch points were typically multifurcated, unlike those in outgrowths occurring more routinely in angiogenesis assays (which were typically bifurcated). Although variation in the extent and rate of angiogenesis was observed, the PVEB mouse aorta angiogenesis assay absent flow produced angiogenic outgrowth typically by day 6 in culture. Prolonged culturing of the aortic ring assays produced angiogenic sprouts that were highly branched and disorganized, with several discontinuities. The morphological changes that accompany prolonged culturing typically occur by day 8 in culture.

After seven days in culture, aortas were retrieved from the PVEB, fixed in 10% formalin for 24 hours, sliced, and H&E stained (middle row of Fig. D.4). Morphological features of the stained aorta were identical to those observed in the whole aorta angiogenesis assay. The aorta that was cultured in the PVEB contrasted strongly with the aorta subjected to prolonged exposure to ambient conditions (room temperature and low CO_2 and humidity).

D.5. Small Molecule and Microsphere Perfusion Experiments

Mindful of the mass transfer characteristics (potentially mimicking that *in vivo*) engendered in the intraluminal perfusion of a vascular explant, initial steps were taken to model mass transport of small molecules in the PVEB. Finite element analyses of Stokes-Poiseuille and Darcy's Law flow equations in section D.5.2. provide a model of bulk fluid flow in the intraluminal and abluminal spaces of the PVEB, respectively. Finite element analyses of Fick's diffusion and convectional mass transport modeled small molecule, salute transport in the PVEB. Section D.5.3. details how fluorescent microspheres facilitated analysis of the transport of larger particles (0.04 μm) in the PVEB.

D.5.1. Hollow Fiber Dye Rinse Out

To quantify transport across a hollow fiber in a PVEB, the abluminal space of PVEB2 was loaded with fluorescein solution in PBS, and rinsed via perfusion of the hollow fiber (with 400 μL/min) with clean PBS. The eluent samples contained dilute amounts of fluorescein. The fluorescent intensity of eluent samples from the PVEB2 were initially high, but decreased toward an asymptotic (average) intensity of 12.5×10^3 ± 385 arbitrary units, eleven minutes after perfusion was initiated (Fig.D.6.). The initial fluorescent intensity of fluorescein in the abluminal space was 142×10^3 arbitrary units. These data when used in equa-

tion (1) give $6x10^{-8}$ m^2s^{-1} as an estimate of small molecule permeability per length of hollow fiber. This estimate of solute permeability was utilized in the COMSOL model of small molecule transport in the PVEB. By the end of the rinsing experiment the intensity of the abluminal space had dropped to $134x10^3$.

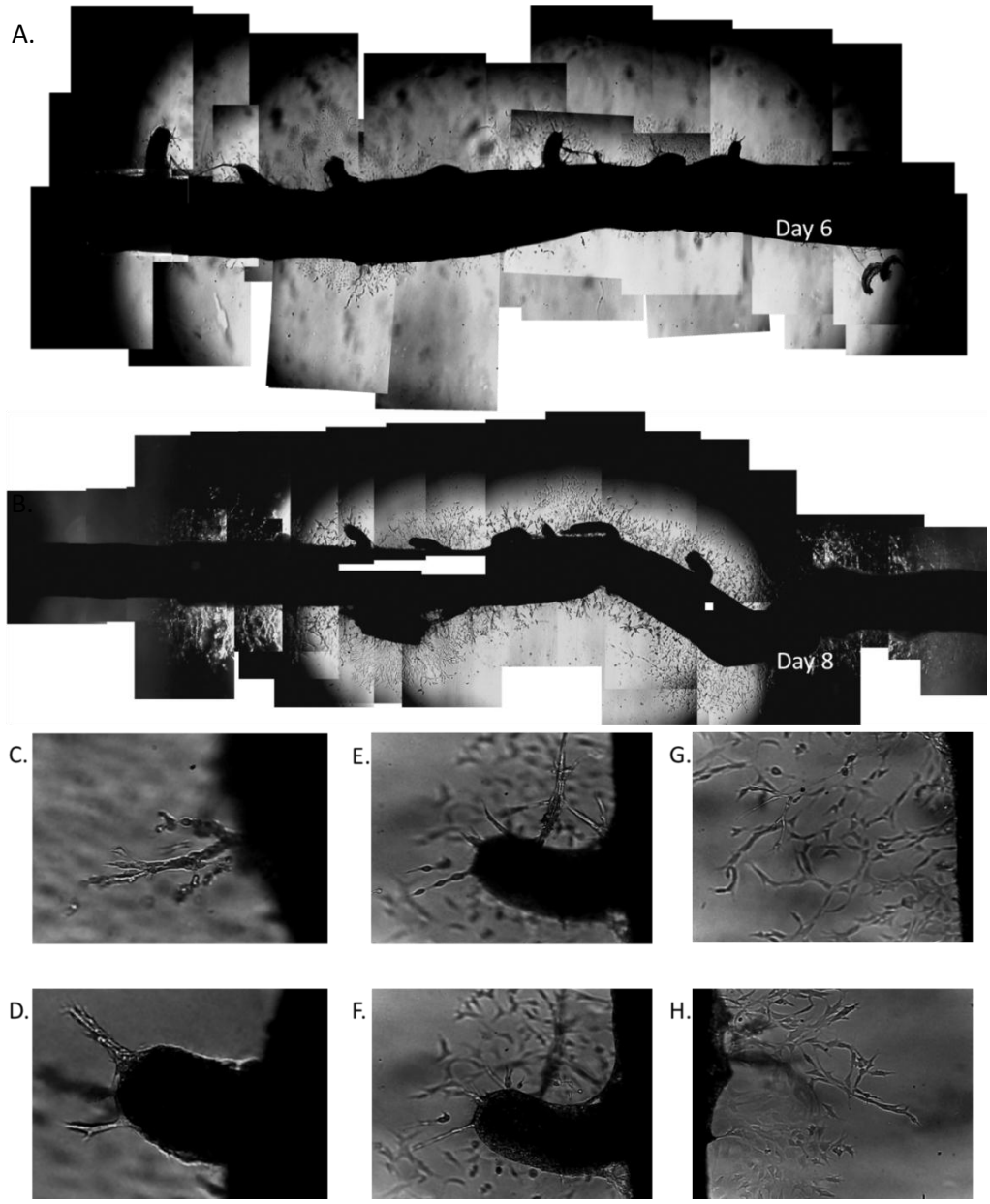

Figure D.3. The PVEB mouse aorta angiogenesis assay absent flow. Aortas, housed in the PVEB without flow, produced angiogenic outgrowth by day 6 in culture (A). Angiogenic outgrowth typically favored severed arterials but also occurred along the sides of the aorta. By day 8 in culture (B) the angiogenic outgrowth began to assume the more disorganized morphology shown in Figure D.1 (C6). Images of specimens inside the PVEB contained an oval shaped shadow that correlated with the rounded opening in the top of the reactor. Tubule networks sprouting from the C) sides and D) severed arterials were morphologically similar to those in the (Fig. D.1) aortic ring and (Fig. D.2) whole aorta angiogenesis assays. Angiogenesis extended vertically into different focal planes (E and F). The angiogenic outgrowth contained regions whose morphology differed from that observed in the mouse aortic ring and whole aorta angiogenesis assays (G and H). Angiogenesis in these regions extended from the aorta without traversing much into vertical axis. The tubules appeared smoother and fainter than those in the aortic ring assay. They are highly branched, and branch points appeared uniformly throughout the outgrowth. These branch points were typically multifurcated, unlike those in outgrowths occurring more routinely in angiogenesis assays (which were typically bifurcated).

D.5.2. COMSOL model of Small Molecule Transport in the PVEB

Numerical analysis (utilizing finite element method in COMSOL) of fluid flow and solute mass transfer in the PVEB2 is shown in Fig D.7. The surface plots that were generated show slight transmembrane pressure difference as the driving force for filtrate flow. Filtrate fluid velocities were approximately 2 nm/s, six orders of magnitude less than perfusate velocity (approximately 1 cm/s at the centerline). The model depicted nonzero tangential fluid velocity in the abluminal space along the wall of the hollow fiber.
In computing a solution to the fluid flow model on a mesh consisting of 11984 elements, 11051 degrees of freedom were solved for by COMSOL 3.4., resulting in convergence standard to the COMSOL code. Filtrate flux across the hollow fiber wall caused perfusate fluid velocities to deviate, but no more than 5 percent along the axis of the hollow fiber. Glucose concentration decreased nonlinearly with increasing distance from the hollow fiber.

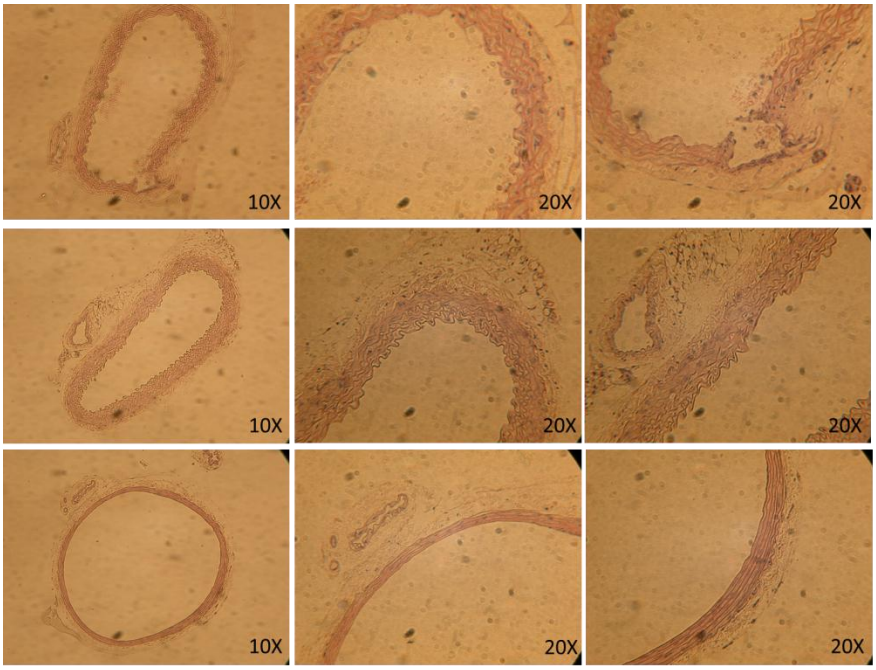

Figure D.4. H&E staining of an aorta cultured six days in Matrigel (top row) or in the aorta bioreactor without flow (middle row) produced dark hemalum stains, indicative of live tissue, throughout the aorta slice. A dead aorta (bottom row) is indicated as such by the lack of hemalum staining of the cell nuclei. An aorta cultured in the PVEB for at least six days without flow was fixed in the 10% buffered formalin and stained with H&E. This aorta was manually separated from the glass it was cultured against, so most of the sprouts were lost before staining. Arteries that extend from the aorta appear in these slices. In the top row there is a small puncture or rupture in the elastic lamina (tunica media) of the aorta. Cells extend into this rupture and slightly behind.

D.5.3. Perfusion of the Aorta with Microspheres

To investigate the potential of the PVEB to independently control properties of the aorta lumen and abluminal space, fluorescent microspheres were loaded into the lumen of the aorta that had undergone angiogenic sprouting. Aortas that were cultured six days in the PVEB without intraluminal perfusion produced angiogenic outgrowth that fluoresced when the aorta lumen was filled with a 1% (w/w) solution of 0.04 µm diameter microspheres and incubated 36 hours. Fluorescent illumination was observed in the aorta, severed arborizing arterials, regions of the nascent vasculature, and regions of the abluminal space. The aorta was twisted during culture Fig. D.8. (A and B). While watching the aorta on the microscope, microspheres were injected into the left side of the aorta. The red hue of the microsphere solution did not go beyond the twist in the aorta. Instead, it was observed in the abluminal space adjacent to

the twist in the aorta. Microspheres were carefully injected into the right side of the aorta and the red hue of the microsphere solution reached the twist in the aorta but did not go further.

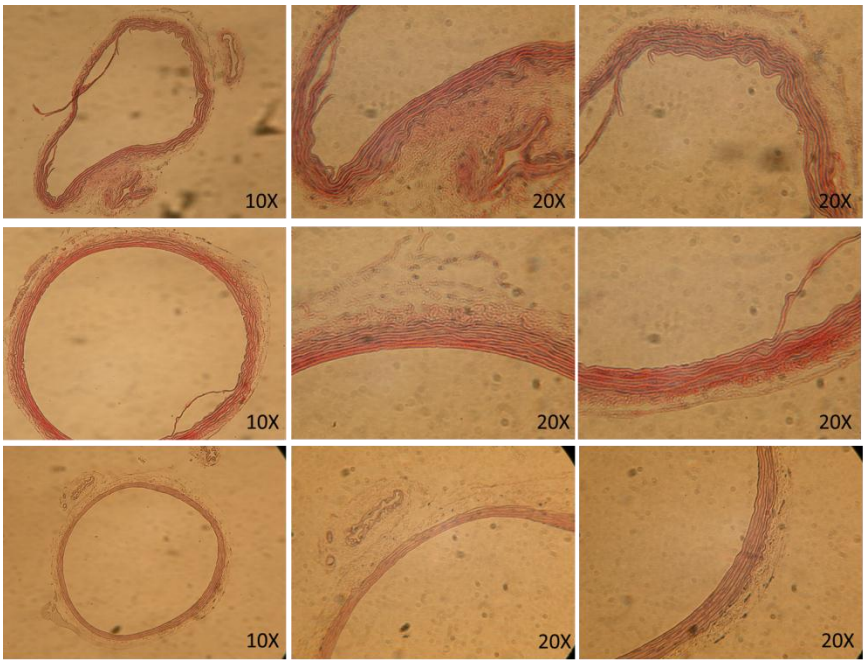

Figure D.5. H&E staining of two aortas cultured four days in the PVEB with flow (top two rows) and of a dead aorta (bottom row). The hydraulic empedence of the aortas was monitored while culturing. Different hydraulic impendance curves were observed for the top two aortas (Fig.D.9). The dead aorta and one of the perfused aortas lack hemalum staining of the cell nuclei. The aortas were manually separated from the glass they were cultured against, so most of the sprouts were lost before staining. Arteries that extend from the aorta appear in these slices.

D.6. Impedance Measurement

Mechanical properties of vascular explants have been conducted on vessels maintained short term (up to 7 hours)[106]. To investigate the potential of the PVEB to monitor a mechanical property of the aorta in long-term culture, impedance to fluid flow imparted by the aorta was monitored during PVEB mouse aorta angiogenesis experiments. Manometers, utilized to determine impedance, provided readings as long as they connected to the operating perfusion circuit (up to 72 hours). Two characteristic curves shown in Fig. D.9. describe the temporal dependence of aortic impedance: 1) Impedance imparted by the aorta gradually increased for 8 to 14 hours, then decreased to less than its initial volume. From there, it would continue to decrease, albeit gradually. 2) More commonly, the impedance imparted by the aorta would increase gradually until it overwhelmed the manometer (i.e., the aorta produced a head in excess of two meters). Since the manometer was open, perfusate would get diverted out of the manometer instead of flowing through the PVEB.

Hematoxylin and eosin (H&E) staining (Fig D.5.) revealed morphological and staining differences between aortas that maintained high impedance to flow and aortas that gradually decreased in impedance. The medial region of aortas that maintain high impedance to flow stained violet and pink with dark spots scattered throughout (Fig. D.5. top row). This resembled hematoxylin and eosin staining of aortas cultured without flow. H&E stains of the tunica media of aortas (Fig. D.5.) which peaked then gradually decreased in impedance were smoother and lacked the dark spots observed in stains of aortas cultured without flow.

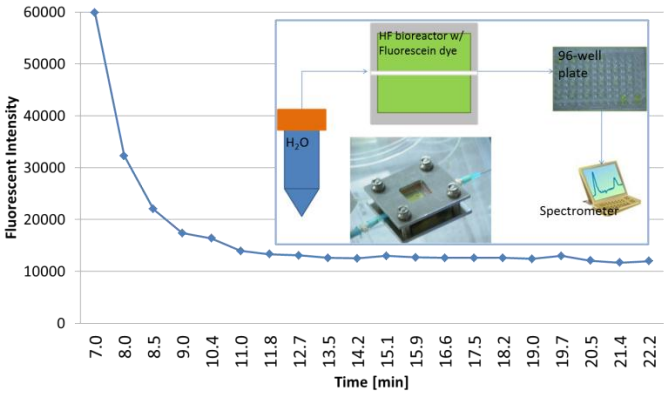

Figure D.6. The fluorescent intensity of eluent samples from the perfused hollow fiber (with 400 μL/min of clean PBS) of the PVEB2 were initially high, but decreased toward an asymptotic (average)intensity of $12.5x10^3$ ± 385 arbitrary units, eleven minutes after perfusion was initiated. The fluorescent intensity of fluorescein in the abluminal space was $142x10^3$ arbitrary units. With these data, Equation (1) gives $6x10^{-8}m^2s^{-1}$ as an estimate of small molecule permeability per length of hollow fiber.

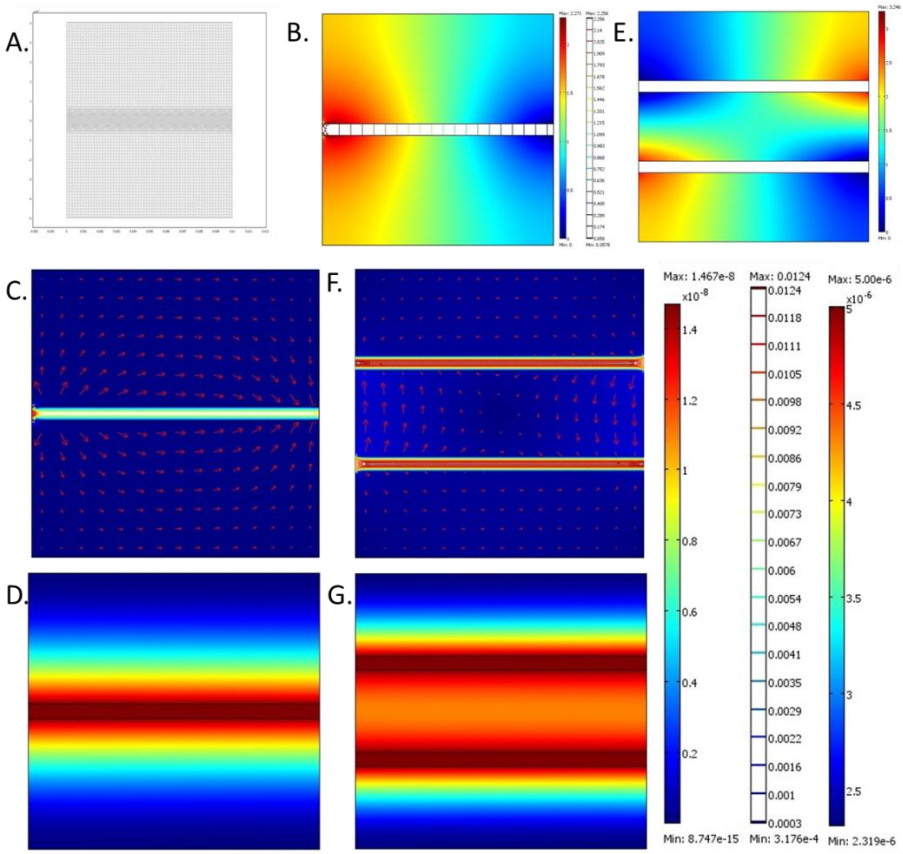

Figure D.7. Model of fluid flow and solute mass transfer in the PVEB2 with one hollow fiber (B,C and D) and two hollow fibers (E, F and G) computed using finite element method in COMSOL 3.4. Surface plots of pressure (B and E) distribution describe the abluminal space as slightly less pressurized than the lumen of the hollow fiber (for the half of the hollow fiber proximal to the inlet). In the half of the hollow fiber close to the outlet, abluminal space is slightly more pressurized. The pressure difference along the length of the hollow fiber was 2.3 Pa in the PVEB with one hollow fiber. Surface and vector field plots (C and F) describe a fluid velocity in the abluminal space as uniform and less than 2 nm/s. In contrast the centerline fluid velocity in the hollow fiber was several orders of magnitude larger (approximately 1 cm/s). The model depicted nonzero tangential fluid velocity in the abluminal space along the wall of the hollow fiber. The two hollow fiber PVEB2 with countercurrent flow created a dead zone (i.e. lacking fluid flow) in the center of the abluminal space of the reactor. Glucose availability (D and G) decreased with increasing distance from its source, the hollow fiber. In computing the flow regime, 11051 degrees of freedom were solved for by COMSOL 3.4.

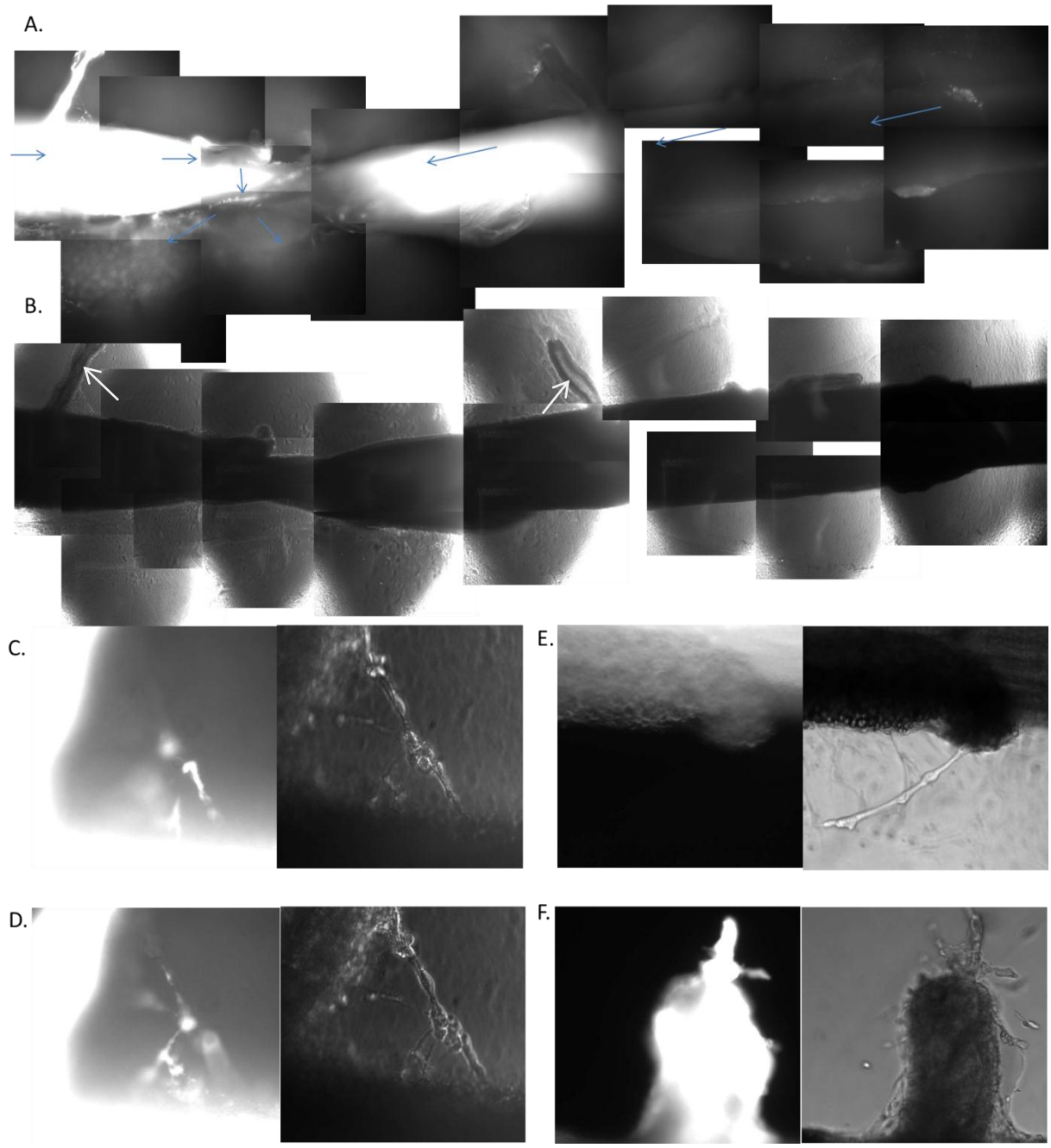

Figure D.8. Aortas that were cultured six days in the PVEB without intraluminal perfusion produced angiogenic outgrowth that fluoresced when the aorta lumen was loaded with a 1% (w/w) solution of 0.04µm diameter microspheres incubated 36hours. Fluorescent illumination in the TRITC emission band pass of wavelengths (590 to 650 nm) was observed A) in the aorta, severed arborizing arterials (indicated by arrows in B)), regions of the nascent vasculature, and regions of the abluminal space. Microspheres were loaded via syringe into both ends of the aorta, while monitoring the aorta on a microscope (10x objective). The arrows in A) indicate the direction of fluid flow that occurred during injection of the microspheres. Microspheres exuded into the abluminal space where the aorta was obstructed by a twist. Regions of the aorta (severed arterials and angiogenic outgrowth) with catheter subjacent did not fluoresce. The fluorescence in the angiogenic outgrowth followed the morphological patterns of vascular sprouts (C and D). Fluorescent images of the vascular sprouts followed the same pattern as those in the phase contrast images or, they formed smaller patterns which fit inside the patterns of the vascular sprouts in the phase contrast images. E) Vascular sprouts along the edge of the aorta fluoresced less often than sprouts near the severed arteries. F) If too much pressure is applied to the syringe when injecting microspheres into the aorta lumen, microspheres would be pushed out of the aorta and damage the vascular sprouts. Aortas not exposed to the fluorescent microspheres did not fluoresce.

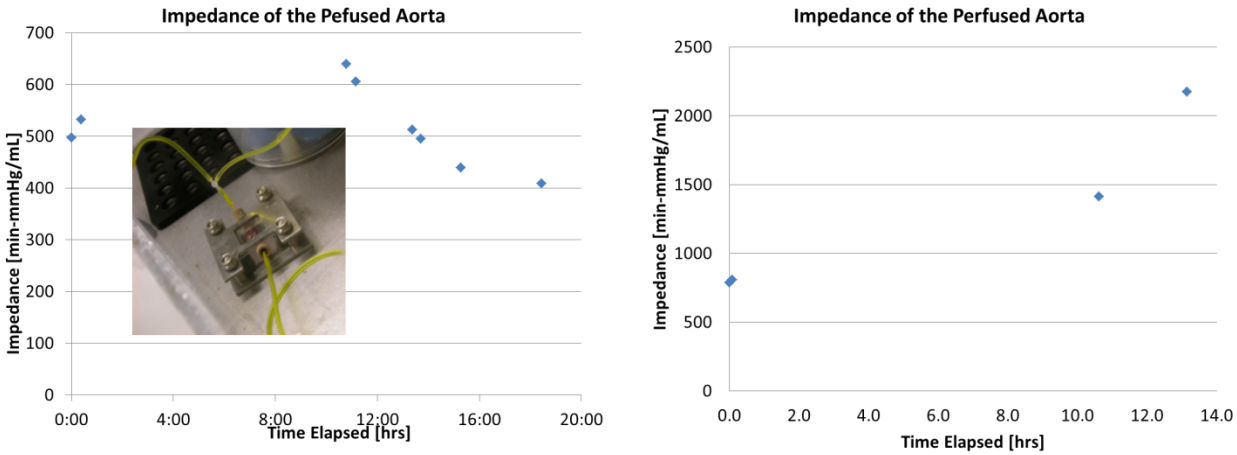

Figure D.9. Two characteristic curves of the temporal dependence of impedance to fluid flow imparted by the aorta. A) Impedance imparted by the aorta gradually increased for 11 hours, then decreased to less than its initial value followed by a gradual decrease from there. B) The impedance imparted by the aorta climbed gradually beyond the range of the manometer. Since the manometer was open, perfusate would get diverted out of the manometer instead of flowing through the PVEB.

D.7. Angiogenic Outgrowth from a Perfused Mouse Aorta

Aortas cultured inside the PVEB with 50 µL/min intraluminal perfusion of EGM-2 produced angiogenic outgrowths. These outgrowths resembled those grown in the whole aorta angiogenesis assay. Tubular networks were largely similar to those observed in the whole aorta angiogenesis assay, and they were highly branched with bifurcating branch points appearing uniformly throughout the outgrowth. A different morphology, identical to that discussed in section D.4.1., was observed in some regions of the angiogenic outgrowths. Although variation in the extent and rate of angiogenesis was observed, the PVEB mouse aorta angiogenesis assay with flow produced angiogenic outgrowth typically by day 6 in culture with initial sprouting occurring by day 4 from severed arterials. Angiogenic sprouting seemed to prefer the severed arterials over the sides and ends of the aorta. If the lumen of the aorta is not flushed prior to culturing, extant blood cells, platelets and debris would exude through severed arterials or other holes in the aorta wall into the abluminal space.

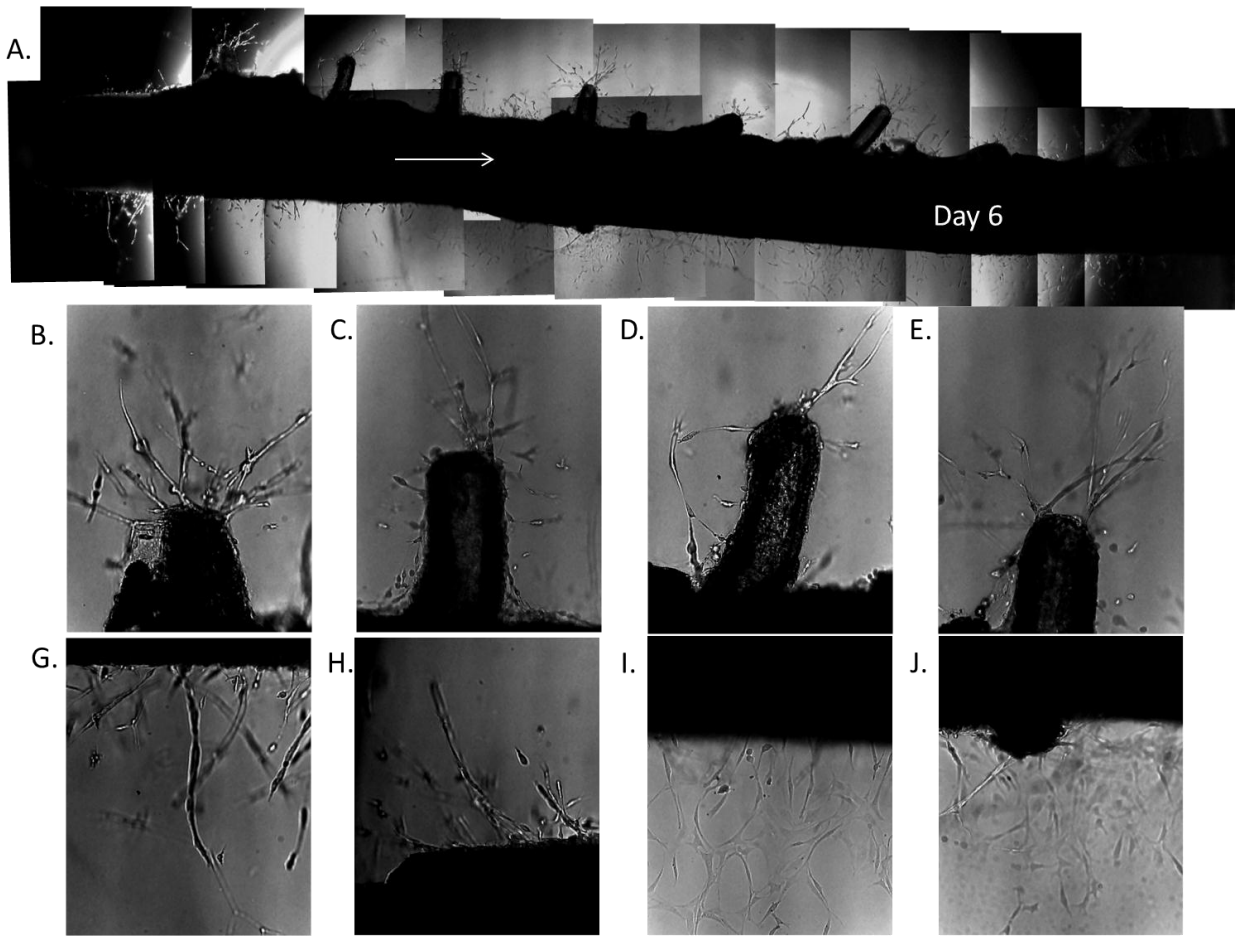

Figure D.10. Angiogenic outgrowth from a perfused aorta. A) The mouse aorta was cultured for six days while also perfusing the aorta lumen with 50 µL/min of EGM-2. The arrow indicates the direction of flow. Regions of the angiogenic outgrowth (B through H) were similar to that in the PVEB mouse aorta assay without flow. Angiogenesis in the PVEB with flow seemed to favor the severed arborizing arterials (B through E), although angiogenesis occurred along the sides of the aorta as well. The angiogenic outgrowth in the PVEB with flow contained regions (I and J) whose morphology differed from that in the aortic ring assay, and bore similarities to that shown in Fig. D.4. (G and H).

CHAPTER V

DISCUSSION

Interest in angiogenesis is growing as researchers realize its impact on several diseases. The picture of angiogenesis is incomplete, however, and although angiogenesis studies have produced useful insights for understanding and treating disease, they suffer from limitations in the current armamentarium of angiogenesis assays. In general, *in vitro* angiogenesis assays permit detailed study of a biological process that poorly represents physiological angiogenesis, while *in vivo* angiogenesis assays limit access to the variables that influence angiogenesis. This trend is more pronounced in studies of the interaction between angiogenesis and hemodynamic stimuli. This study sought to address limitations of current *in vitro* and *in vivo* angiogenesis assays by designing and implementing a device that incorporates into the vascular explant assay measurement and actuation of mechanical and chemical stimuli (engendered in blood flow). The perfused vascular explant bioreactor (PVEB) permitted long-term culture of and facilitated angiogenic outgrowth from a perfused vascular explant *in vitro*. Results of this study support the hypothesis that the PVEB will facilitate angiogenic outgrowth from a vascular explant whose lumen is accessible to perfusion, and that this enhancement will allow measurement and actuation of mechanical and chemical stimuli (those accompanying blood flow) in a vascular explant angiogenic culture. This enhancement to the body of angiogenesis assays will allow researchers to uncover more of the angiogenic process, and insights gained from the use of the PVEB may inform the development of future disease treatments. In the following sections, I describe and interpret the results of the study, state the significance of the findings, and propose future improvements to and applications of this technology.

E.1. Interpretation of the results

E.1.1. Long-Term Viable Culture of Perfused or Perfusable Aorta *In Vitro*

Hematoxylin and eosin staining of the whole aorta that possessed angiogenic sprouting produced dark spots indicative of stained intact nuclei. This is typical of live tissues. Hematoxylin, when in complex with iron (III) or aluminum (III) ions, produces a dark colored stain. The hematoxylin-metal complex stains the nucleus by binding to arginine-rich nucleoproteins such as histones[123]. Fragmentation of the chromosomal materials, via apoptosis or necrosis, causes a lack of hematoxylin staining. Eosin, an acidic pink stain, stains the cell contents. Dark dots present in the hematoxylin and eosin stains of the aorta indicated the presence of intact nuclei (a marker of live cells). Hematoxylin and eosin staining of aortas that were cultured without perfusion for six days and aortas that were cultured with perfusion for four days had the same morphology and dark staining dots (Fig. D.4. and D.7.). In contrast, aortas that were intentionally

killed via prolonged exposure to ambient temperature and CO_2 levels lacked the dark dots. Hematoxylin and eosin staining of aortas cultured in this study suggests that the PVEB can maintain long-term viability of a perfused and perfusable aorta in *in vitro* culture. An uncertainty inherent in hematoxylin and eosin stains is that hematoxylin will stain other arginine-rich content in the cell, thereby generating false positives.

The aorta and large arteries are supported by a layer of elastin fibers in the tunica media called the elastic lamina. Hematoxylin and eosin stains of the elastic lamina in the aorta feature layers of wavy, ribbon-like structures that stain pink[124]. Interestingly, the wavy, ribbon-like morphology of the elastic lamina was largely absent in hematoxylin and eosin stains of dead aortas. The smooth muscle cells that line the aorta contain a resting (i.e., in the absence of tensional load on the wall) vascular tone. I suspect that this resting contractile force in the smooth muscle causes it to contract the elastic lamina into bundles or ribbon-like structures. The dead aorta has lost this capability and the elastic lamina unfolds as the aorta takes on a passive cylindrical shape.

The elastic lamina of aortas cultured in the presence of perfusion appeared less ribbon-like than that of aortas cultured in the absence of perfusion. If the wavy morphology of the elastic lamina correlates with smooth muscle cell activity, then this would imply that perfusion of the lumen of the aorta in the PVEB had a deleterious effect on aortic smooth muscle cell function or vessel viability. Some procedural uncertainties that may have contributed to this result are inaccuracies of the temperature in the reactor and perfusate. Perfused aortas were cultured in the Bioscience Tools miniature incubator. The incubator presented spatial variations ranging from 34-37 degrees. The perfusate temperature was not measured, but circulated from a media reservoir which rested on top of a 37°C heating element, then down a 3–feet-long room-temperature path to the incubator and 4 times around the heating element within the incubator (Fig. C.4.). In contrast, the non-perfused aortas were cultured in conventional tissue culture incubators which maintain 37°C throughout. I speculate that the temperature of the Bioscience Tools incubator (and concomitantly, the PVEB) and/or perfusate drifted out or the livable range for mammalian tissues.

E.1.2. Angiogenic Outgrowth from a Perfused or Perfusable Aorta *In Vitro*.

Aortic ring assays conducted in this study produced proliferative outgrowths that were similar in morphology to that reported by Nicosia et al. as angiogenic outgrowth in the aortic ring assay[121, 125]. Nicosia (who pioneered much of the development of the aortic ring assay) described various morphological features that distinguish angiogenesis from the proliferative outgrowth of fibroblast resident in the aorta (e.g., the bifurcating branch points). These heuristics suggest that the outgrowths observed in this study were angiogenic.

Sato et al. engineered a Tie-2::GFP mouse that uniformly fluoresces throughout the vasculature[126]. This mouse expresses green fluorescent protein (GFP) under the direction of the endothelial specific receptor tyrosine kinase Tie-2 promoter. The Tie-2 promoter is active principally in proliferating vascular endothelial cells and, to a lesser extent, quiescent endothelial cells. Aortas from this mouse produced (in the

aortic ring assay) fluorescent outgrowths that were morphologically similar to those in other aortic ring assays. Since Tie-2 is expressed principally in the vascular endothelium, this experiment identifies the outgrowth as endothelial and distinguishes it from expansion and tube formation by resident non-fluorescent fibroblasts in the PVEB[127]. The morphology and fluorescent illumination of angiogenic sprouts shown in Fig. D.1. demonstrates angiogenesis in the aortic ring assay. Figures D.2, D.3, D.5, and D.10 depict outgrowth from catheterized whole aortas, and aortas cultured in the PVEB with or without intraluminal perfusion. These outgrowths contained regions that are morphologically similar to the angiogenic outgrowth that occurred in the aortic ring assay. These data suggest that angiogenesis occurred in the PVEB and support the hypothesis that the PVEB will facilitate angiogenic outgrowth from a vascular explant whose lumen is accessible to perfusion.

Fluorescent illumination varied throughout the angiogenic outgrowth. This may result from spatial variations in nutrient oxygen availabilities. For example, Tie-2 mRNA expression declines in hypoxia (in rat lung, liver, cerebellum, and heart microvasculature)[128]. Fainter fluorescence may also have occurred in vessels that were smaller (i.e., producing less of a signal). The quiescent cells of the endothelium fluoresced as much if not more than the angiogenic sprouts; however, Tie-2 is down-regulated in quiescent endothelial cells (i.e., those lining the aorta wall). This is explained by Thomas Sato and colleagues, who noted that the non-proliferating cells that line the aorta permit slow accumulation of Tie-2 (and GFP), whereas proliferating cells thin their Tie-2 or GFP content with every division[127]. When using Tie-2::GFP mice to identify angiogenesis one should consider that Tie-2 expression also characterizes a subpopulation of $CD11b^{+}$ myeloid tumor-infiltrating cells called Tie-2 expressing monocytes (TEMs)[130]. These cells form in the bone marrow and circulate in the peripheral blood. As monocytes, TEMs can localize in the endothelium or extravascular tissue; therefore, TEMs conceivably may be in the vascular explant. However, TEMs are incapable of forming the tubule networks depicted in the aortic ring assay.

Proliferative outgrowths from aortas cultured in the PVEB were, in general, morphologically similar to angiogenic outgrowths that were identified as angiogenesis in the aortic ring assay. Nicosia et al. distinguished vascular endothelial cells from fibroblasts by their greater thickness and more cohesive tubule networks and their bifurcating branch points[125]. An alternate morphology, shown in Fig. D.3. (G and H), that lacked these characteristics was observed in the PVEB. I speculate that these were fibroblasts. The morphologically was similar to that which was identified, by other labs, as fibroblasts in the aortic ring assay[130]. The outgrowth bearing this morphology stayed within a thin layer on the z-axis, presumably on the glass underpinning the reactor. In angiogenesis, fibroblasts migrate away from the aorta before the endothelial cells[130]. I speculate that regions of aorta that were pressed against the glass made cellular movement along the glass more probable, and that fibroblasts were more capable of outward migration than were the trailing endothelial cells. This may have given rise to the regions bearing the alternate morphology. The alternate morphology was not observed in aortas cultured on polystyrene culturing dishes.

The PVEB facilitated the growth of functional angiogenic sprouts.

To identify functional nascent vessels in the PVEB mouse aorta assay, fluorescent microspheres were loaded into the lumen of the aorta. As a result, the aorta lumen, severed arterials, and parts of the angiogenic outgrowth fluoresced (under the TRITC band pass). There was clear contrast between the fluorescence in the vasculature and in the adjacent Matrigel. Clusters of microspheres that had escaped into the abluminal space appeared randomly distributed and cast a generally diffuse fluorescence haze. The fluorescence in the abluminal space was not as bright as that in the aorta and in the angiogenic outgrowth. The fluorescence of aortas not exposed to the fluorescent microspheres was very low and indistinguishable from that of the background or abluminal space. These data suggest that microspheres were inside the nascent vasculature. If so, these microspheres arrived at their position via a contiguous network of angiogenic sprouts that were accessible to the lumen of the aorta (i.e., the vasculature was patent). Patent vascular sprouts were observed predominantly in the proximity of severed arterials. Angiogenic outgrowth along the side of the aorta and outgrowths bearing the alternate morphology (Fig. D.3. (G and H)) did not fluoresce when the aorta was loaded with microspheres.

The sharp contrast in fluorescence between the angiogenic outgrowth and the adjacent Matrigel in this experiment suggests that the angiogenic outgrowth was not leaky to particles greater than 0.04 μm. This agrees with literature which states that most healthy vessels in the body contain 10 nm pores between the endothelial cells that line the vasculature[21]. Davis et al. review the formation of patent endothelial tubes in *in vitro* 3D assays[131]. Tubule formation of endothelial cells occurs in a 3D extracellular matrix and minimal media supplemented with fetal bovine serum and angiogenic growth factors. The aortic ring features these, as well as fibroblasts, monocytes, and pericytes which enhance the formation and stabilization of vascular tubes[131]. I was initially uncertain whether angiogenic outgrowth from the catheterized aorta would have connections to the lumen of the aorta, and whether those connections would be identifiable using these microspheres. Endothelial cells in a confluent layer plated on a thick layer of collagen will migrate into the collagen, forming hollow tubes that maintain a patent connection with the collagen surface. It is conceivable that a similar patent connection is maintained between the migrating/tube-forming endothelial cells and the intimal wall of the aorta. It is accepted that in the aortic ring assay angiogenesis occurs at the ends of the aortic segment, where endothelial cells in the tunica intima have access to the abluminal space[73]. However, if nascent tubes grow from the ends or from severed arterials, there is the possibility that microspheres would diffuse out of the aorta without entering the angiogenic sprouts. This did not occur. Fluorescent illumination of severed arterial sprouts abruptly stopped at the ends of the arterials. I speculate that the constriction of the arterial lumen and the surrounding Matrigel plugged the end of the arterial, thereby impeding flow of the microspheres into the abluminal space from the severed arterial. Non-patent vasculature was also observed, and I speculate that it arose from endothelial cells resident in extant fibroadipose tissue on the outside of the aorta.

As shown in Figure D.8 (C and D), endothelial sprouts formed spokes around a circular cell. This circular cell did not fluoresce. I speculate that this was a monocyte that positions itself at the end of two vascular sprouts and when subjected to blood flow causes the vascular sprouts to form an anastomotic con-

nection. That microspheres did not occur in that region suggests that the anastomosis did not occur. In this experiment, the aorta was cultured in the absence of flow.

Skill was required to inject microspheres into the lumen of the aorta without damaging (via pressurization) the angiogenic sprouts. Fluid that entered the abluminal space as a result of mechanical rupture of the vessels formed a blob of fluorescent microspheres that did not diffuse into the surrounding Matrigel (Fig. D.8. (E)). The intense fluorescence of the microspheres that escaped, via this mechanism, into the abluminal space obscured the fluorescence of the angiogenic sprouts.

Angiogenesis varies in rate and extent

After six days in culture, aortas typically produced continuous angiogenic outgrowths with several bifurcating branch points. Some aortas will have by day 6 begun to display a spatially disorganized outgrowth. This disorganization is vessel regression and apoptosis, which occur with prolonged culturing in the absence or depletion of pro-angiogenic signals[121]. Larger slices of aorta tended to regress before small slices (from the same mouse). I speculate that the larger slices more rapidly depleted the pro-angiogenic signals from the culture. Variability in the rate and extent of angiogenesis is a documented limitation of the vascular explant assay. The extent of angiogenesis was quantitated in this study; however, notable variability was observed in the angiogenic outgrowths grown in the PVEB. The mice utilized in this study were largely “trash” mice with unknown genetic back ground. This genetic variability may have translated to observed variability in the extent of angiogenesis. Though variable, the extent of angiogenesis (by day 6 in culture) tended to be greater in the aortic ring assay than in the PVEB. Aortas cultured in the PVEB without intraluminal perfusion tended to produce more angiogenic outgrowth than aortas cultured with intraluminal perfusion. This trend may be the result of the increased preparatory time for the PVEB mouse aorta assay. It takes roughly forty minutes to load the explant and load the aorta into the PVEB. During this time, exposure to subphysiological temperature and CO_2 pressure decreases the angiogenic potential of endothelial cells in the aorta[132]. Catheterization blocks the main escape route for endothelial cells in the aortic ring assay (i.e., the ends). Endothelial cells can also escape through the severed arborizing arterials and punctures/tears in the aorta wall, but it is expected that the wall of the aorta is a barrier to endothelial cells undergoing angiogenesis.

Angiogenesis in the PVEB occurred along the sides of the aorta and from severed arborizing arterials. In many experiments, angiogenesis appeared more frequent near severed arterials, although quantitation of this effect was not conducted. The severed ends of vascular explants provide an escape route from the tunica intima for migrating endothelial cells. I speculate that in the PVEB, angiogenesis occurs from severed arterials because the severed arterials provide intimal endothelial cells an escape route into the abluminal space. Angiogenesis occurs along the side of the aorta as well. This may result from microvasculature in extant fibroadipose tissue or from holes/tears in the aorta incurred during explantation. Both of these phenomena would place endothelial cells in contact with the abluminal space.

In regions near the suture knot (Fig. D.2.), angiogenesis was sparse or not present; however experiments (Fig. D.3) in which suture thread was not used produced angiogenic outgrowths in the regions of the

aorta that had underlying catheters, suggesting that silk threads have a role in the inhibition of angiogenesis. I speculate that the sutures compressed the aorta and prevented adequate growth factor, nutrient and oxygen exchange, thereby compromising the angiogenic potential and the viability of the tissue. Another explanation for the decrease in angiogenesis near the silk thread knot is the higher concentration of salts and the of presence residual sterilizing solvents in the thread. Ethicon thread alone is bioinert. Prior to experimentation, silk thread is sterilized in ethanol then stored in PBS until use. Ethanol desorption from the thread is limited by the solubility of ethanol in the thread. Ethanol retained in the thread (particularly shortly after sterilization) does not dissolve the salts in PBS, and can precipitate salts from the PBS and cause salt crystals to be deposited on the suture thread[133]. Once on the aorta, this suture thread serves as a potentially toxic source of ethanol and excess salt. To alleviate this concern, one might consider sterilizing the suturing thread via autoclaving.

Less angiogenic outgrowth was observed from aortas subjected to intraluminal perfusion.

Angiogenic outgrowth appeared to occur to a lesser extent from aortas that were subjected to flow than aortas that were left static. Quantification of the angiogenic outgrowth should be carried out in order to determine if there is a statistical difference in the rate and/or extent of angiogenic outgrowth from the aorta when perfused versus the static aorta. Intraluminal perfusion generates mechanical stimuli (shear stress, pressurization or compression, and transmural pressure differences which distend the vessel). Chemical stimuli that are direct consequences of flow include transendothelial concentration differences and standing gradients of concentration in the interstitium. The mechanical and chemical stimuli engendered in blood flow have an impact on angiogenesis; however, their effect is undercharacterized. A general consensus regarding the impact of flow on angiogenesis has yet to be reached. The activation or inhibition of angiogenesis in response to shear stress, for example, depends on the magnitude and temporal pattern of the shear stress. High shear stress, in excess of 15 dyne/cm^2, induces quiescence, whereas low or oscillating wall shear stresses are typically identified in arteriogenesis[134]. Endothelial cell (and/or vasculature) behavior in the presence of the mechanical stimuli is also context-dependent: *in vivo*, increases in fluid flow via injection of prazosin caused increased angiogenic ingrowth in the rabbit ear chamber[135]. In contrast, *in vitro* studies of the effect of shear stress on angiogenes yielded varying results that depended on the source (along the vascular tree) of the endothelial cells and extracellular matrix used. Tressel et al. report an inhibitory effect of shear stress on HUVEC tubulogenesis in Matrigel, whereas shear stress enhanced HUVEC mediated angiogenesis in collagen[136, 137]. The impact of shear stress on angiogenesis in the presence of pericytes, smooth muscle cells, fibroblasts and monocytes (cells present in the vascular explant assay) has not been researched in depth. *In vitro*, endothelial cell monolayer cultured on collagen that was loaded with smooth muscle cells showed reduced proliferation in the presence of shear stress[138]. I suspect that unique circumstances provided by an intact perfused aorta *in vitro* caused the somewhat unexpected reduction of angiogenesis in the presence of flow. Chemical factors engendered in the perfusion may have also contributed. For instance, VEGF, though pro-angiogenic, has been shown to maintain endothelial cell quiescence when presented as an autocrine signal to endothelial cells subjected to blood flow[4].

Hydraulic impedance measurements conducted on the perfused aorta revealed that the aorta strongly impeded fluid flow and generated a backpressure in excess of 150 mmHg (Section D.7.). The backpressure generated by the aorta exceeds mean arterial blood pressure for normotensive mice. I speculate that perfusion of the aorta and/or the aorta's response to perfusion created an *in vitro* condition that mimics aspects of hypertension. A principal observation in hypertensive animal models and patients is rarefarction (i.e., decreased amount of capillaries). The cause of hypertensive rarefarction is unclear. Insufficient stimulation of angiogenesis overtime possibly generates capillary rarefarction and hypertension[139]. The response of arterioles to hypertension causes downstream capillaries to collapse and over time to regress[139]. Hypertension generates pro- and anti-angiogenic signals[139]. These signals are not entirely recapitulated in the PVEB. For instance, endocrine signaling pathways which modulate angiogenesis, e.g., the renin-angiotension pathway, were absent from the PVEB[139]. An explanation for the perceived decrease in angiogenesis that resulted from intraluminal perfusion of the aorta is that hypertension-responsive signals extant in the PVEB had an overall anti-angiogenic effect.

E.1.3. Actuation and Measurement of the Mechanical Stimuli In the PVEB

Mechanical stimulation of the aorta in long-term *in vitro* culture was accomplished via intraluminal perfusion. The peristaltic pump that delivered media to the PVEB was calibrated prior to use, and therefore the volumetric flow rate of perfusate entering the aorta was not monitored. A mechanical response of the aorta to perfusion (i.e., hydraulic impedance to fluid flow) was monitored long-term (>20 hours). Manometers were placed upstream and downstream of the device, thereby providing a measurement of axial pressure difference across the aorta for a particular flow rate. This is proof of principle that a mechanical stimulus can be incorporated into the vascular explant assays using the PVEB.

Perfusion of the aorta with 50 – 100 µL of complete EBM-2 media resulted in two characteristic hydraulic impedance curves (Fig. D.9.) : 1) The hydraulic impedance imparted by the aorta would gradually increase until, at 4 to 16 hours in culture, it generated a backpressure that overwhelmed the upstream manometer (i.e., in excess of 150 mmHg); 2) the hydraulic impedance imparted by the aorta would increase, decrease to less than its initial value, then continue to decrease from there. Hematoxylin and eosin stains (Fig. D.5.) of an aorta that maintained high hydraulic impedance contained dark hematoxylin stained dots characteristic of live tissue. In contrast, hematoxylin and eosin stains of aortas whose impedance decreased to less than its initial value lacked the dark hemalum stains characteristic of live cells. This suggests that the characteristic hydraulic impedance curves correlate with the state (live or dead) of the aorta. A dead aorta (i.e., incapable of active force generation) would behave like a passively deformable viscoelastic tube. The elastic properties of the aorta would cause it to distend until the transmural pressure difference is balanced by the tension generated in the stretched aorta walls. The aorta would continue to distend via viscoelastic creep. Hydraulic impedance would decrease with increasing radius of the distended aorta.

Hydraulic impedance is dependent on the geometric features of the aorta. These include bends, tapers and forks in the aorta, but the most important influence on the hydraulic impedance of the aorta is its

radius. The impedance of a vessel is roughly inversely proportional to the fourth power of its radius. The aorta is the major conduit for systemic blood flow. Connected directly to the heart, it experiences pulsatile shear and pressurization *in vivo*. In response, the aorta largely passively distends and recoils in order to maintain throughout the cardiac cycle a constant flow to downstream arteries and arterioles. Principal function of the aorta does not require or give rise to active dilation or constriction, and the aorta typically has a low hydraulic impedance. In contrast, the aorta (i.e., a live aorta) cultured in the PVEB generated a backpressure in excess of 150 mmHg (more than the mean arterial blood pressure for the mouse, 80mmHg)[140]. Vasodilation and vasoconstriction are important to maintaining mean arterial blood pressure and adequate blood flow to the target organs. It is carried out by resistance arteries (or arterioles). However, the aorta retains some measure of constriction and/or dilation potential. *In vivo*, the aorta has demonstrated contractile capabilities. *In vitro*, the aorta has demonstrated vasoconstriction in response to endothelin-1, a vasoactive protein secreted by the endothelium in response to shear stress, adrenaline, hypoxia and ischemia[141]. Endothelin-1 signals to the ET_A receptor on smooth muscle cells, affecting vasoconstriction. Vasodilation of the mouse aorta *in vitro* in response to shear stress and other dilatory factors was demonstrated as well[142]. Shear stress can trigger both dilation and constriction of the aorta *in vitro*. I speculate that the vasoactive response of the aorta to shear stress depends in part on the magnitude of the shear stress. Jen et al. induced vasodilation of the aorta using physiological values for thoracic aortic shear stress (50dyne/cm^2)[142]. Since the PVEB was designed to study angiogenesis (a phenomenon located in the microvasculature), we used a flow rate that would achieve a shear stress that was comparable to that in the post capillary venules (i.e. orders of magnitude lower at app. 1 dyne/cm^2). I speculate that the low shear stress of the PVEB aorta angiogenesis culture induced the vasoconstrictive response and not a vasodilation response. Alternate explanations for the aorta constriction which generated the observed high impedance exist. The constriction may also be a myogenic response of the aorta to stretching of the aorta wall by the catheter inserts. Extant platelets in the aorta may generate hemostatic vasoconstrictive response to vessel injury incurred during dissection. As modeled in Fig. D.7., perfusate leaves the aorta and re-enters it near the exit of the PVEB. The aorta is malleable, and it is conceivable that the momentum or driving force of fluid reentering the downstream end of the aorta could cause it to collapse, thereby occluding axial flow.

The PVEB offers actuation and measurement of spatially averaged mechanical properties. Figure D.7. demonstrates that local shear forces can be predicted using a mathematical model of the PVEB, if the perfused vessel (or hollow fiber) has a defined rigid shape and the porosity of the vessel and the matrix material in the abluminal space are precisely known. However, the thoracic aorta has an unpredictable, deforming, and non-uniform geometry. The movement of fluid into and out of the aorta via severed arterials and other holes in the aorta impairs precise control of local shear stress, transmural pressure difference, and pressure experienced by the aorta. This suggests that the PVEB can actuate a spatially averaged mechanical stimulus (i.e., perfusate flow rate into the PVEB) but lacks, in its current implementation, spatial control of the mechanical stimuli engendered in perfusion. In response to fluid flow, shear stress, and transmural pressure difference, arteries (e.g., the aorta) modulate their hydraulic impedance, thereby protecting downstream arterioles and capillaries. Impedance is a spatially averaged property arising from spatially varying properties of contour and the inner diameter of the aorta.

E.1.4. Solute and Particulate Mass Transport in the PVEB

Nutrient and oxygen concentrations in the interstitium form spatial patterns that are a direct consequence of blood flow to nearby capillaries. The spatial presentation of oxygen, nutrients, and growth factors is a chemical stimulus engendered in blood flow. A mathematical model of the mass transfer of a small molecule test substance (e.g., glucose) from a leaky tube (hollow fiber), as in Fig. D.7., suggests that in the cases where the diffusion, convection, and consumption of a test substance follow known formulas or values, the spatial distribution of the test substance can be controlled by controlling the concentration of the perfusate. Concentration differences between the abluminal space and hollow fiber lumen resulted *in silico* in neatly patterned gradients of concentration. Since the aorta has non-uniform, unpredictable, and time-varying (when perfused) geometry, and mass transfer across the wall or out of the aorta through holes is not uniform, gradients in the concentration of a test substance cannot be defined as suggested in Fig. D.9. However, the PVEB may be capable of defining a concentration difference of a macromolecule or microparticle between the lumen and abluminal space in the PVEB.

Mathematic model of small molecule diffusive mass transport in the PVEB

In the mathematical model of small molecule diffusive mass transport in the PVEB, the hollow fiber was selected as the model of the vascular explant. Small molecule permeability of the hollow fiber membrane was measured to be $6x10^{-8}$ m/s. This is consistent with measurements of other hollow fibers or porous membranes ($10^{-8} – 10^{-10}$)[143]. In this measurement dilute solutions were used and therefore osmotic pressure differences were neglected. This measurement was obtained by perfusing the hollow fiber lumen, and convective transport of the fluorescein across the hollow fiber membrane presumably occurred as perfusion pressurized regions of the hollow fiber. Convective mass transport across the hollow fiber would have inflated our measurement of small molecule diffusive permeability, and a more rigorous measurement would be required in applications requiring high accuracy. Ultimately, this permeability term was not incorporated into the mathematical model of mass transport in the PVEB. A measure of the hydraulic permeability of the hollow fiber is also needed in order to sufficiently model the hollow fiber's impact on mass transport in the PVEB2. However, if the hollow fiber walls were thin relative to the geometry of the PVEB, and the hydraulic and diffusive permeabilities of the extracellular matrix material that fills the abluminal space were less than or equal to those of the hollow fiber, then one might justify neglecting the hollow fiber's impact on mass transport in the PVEB. Klein et al. report the hydraulic permeability of commercially available hollow fibers as $8.5\text{-}4.2x10^{-7}$m/atm-s[143]. In comparison, the hydraulic permeability (L_P) of collagen (which was used in the mathematical model) was computed by the following equation to be $1.3x10^{-7}m^2$/atm-s; K is Darcy's Law Coefficient for water in collagen and the viscosity of water[144]

$$L_P = \frac{K}{\mu} \ . \qquad 8$$

The similar values of permeability between the hollow fiber and the surrounding extracellular matrix material suggest that the hollow fiber can be neglected without a severe impact on the accuracy of the mathematical model.

The mathematical model of mass transport in the PVEB predicted that fluid would flow through the matrix material in the abluminal space of the PVEB at roughly eight orders of magnitude slower than along the lumen of the lumen of the hollow fiber. Nutrient availability decreased gradually with increasing distance from the hollow fiber, in ways similar to the theorized Krogh cylinder of nutrients that surrounds a capillary tube[120]. The model predicts a nearly constant solute concentration in the lumen of the hollow fiber. The spatial patterns of fluid flow and nutrient availability predicted by the model did not accurately reflect mass and solute transfer in the PVEB with an aorta. Perfusing the aorta with fluorescent dyes or microspheres would cause non-uniform fluorescent illumination of the abluminal space. It appeared that the fluorescent materials would exit the aorta near the ends of the aorta and at severed arterials. Fluid flow in the abluminal space seemed to stem from severed arterials. The ability of the mathematical model of mass transport in the PVEB as computed using COMSOL to predict bulk fluid and small molecule transport patterns relied on the regular geometry of the hollow fiber and the spatially uniform, or determined, permeability of the abluminal space. The irregular geometry and the heterogeneous barrier the aorta presents, and the spatial and temporal variations in the permeability of the Matrigel in the abluminal space, cannot be adequately predicted using the model.

Mass transport of fluid flow in the abluminal space in the PVEB (with the aorta) is influenced by spatial and temporal variations in the permeability of the Matrigel. This problem exists in other three-dimensional angiogenesis assays which incorporate mechanical stimuli (e.g., shear stress, hydrostatic pressure) and utilize matrix materials to facilitate angiogenic migration and tube formation steps. For instance, matrix metalloproteases (MMPs) which become active in cell migration in angiogenesis locally degrade the surrounding matrix. Fibroblasts synthesize matrix material substrates to provide traction to migrating cells. These processes alter the permeability of the matrix in unpredictable ways, and pose an obstacle to future models of mass and solute transport in the PVEB and other three-dimensional angiogenesis assays. Imaging techniques that allow precise characterization of blood vessel geometries exist and have been utilized in mathematical models of blood vessel properties. These techniques may be applicable to future studies that utilize the PVEB.

E.2. Significance

This study details the long-term maintenance of and angiogenic outgrowth from a perfused or perfusible vascular explant *in vitro*. This enhancement to the conventional vascular explant assay expands the capabilities of the current armamentarium of angiogenesis assays. With this technology, researchers may discover new properties of and mechanisms of angiogenesis. Insights gained from studies that utilize the PVEB may prove necessary to the treatment of several diseases, including cancer, heart disease, and ischemia (i.e., leading causes of death in the United States).

The study of angiogenesis and diseases associated with pathological angiogenesis is slowed by the limitations of the currently available assays. *In vitro* angiogenesis assays allow detailed study of a biological process that does not fully recapitulate angiogenesis *in vivo*. In contrast, *in vivo* models of angiogenesis limit access to several mechanisms and variables that drive angiogenesis. The vascular explant assay is considered the best *in vitro* mimic of *in vivo* angiogenesis. It provides near-physiological spatial organization of cells and allows recapitulation of several of the paracrine and juxtacrine signals that direct angiogenesis. The vascular explant assay facilitates more "steps" of angiogenesis and generates vascular sprouts that are functionally similar to those *in vivo*. The angiogenesis in the PVEB produces vasculature that is morphologically identical to that in the vascular explant assay. This suggests that the physiologically relevant features of the aortic ring assay were retained in the PVEB. If this is the case, then the addition of flow potentially makes this PVEB an even better *in vitro* mimic of *in vivo* angiogenesis. *In vitro* qualities of the vascular explant assay (e.g., time-lapsed imaging, precise control and measurement of angiogenic stimuli, absence of confounding inflammatory responses) are maintained in the PVEB.

The connection between hemodynamic factors and angiogenesis is known[54-56, 146] . Changes in hemodynamic factors have been implicated in several diseases that stem from pathological angiogenesis (e.g., cancer, hypertension, and inflammatory pathologies). However, the details of the interactions between hemodynamic factors and angiogenesis are largely uncharacterized. Investigations of these interactions were largely conducted *in vivo,* where the detailed study of the mechanisms is limited. *In vitro* angiogenesis assays that incorporate the mechanical and/or chemical stimuli that directly result from blood flow are required in order to better understand the hemodynamic influences on angiogenesis (and associated diseases). The PVEB may fill that need. The PVEB mimics aspects of hemodynamic angiogenic stimuli in the most physiologically relevant model of angiogenesis. Results of this study suggest that vascular function (vasoconstriction and angiogenesis) were modulated by long-term intraluminal perfusion. Since the PVEB is amenable to molecular biology and culturing techniques conducted in the vascular explant assay, continued study of the effect of long-term intraluminal perfusion and vascular function using the PVEB can yield meaningful insights about the detailed mechanisms of these interactions. Insight gained from studies of vascular function and angiogenesis using the PVEB may prove necessary to the development of treatments for diseases that affect angiogenesis.

E.3. Future Directions

The angiogenic outgrowths grown in the PVEB were morphologically similar to those of the aortic assay and displayed features of healthy (*in* vivo) vasculature. They appeared patent to the aorta lumen, and were non-leaky to particles greater than 0.04 µm. The PVEB allows researchers to characterize angiogenic outgrowth from a vascular explant in ways not possible in the conventional vascular explant assay. An obvious next step in the development and implementation of the PVEB is to better characterize and quantitate angiogenesis in the PVEB.

Perfusion with fluorescent dyes, nanoparticles, and microspheres is commonly utilized to assess the extent and functional quality of angiogenesis *in vivo*[83, 147]. Patent vessels are identified in *in vivo* angiogen-

esis assays by fluorescent illumination via injection of fluorescent material into upstream arteries or vessels. Malformed (e.g., arising from tumor angiogenesis) and damaged vasculature can be identified *in vivo* by its leakiness to large particles. For instance, the microvasculature endothelium typically contains 10 nm pores but tumor microvasculature contains fenestrae that cause leakage of particles greater than 50-100 nm[71]. The perfusion access provided by the PVEB allows researchers to, for the first time, similarly assess the functional qualities of the nascent vasculature in *in vitro* vascular explant angiogenesis assays. I recommend perfusing or charging the aorta with microspheres and nanoparticles of varying size to assess the functional quality of nascent vasculature in the PVEB. The size of the largest particle that leaks from the vasculature would provide a measure of the pore size in the nascent vasculature endothelium

In this study perfusion of the aorta resulted in a noticeable decline in angiogenesis. This effect was not quantitated, therefore it is uncertain whether the perceived decrease in angiogenesis is significant. Quantification strategies should be explored in future work. Though no standard technique for quantitating the angiogenesis in the vascular explant assay exists, Nicosia et al. describe various methods of scoring angiogenesis in the vascular explant assay[125]. Some of these methods are gaining ground and should be modified for use in the PVEB. Similarly, quantification strategies should be employed to determine what fraction of the angiogenic outgrowth is patent.

The vascular explant assay carries out nearly all of the "steps" of angiogenesis. The final steps of vessel regression (adaption to tissue needs) and vessel stabilization, or vessel maturation, are mediated in part by blood flow. The PVEB recapitulates aspects of fluid flow, and it is plausible that nascent vessels in the PVEB would mature further than those in the vascular explant assay. I recommend incorporating ways of assessing vessel maturity in the PVEB. The amount of pericytes that bind to a nascent vessel is a common marker of vessel maturity. Pericytes are identified via histochemical staining cell markers (desmin, calponin, and proteoglycan NG2)[121]. Aortas cultured in the PVEB produced outgrowths that featured, in regions, a distinct second morphology. I speculate that this was proliferative expansion of fibroblasts in the PVEB. To settle uncertainties about this, one should stain the vasculature for fibroblast-specific markers and markers specific to other cell types resident in the vascular explant assay (macrophages, monocytes, dendritic cells, endothelial cells, and smooth muscle cells). Staining of angiogenesis in the vascular explant assay poses a significant obstacle: attempting to remove the specimen from its culturing dish or reactor distorts or obliterates the nascent vasculature. A "thin prep" assay was developed to allow whole mount staining of the angiogenic outgrowth from a vascular explant. This method should be adapted to use in the PVEB.

The PVEB provides researchers a measure of control over hemodynamic stimuli in the vascular explant model. In this study, the PVEB was utilized to facilitate angiogenesis from an aorta that was either perfused with 50µL/min EGM or cultured without perfusion. The effect of shear stress and pressures generated by fluid flow depend on their magnitude and temporal pattern. Therefore, I recommend using the PVEB to investigate the effects of a wider range of perfusate flow rates and temporal patterns. Several molecules that induce angiogenesis (e.g., VEGF) also inhibit angiogenic maturation steps, and vice versa (Ang-1 which activates angiogenic maturation steps inhibits endothelial cell proliferation required for initiation of angiogenesis.) Nitric oxide, produced in response to shear stress, has a role in the earlier

and later 'steps' of angiogenesis. By starting intraluminal perfusion of an aorta in the PVEB after day 4 or day 6 in culture, may allow us to elucidate details about the role of shear stress on different steps of angiogenesis.

Currently, the PVEB offers only spatially averaged measurements and actuation of mechanical/chemical stimuli resultant of intraluminal perfusion. Frequently, researchers employ mathematical models to better characterize the spatial variation of the stimuli in mechanotransduction assays and assays that incorporate chemical gradients. The mathematical model of the mass transport in the PVEB must be improved before it can provide local measures of the mechanical/chemical stimuli engendered in intraluminal perfusion of the vascular explant. One drawback of this mathematical model is that it approximated the vascular explant as a rigid uniform geometry. Optical image processing strategies exist that can be used to better model the geometry of the vascular explant[116]. A precise three-dimensional characterization of the aorta geometry may require MRI imaging of the vascular explant[148]. Two-photon microscopy might also accomplish more precise three dimensional characterization. I speculate that mass transport in the PVEB can be adequately modeled by incorporating more precisely characterized vessel geometries.

In vivo, angiogenesis in postnates typically occurs from microvasculature and post-capillary venules. In comparison to other vascular explants, the aorta poorly represents the phenotype of angiogenic vessels. In addressing this, researchers have used smaller arteries, embryonic vessels, the saphenous vein, and the vena cava to better model *in vivo* angiogenesis in the vascular explant assay. I recommend incorporating these vessels into the PVEB. The PVEB may have to be scaled in order to accommodate this. A further modification to the PVEB should be done, in order to allow co-culture of the aorta and vena cava.

Ultimately, the PVEB should be utilized to investigate pathological angiogenesis. For example, cancer progression accelerates when the vasculature innervates the primary tumor. Tumors recruit new vessels by secreting pro-angiogenic cytokines, then use the vessels to supply their oxygen and nutrient needs, and metastasize. Tumor angiogenesis differs considerably from physiological angiogenesis. Tumor vasculature that results is malformed, leaky, and less stable or mature. Blood flow and other hemodynamic stimuli are also abnormal in tumor vasculature[71, 90]. Massive effort is aimed at elucidating the molecular details of tumor angiogenesis. Hemodynamic factors influence tumor angiogenesis, and their impact should be studied more. The addition of tumors or cancer cells to the abluminal space in the PVEB would provide a platform for studying molecular mechanisms of tumor angiogenesis, functional qualities of the resulting tumor vasculature, and the impact of hemodynamics on angiogenesis and tumor vasculature.

BIBLIOGRAPHY

1. Kochanek, K. D. et al. “Deaths: preliminary data for 2009” National Vital Statistics Reports **59** (4) **(**2011)
2. “Cancer -- addressing the cancer burden” US CDC National Center for Chronic Disease Prevention and Health Promotion Division of Cancer Prevention and Control (2011)
3. “Heart disease and stroke – addressing the nation’s leading killers” US CDC National Center for Chronic Disease Prevention and Health Promotion Division for Heart and Stroke Prevntion (2011)
4. Carmeliet, P. “Angiogenesis in life, dieases and medicine” Nature **438** 932-936 (2005)
5. Risau, Wener and Ingo Flamme “Vasculogenesis” Annual Review Cell and Developmental Bioliology **11** 73-91(1995)
6. Carmeliet, P. “Molecular mechanisms and clinical application of angiogenesis” Nature **473** 298-307 (2011)
7. Folkman, J., “Angiogenesis in cancer, vascular, rheumatoid and other disease” Nature Medicine **1** 27-30 (1995)
8. Adam R. H., “Molecular regulation of angiogenesis and lymphangiogenesis” Nature Reviews Molecular Cell Biology **8** 464-478 (2007)
9. Risau W., Flamme I., “Vasculogenesis” Annual Review Cell and Developmental Biology (1995) **11** 73-91
10. Breier, G., “Angiogenesis in Embryonic Development – A review” Placenta **21** S11-S15 (2000)
11. Carmeliet, P., “Angiogenesis in health and disease” Nature Medicine **6** 389-395 (2003)
12. Tuma R. F. et al. (Eds.), *Handbook of physiology: Microcirculation* (2nd ed.). Elsevier San Diego (2008)
13. Nicosia et al., “A new *ex vivo* model to study venous angiogenesis and arterio-venous anastomosis formation” Journal of Vascular Research **42**(2) 111-119 (2005)
14. Makanya et al., “Intussusceptive angiogenesis and its role in vascular morphogenesis, patterning, and remodeling” Angiogenesis **12**(2) 113-123 (2009)
15. Phelps, E. A. and A. J. Garcia “Update on therapeutic vascularization strategies” Regenerative Medicine **4**(1) 65-80 (2009)
16. Carmeliet, P., “Mechanisms of angiogenesis and arteriogenesis” Nature Medicine **6**, 389 - 395 (2000)
17. Van Royen, N., et al., “A Critical Review of Clinical Arteriogenesis Research” Journal of the American College of Cardiology **55**(1) 17-25 (2009)
18. Brady, N., et al., “Differential Effects of Pressure and Flow on DNA and Protein Synthesis and on Fibronectin Expression by Arteries in a Novel Organ Culture System” Circulation Research. **77** 684-694 (1995)
19. Rezvan,A., et al. “Animal, in vitro, and ex vivo models of flow-dependent atherosclerosis: role of oxidative stress” Antioxidants and Redox Signaling **15**(5) 1433-48 (2011)

20. Tammela, T. and Kari Alitalo “Lymphangiogenesis: Molecular mechanisms and future promise” Cell **140**(4) 460-476, (2010)
21. Ganong, W. F., *Review of Medical Physiology* (18th ed). Appleton & Lange (1997)
22. Bouïs D., et al. “A review on pro- and anti-angiogenic factors as targets of clinical intervention” Pharmacological Research **53**(2) 89-103 (2006)
23. Gerhardt ,H., and C. Betsholz “Endothelial-pericyte interactions in angiogenesis” Cell and Tissue Research 314(1) 15-23
24. Moldovan, N. I., “Role of monocytes and macrophages in adult angiogenesis: A light at the tunnel’s end” Journal of hematotherapy and Stem Cell Research **11** 179-194 (200)
25. Cheresh, D. A., and D. G. Stupack “Regulation of angiogenesis: apoptotic cues from the ECM” *Oncogene* (2008) **27,** 6285–98
26. Scottile, J., “Regulation of angiogenesis by extracellular matrix” Biochimica et Biophysica Acta (BBA) - Reviews on Cancer **1654**(1) 2004
27. Pugh, C. W., and P. J. Ratcliffe “Regulation of angiogenesis by hypoxia: role of the HIF system” Nature Medicine **9** 677 - 684 (2003)
28. Diaz-Gonzalez, J. A. et al., “Targeting hypoxia and angiogenesis through HIF-1α inhibition” Cancer Biology and Therapy **4(**10), 1055-62, (2005)
29. Zhu, K., et al., “Mechanism by which H-2g, a glucose analog of blood group H antigen, mediates angiogenesis” Blood **105**(6) 2343-2349 (2005)
30. Zhu, K., et al., “A novel function for a glucose analog of blood group H antigen as a mediator of leukocyte-endothelial adhesion via intracellular adhesion molecule 1” Journal of Biological Chemistry **278**(24) 21869-77 (2003)
31. Asif Amin, M., et al., “H-2g, a glucose analog of blood group H antigen, mediates mononuclear cell recruitment via Src and phosphatidylinositol 3-kinase pathways” Arthritis and Rheumatism **58**(3) 689-695 (2008)
32. Svendsen, M. N., et al., “VEGF and tumour angiogenesis. Impact of surgery, wound healing, inflammation and blood transfusion” Scandinavian Journal of Gastroenterology **4** 373-379 (2002)
33. Aplin, A. C., et al., “Angiopoietin-1 and vascular endothelial growth factor induce expression of inflammatory cytokines before angiogenesis” Physiological Genomics **27** 20-28 (2006)
34. Dai Fukumura., et al., “Predominant role of endothelial nitric oxide synthase in vascular endothelial growth factor-induced angiogenesis and vascular permeability” Proceeding of the National Academy of Sciences (PNAS) **98**(5) 2604-2609 (2001)
35. Hellström M., et al., “Dll4 signalling through Notch1 regulates formation of tip cells during angiogenesis” Nature **445** 776-780 (2007)
36. Geudens , I. and H. Gehardt., “Coordinating cell behaviour during blood vessel formation” Development **138** 4569-4583 (2011)
37. Davis, G. E. and D. R. Senger “Endothelial extracellular matrix – Biosynthesis, remodeling and functions during vascular morphogenesis and neovessel stabilization” Circulation Research. **97** 1093-1107 (2005)
38. Bach, T. L., et al. “VE-Cadherin mediates endothelial cell capillary tub formation in fibrin and collagen gels“ Experimental Cell Reseacrch **238**(2) 324-334 (1997)

39. Berthod F., et al "Extracellular matrix deposition by fibroblasts is necessary to promote capillary-like tube formation in vitro" Journal of Cellular Physiology **207**(2) 491-498 (2006)
40. Arnaoutova, I. and H. K. Kleinman, "*In vitro* angiogenesis: endothelial cell tube formation on gelled basement membrane extract" Nature Protocols **5** 628 - 635 (2010)
41. Leslie, J. D., et al., "Endothelial signalling by the Notch ligand Delta-like 4 restricts angiogenesis" Development **134** 839-844 (2007)
42. Krueger, K., et al., "Flt1 acts as a negative regulator of tip cell formation and branching morphogenesis in the zebrafish embryo" Development **138** 2111-20 (2011)
43. Dimmeler, S. and A. M. Zeiher "Endothelial cell apoptosis in angiogenesis and vessel regression" Circulation Research **87** 434-439 (2000)
44. Lobov, I. B., et al, "Angiopoietin-2 displays VEGF-dependent modulation of capillary structure and endothelial cell survival *in vivo*" Proceeding of the National Academy of Sciences (PNAS) **99**(17) 11205-10 (2002)
45. Yancopoulos, G. D., et al., "Vascular-specific growth factors and blood vessel formation" Nature **401** 242-248 (2000)
46. Uriel, S., et al., "Sustained low levels of fibroblast growth factor-1 promote persistent microvascular network formation" American Journal of Surgery **192**(5) 2006
47. Iozzo, R. V., "Heparan sulfate proteoglycans: heavy hitters in the angiogenesis arena" Journal of Clinical Investigation **108**(3) 349-355 (2001)
48. Jain, R. K., "Molecular mechanisms of vessel maturation" Nature Medicine **9**(6) 2003
49. Takuwa, Y., "Roles of sphingosine-1-phosphate signaling in angiogenesis" World Journal of Biological Chemistry **1**(10) 298-306 (2010)
50. Fantin, A., "Tissue macrophages act as celluar chaperones for vascular anastomosis downstream of VEGF-mediated endothelial tip cell induction" Blood **116** 829-840 (2010)
51. Stetler-stevenson, W. G., "TIMP-2: an endogenous inhibitor of angiogenesis" Trends in Molecular Medicine **11** (3) 97-103 (2005)
52. Conway, E. M., D. Collen and P. Carmeliet "Molecular mechanisms of blood vessel growth" Cardiovascular Research **49** 507-521 (2001)
53. Maragoudakis, M. E. (Ed), *Angiogenesis models, modulators and clinical applications* pp. 19-33 Plenum Press, New York (1997)
54. Egginton, S., "Unorthodox angiogenesis in skeletal muscle" Cardiovascular Research **49** 634-646 (2001)
55. Egginton, S., "Physiological factors influencing capillary growth." Acta Physiologica 202, 225–239 (2011)
56. Egginton, S., "*In vivo* shear stress response" Biochemical Society Transactions **39** 1633–1638 (2011)
57. Ando, J. and K. Yamamoto "Vascular Mechanobiology" Circulation Journal **73** 1983-1992 (2009)
58. Isshiki, M., et al., "Endothelial Ca2+ waves preferentially originate at specific loci incaveolin-rich cell edges." Proceeding of the National Academy of Sciences (PNAS) **95** 5009 –5014 (1998)
59. Mitsumata, M., et al., "Fluid shear stress stimulates platelet-derived growth factor expression in endothelial cells." American Journal of Physiology **265** (1 Pt 2) H3-8 (1993)

60. Gloe, T., “Shear stress-induced release of basic fibroblast growth factor from endothelial cells is mediated by matrix interaction via integrin $\alpha_V\beta_3$” Journal of Biological Chemistry **277** 23452-58 (2002)
61. Malek, A. M., et al., “Fluid shear stress differentially modulates expression of genes encoding basic fibroblast growth factor and platelet-derived growth factor B chain in vascular endothelium” Journal of Clinical Investigation **92**(4) 2013-2021 (1993)
62. Ohno, M., et al., “Fluid shear stress induces endothelial transforming growth factor beta-1 transcription and production” Journal of Clinical Investigation **95** 1363-1369 (1995)
63. Dulak, J., et al., “Nitric oxide induces the synthesis of vascular endothelial growth factor by rat vascular smooth muscles cells” Arteriosclerosis, Thrombosis, and Vascular Biology **20** 659-666 (2000)
64. Ziche, M. et al., “Nitric oxide promotes proliferation and plaminogen activator production by coronary venular endothelium through endogenous bFGF” Circulation Research **80** 845-852 (1997)
65. Matsunaga, T., et al., “Angiostatin inhibits coronary angiogenesis during impaired production of nitric oxide” Circulation **105**(18) 2185-91 (2002)
66. Cooke, J. P., and D. w. Losordo, “Nitric oxide and angiogenesis” Circulation **105** 2133-2135 (2002)
67. McMahon, T. J., “Nitric oxide in the human respiratory cycle” Nature Medicine **8** 711 - 717 (2002)
68. Isbell, T. S., “SNO-hemoglobin is not essential for red blood cell-dependent hypoxic vasodilation” Nature Medicine **14** 773 - 777 (2008)
69. Carmeliet, P., “Angiogenesis in health and disease” Nature Medicine **9** 653 - 660 (2003)
70. Albini, A., et al., “The angiogenesis induced by HIV−1 Tat protein is mediated by the Flk−1/KDR receptor on vascular endothelial cells” Nature Medicine **2** 1371 - 1375 (1996)
71. Jain, R. K., “Normalization of tumor vasculature: an emerging concept in antiangiogenic therapy” Science **7**(5706) 58-62 (2005)
72. Auerbach, R., et al., “Angiogenesis assays: a critical overview” Clinical Chemistry **49**(1) 32-40 (2002)
73. Staton, C. A., et al., “Current methods for assaying angiogenesis *in vitro* and *in vivo*” International Journal of Experimental Pathology **85**(5) 233-248 (2004)
74. Staton, C. A., M. W. R. Reed and N. J. Brown “A critical analysis of current in vitro and in vivo angiogenesis assays” International Journal of Experimental Pathology **90**(3) 195-221 (2009)
75. Bouïs, D., et al. “Endothelium *in vitro*: a review of human vascular endothelial cell lines for blood vessel-related research” Angiogenesis **4** 91-102 (2001)
76. Brown, T. D., “Techniques for mechanical stimulation of cells in vitro: a review” Journal of Biomechanics **33**(1) 3-14 (2000)
77. Patent: Zijlstra, A., et al. (2011) “Magnetic reversibly attached template (MRAT) and uses therefor” Patent number WO/2011/068,951, 2011
78. Arnaoutova, I. et al, “The endothelial cell tube formation assay on basement membrane turns 20: state of the science and the art” Angioenesis **12** 267-274 (2009)

79. Vickermann, V., et al., “Design fabrication and implementation of a novel multi-parameter control microfluidic platform for three-dimensional cell culture and real-time imaging” Lab on a Chip **8** 1468-1477 (2008)
80. Hetheridge, C., G. Mavria and H. Mellor “Uses of the in vitro endothelial–fibroblastorganotypic co-culture assay in angiogenesis research” Biochemical Society Transactions **39**(6) 1597-1600 (2011)
81. Chang, C. C., et al., “Angiogenesis in a Microvascular Construct for Transplantation Depends on the Method of Chamber Circulation” Tissue Engineering: Part A **16**(3) 795-805 (2010)
82. Ribatti, D., “The gelatin spong- chorioallantoic membrane assay” Nature Protocols **1** 85-91 (2006)
83. Weinstein, B.M., Stemple D.L., Driever W., Fishman M.C. “Gridlock, a localized heritable vascular patterning defect in the zebrafish” Nature Medicine **1** (11), 1143-1147 (1995)
84. Akhtar, N., E. B. Dickerson and R. Auerbach, “The sponge/ matrigel angiogenesis assay” Angiogenesis **5** 75-80 (2002)
85. Guedez, L. “Quantitative assessment of angiogenic responses by the directed *in vivo* angiogenesis assay” American Journal of Pathology **162**(5) 1431-1439 (2003)
86. Yonezawa, S., Asai, T. and Oku, N. “Dorsal Air Sac Model”, in *Angiogenesis Assays: A Critical Appraisal of Current Techniques* (eds C. A. Staton, C. Lewis and R. Bicknell), John Wiley & Sons, (2007)
87. Yanni S. E., Penn J.S. “Animal models of retinopathy of prematurity” in *Animal Models for Retinal Diseases*(eds Pang, I. and A. F. Clark) Series: Neuromethods **46** (2010)
88. Penn, J. S., (ed) *Retinal and Choroidal Angiogenesis* Springer (2008)
89. Sakai K., et al., “Potential withdrawal of rheumatoid synovium by the induction of apoptosis using a novel in vivo model of rheumatoid arthritis” **41** (7) 1251-1257 (1998)
90. Bergers, G. and L. E. Benjamin “Angiogenesis: Tumorigenesis and the angiogenic switch” Nature Reviews Cancer **3** 401-410 (2003)
91. Yang, M., et al., “Dual color fluorescence imaging distinguishes tumor cells from induced host angiogenic vessels and stromal cells Proceeding of the National Academy of Sciences (PNAS) **100** 14259-62 (2003)
92. Liang, C., A. Y. Park and J. Guan “*Invitro* scratch assay: a convenient and inexpensive method for analysis of cell migration *in vitro*” Nature Protocols **2**(2) 2007 329-333
93. Aplin A. C., et al., “The aortic ring model of angiogenesis” in *Methods in Enzymoogy: Angiogenesis Systems* vol. **443** (ed Cheresh, D. A.) Elsevier academic press(2008)
94. Burbridge, M. F. and D. C. West “Rat aortic ring: 3D model of angiogenesis *In vitro*” in *Methods in Molecular Medicine* vol. **46**: Angiogenesis Protocols (ed. J. C. Murray) Humana Press Inc., 2001
95. Serbedzija, G. N., E. Flynn and C. E. Willett “Zebrafish angiogenesis: a new model for drug screening.” Angiogenesis **3**(4) 353-359 (1999)
96. Amoh, Y., K. Katsuoka and R. M. Hoffman “ Color-coded fluorescent protein imaging of angiogenesis: the AngioMouse® Models” Current Pharmaceutical Design **14** 3810-3819 (2008)

97. Nicosia, R. F., R. Tchao and J, Leighton. “Histotypic angiogenesis *in vitro* – light microscopic, ultrastructural and autoradiographic studies” *In vitro*- Journal of the tissue culture association **18**(6) 538-549 (1982)
98. Zhu, Wen-Hui and Roberto Nicosia “The thin prep rat aortic ring assay: A modified method for the characterization of angiogenesis in whole mounts” Angiogenesis **5**, 81–86, (2002)
99. Zhu, et al., “The Mouse Aorta Model: Influence of Genetic Background and Aging on bFGF- and VEGF-Induced Angiogenic Sprouting" Angiogenesis **6**, 193-199, (2003)
100. Nicosia, R. F., et al., “A new ex vivo model to study venous angiogenesis and arterio-venous anastomosis formation” Journal of Vascular Research **42**, 111-119 (2005)
101. Gelati, et al., “The angiogenic response of the aorta to injury and inflammatory cytokines requires macrophages” Journal of Immunology, **181**, 5711 – 5719 (2008)
102. Jang, H., et al., “A novel *ex vivo* angiogenesis assay base on electroporation-mediated delivery of naked plasmid DNA to skeletal muscle” Molecular Therapy **9** 464-474 (2004)
103. Rymo, Simin F., et al. “A two-way communitaction between microglial cells and angiogenic sprouts regulates angiogenesis in aortic ring cultures” PLoS ONE **6**(1) e15846 (2011)
104. Kredo-Russo, S. and E. Hornstein “MicroRNA Knock Down by Cholesterol-Conjugated Antisense Oligos in Mouse Organ Culture.” Methods Mol ecular Biology **732** 89-97 (2011)
105. Barkefors, Irmeli., et al., “A fluidic device to study directional angiogenesis in complex tissue and organ cultures models” Lab on a Chip, **9**, 529-535 (2009)
106. Günther, Axel,. et al. “A microfluidic platform for probing small artery structure and function” Lab on a Chip, **10**, 2341-2349 (2010)
107. Humphrey J.D. and S. L. Delange *An introduction to biomechanics: solids and fluids analysis and design* Springer-Verlag New York, Inc (2004)
108. Silvestre J. S., B. I. Levy and A. Tedqui., “Mechanisms of angiogenesis and remodeling of the microvasculature” Cardiovasc Research **78** (2) 201-202 (2008)
109. Resnick, N., et al., “Fluid shear stress and the vascular endothelium: for better and for worse” Progress in Biophysics and Molecular Biology **81**(3) 177-199 (2003)
110. Addae-Mensah, K. A., and J. P. Wikswo, “Measurement techniques for cellular biomechanics *in vitro*” Experimental Biology and Medicine **233** (7) 792-809 (2008)
111. Desmaele, D., M. Boukallel and S. Regnier “Actuation means for the mechanical stimulation of living cells via microelectromechanical systems: A critical review” Journal or Biomechanics **44**(8) 1433-46 (2011)
112. Brown, T. D., et al., “Loading paradigms-intentional and unintentional-for cell culture mechanostimulus” American Journal of the Medical Sciences **316** (3) 162-168 (1998)
113. Olsen, S. D., D. Clapham and P. Davies “Haemodynamic shear stress activates a K^+ current in vascular endothelial cells” Nature **331** 168-170 (1988)
114. Kolodney, M. S. and R. B. Wysolmerski “Isometric contraction by fibroblasts and endothelial cells in tissue culture: a quantitative study” Journal of Cell Biology **117** 73-82 (1992)
115. Freyman, T.M., et al. “Fibroblast contractile force is independent of the stiffness which resists the contraction.” Experimental Cell Research **272** 153–162 (2002)
116. Zeng, D., et al., “Three-dimensional modeling of mechanical forces in the extracellular matrix during epithelial lumen formation.” Biophyisical Journal **90** 4380-91 (2006)

117. Pedersen, J. A. and M. A. Swartz “Mechanobiology in the third dimension” **33**(11) Annals of Biomedical Engineering
118. Kluge, J. A., “Bioreactor system using noninvasive imaging and mechanical stretch for biomaterial screening” Annals of biomedical engineering **39**(5) 1390-1402 (2011)
119. Powers, M. J. et al., “A microfabricated array bioreactor for perfused 3d liver culture” Biotechnology and bioengineering **78**(3) 257-268 (2002)
120. Apelblat, A , A. Katzir-Katchalsky, and A. Silberberg, “A Mathematical Analysis of Capillary-Tissue Fluid Exchange” Biorheology **11** (1974)
121. Nicosia, R. F., “Aortic ring model of angiogenesis”as part of the *Analytical Techniques for the Quantitation of Angiogenesis and Lymphoangiogenesis Course, TRAC28* (developed by Mark Nardone) National Institutes of Health and the Foundation for the Advanced Education in the Sciences (NIH/FAES) 2010
122. Bellacen, K. and E. C. Lewis “Aortic Ring Assay” Journal of Visuallized Experiments **33** e1564 (2009)
123. Fischer, A. H., et al., “Hematoxylin and eosin staining of tissue and cell sections” Cold Spring Harbor Protocols (2008)
124. Gunin A., (2000) Histology Images: Circulatory system in *Histology textbook and atlas of microscopic images* Retrieved 2011, from http://histol.narod.ru/atlas-en/circulatory-en.htm
125. Nicosia, R. F. and W. Zhu “Rat aortic ring assay of angiogenesis” in Sringer Lab Manual: Methods in Endothelial Cell Biology (H. Augustin ed.) 2004
126. Schlaeger, T. M., et al., “Uniform vascular-endothelial-cell-specific gene expression in both embryonic and adult transgenic mice” Proceeding of the National Academy of Sciences (PNAS) **94**(7) 3058-63 (1997)
127. Peters, K. G., et al., “Functional significance of Tie2 signaling in the adult vasculature” Recent progress in Hormone Research **59** 51-71 (2004)
128. Abdulmalek, K., et al., “Differential expression of Tie-2 receptors and angiopoietins in response to *in vivo* hypoxia in rats” American Journal of Physiology – Lung Cellular and Molecular Physiology **281** L582-L590 (2000)
129. De Palma, M., et al., “Tie2-expressing monocytes: regulation of tumor angiogenesis and therapeutic implications” Trends in Immunology **28**(12) 519-524 (2007)
130. Suda, H., et al., “Immuno-histochemical expression of α1, α2 and α3, integrin subunits during angiogenesis *in vitro*” Histology and Histopathology **19** 735-742 (2004)
131. Davis, G. E., et al., “Molecular basis for endothelial lumen formation and tubulogenesis during vasculogenesis and angiogenic sprouting” International Review of Cell and Molecular Biology **288** 101-165 (2011)
132. Burbridge, M. F., et al., “The effect of extracellular pH on angiogenesis *in vitro*” Angiogenesis **3**(3) 281-288 (1999)
133. Pinho, S. P., and E. A. Macedo “Solubility of NaCl, NaBr, and KCl in water, methanol, ethanol and their mixed solvents” Journal of Chemical Engineering Data **50**(1) 29-32 (2005)
134. Kaunas, R., H. Kang and K. J. Bayless “Synergistic regulation of angiogenic sprouting by biochemical factors and wall shear stress” Cellular and Molecular Bioengineering **4**(4) 547-559 (2011)

135. Ichioka, S., et al., “Effects if shear stress on wound-healing angiogenesis in the rabbit ear chamber” Journal of Surgical Research **72**(1) 29-35 (1997)
136. Tressel, S. L., et al., “Laminar shear inhibits tubule formation and migration of endothelial cells by an angiopoietin-2 dependent mechanism” Arteriosclerosis, Thrombosis and Vascular Biology **27** 2150-56 (2007)
137. Gloe, T., et al., “Shear stress-induced release of basic fibroblast growth factor from endothelial cells is mediated by matrix interaction via integrin $\alpha_V\beta_3$.
138. Fisher, A. B., et al., “Endothelial cellular response to altered shear stress” American Journal of Physiology – Lung Cellular and Molecular Physiology **281**(3) L529-L533 (2001)
139. Feihl, F., et al., “Hypertension: A disease of the microcirculation?” Hypertension **48** 1012-17 (2006)
140. Huang, Y., et al., “Axial nonuniformity of geometric and mechanical properties of mouse aorta is increased during postnatal growth” American Journal of Physiology Heart and Circulatory Physiology **290**(2) H657-H664
141. Nassar, T., et al., “In vitro and in vivo effects of tPA and PAI-1 on blood vessel tone” Blood **103**(3) 897-902 (2004)
142. Jen, C. J., S. J. Jhiang and H. I. Chen “Invited review: effects of flow on vascular endothelial intracellular calcium signaling of rat aortas ex vivo” Journal of Applied Physiology **89**(4) 1657-62 (2000)
143. Klein, E., et al., “Diffusive and hydraulic permeabilities of commercially available cellulosic hemodialysis films and hollow fibers” Journal of Membrane Science **2** 349-364 (1977)
144. Ramanujan, S., et al., “Diffusion and convection in collagen gels: implications for transport in the tumor interstitium” Biophysical Journal **83** 1650-60 (2002)
145. Shiu, Y. T., et al., “The role of mechanical stresses in angiogenesis.” Critical Reviews in Biomedical Engineering **33**(5) 431-510 (2005)
146. Egginton, S., “Angiogenesis – may the force be with you!” Journal of Physiology **588** 4615-16 (2010)
147. Karathanasis, E., et al., “Tumor vascular permeability to a nanoprobe correlates to tumor-specific expression levels of angiogenic markers” PLoS ONE **4**(6) e5843
148. Auer, M., et al., “*In vitro* angioplasty of atherosclerotic human femoral arteries: analysis of the geometrical changes in the individual tissues using MRI and image processing” Annals of Biomedical Engineering **38** 1276-87 (2010)
149. Aaa[Martin-Green]
150. Liu,Y, Markov,D, Wikswo,J, McCawley,L. Microfabricated Scaffold-Guided Endothelial Morphogenesis in Three-Dimensional Culture, Biomed. Microdevices, **13** 837-846 (2011)
151. Dohle, D. S., Pasa, S. D., Gustmann, S., Laub, M., Wissler, J. H., Jennissen, H. P., Dünker, N. “Chick *ex ovo* Culture and *ex ovo* CAM Assay: How it Really Works.” J. Vis. Exp. **33** e1620, (2009).
152. Palmer, T. D., Lewis, J., Zijlstra, A. “Quantitative Analysis of Cancer Metastasis using an Avian Embryo Model.” J. Vis. Exp. **51** e2815 (2011).

153. Georgescu W, Jourquin J, Estrada L, Anderson ARA, Quaranta V, Wikswo JP, “Model-Controlled Hydrodynamic Focusing to Generate Multiple Overlapping Gradients of Surface-Immobilized Proteins in Microfluidic Devices”, Lab on a Chip, **8** 238-244 2008